



## **DEVELOPMENT OF SUSTAINABLE PROCESSES FOR LEATHER SURFACE AND STRUCTURE DEFECTS MINIMIZATION**

**Matías Joaquín Penayo Bernal**

*Final dissertation submitted to Escola Superior de Tecnologia e Gestão of Instituto Politécnico de Bragança to obtain the Master's degree in Chemical Engineering in the ambit of the double diploma with Universidad Nacional de Asunción*

Supervisors:

**Prof. Dr. Maria Filomena Barreiro**

**Dr. Arantzazu Santamaria-Echart**

**Dr. Juan Daniel Rivaldi Chávez**

Bragança

July 2023

This work was made possible thanks to the Foundation for Science and Technology (FCT, Portugal) for the financial support through national funds FCT/MCTES (PIDDAC) to CIMO (UIDB/00690/2020 and UIDP/00690/2020), and SusTEC (LA/P/0007/2021). This work was developed within the scope of the project GreenShoes 4.0 (POCI-01-0247-FEDER-046082).



**UNIÃO EUROPEIA**  
Fundo Europeu  
de Desenvolvimento Regional



## Acknowledgements

Firstly, I would like to thank the Polytechnic Institute of Bragança, Dr. Omayra Ferreiro, and the General Postgraduate and International Relations Office of the National University of Asunción for granting me with a scholarship and allow me to graduate as a master in chemical engineering at the IPB.

My deepest and most sincere thanks to my closest and dearest fans, my family, who even at the distance never stopped providing me with their relentless and unconditional support under any circumstance, encouraging me to always aim for self-improvement and integrity.

Also, my thanks and gratitude to Prof. Dr. Filomena Barreiro, who gave me the opportunity to work under her wings and has believed in my capacities since the moment we met, sharing her support, enthusiasm, and experience with me throughout the whole development of this work.

Many thanks to Dr. Arantzazu Santamaria-Echart for accompanying and helping me with continuous support, patience, and optimism during the progress of this work, lending her invaluable wisdom and time whenever I needed it.

A special thanks to Dr. Juan Daniel Rivaldi for his availability and assessment in the elaboration of this work, granting me words of encouragement and positivity at all moments.

To all my colleagues from CIMO-IPB, who welcomed me into their facilities and most importantly, into their lives, allowing me to be part of their family with great joy and partnership, making my stay a lighthearted and unforgettable experience.

A heartfelt thanks to my friends in Paraguay, who always showed their support and believed in me, even before I did it.

To everyone who contributed in one way or another to the making of this work, you have my gratitude.

## Abstract

In pursuit of a greener future, the European Union and the United Nations encourage industries to renew their practices by adopting new sustainability principles and circular economy strategies. The waste produced by the leather industry takes part in this initiative by proposing a sustainable approach to minimizing leather's superficial and structural defects. In this context, the objective of this work aims to minimize structural and superficial defects of discarded leather by employing leather hydrolysate and commercial fillers (nanoclay particles, expandable and glass microspheres) and employing the combination of additives that proves more effective in improving the leather's mechanical properties. The reduction of superficial defects was achieved by combining 0.2%, 0.7% and 4.0% of expandable microspheres, glass microspheres, and nanoclay particles, respectively, and 20.0% polyurethane binder with each one of the fillers. However, the most effective additive was the addition of 25.0% leather hydrolysate and 10.0% transglutaminase (mTG), resulting in lighter, smoother, and more elastic leather without a significant dimensional variance. The effect of the former additive's concentration over the leather's mechanical properties was analyzed with a rotational central composite design  $2^2$  with 3 central points, defining 15.0 and 45.0% (OHW) leather hydrolysate, and 5.0 and 15.0% (OLW) mTG as boundary values. The ANOVA revealed that in the studied region, a significant effect of the concentration of mTG on the elongation percentage of leather. In contrast, the leather hydrolysate demonstrated a weak, yet significant, influence on the tensile strength. No significant effect of the additives on Young's modulus was found. The mathematical model generated to estimate the elongation percentage values was validated, predicting a value close to the one obtained from the experimental procedure. Overall, this work demonstrated the applicability of leather hydrolysate in the minimization of leather defects.

**Keywords:** *leather defects, leather hydrolysate, transglutaminase.*

## Resumo

Na busca por um futuro mais verde, a União Europeia e as Nações Unidas incentivam as indústrias a renovarem as suas práticas de trabalho adotando princípios de sustentabilidade e estratégias de economia circular. Os resíduos produzidos pela indústria de curtumes fazem parte desta iniciativa, propondo-se uma abordagem sustentável para minimizar os defeitos superficiais e estruturais do couro. Neste contexto, o objetivo deste trabalho consiste em estudar estratégias para minimizar defeitos estruturais e superficiais de couros rejeitados, empregando hidrolisado de couro e cargas comerciais (partículas de nanoargila, partículas expansíveis e microesferas de vidro), incluindo a combinação de aditivos que se mostre mais eficaz em melhorar as propriedades de resistência mecânica do couro. A redução dos defeitos superficiais foi obtida combinando-se 0,2%, 0,7% ou 4,0% de microesferas expansíveis, microesferas de vidro e partículas de nanoargila, respectivamente, com 20,0% de um ligante de poliuretano. Não obstante, a estratégia mais eficaz consistiu na adição de 25,0% de hidrolisado de couro e 10,0% de transglutaminase (mTG), resultando num couro mais leve, macio e elástico, sem variação dimensional significativa. O efeito da concentração do hidrolisado sobre as propriedades mecânicas do couro foi analisado recorrendo a um desenho de experiências composto rotacional central  $2^2$  com 3 pontos centrais, definindo 15,0 e 45,0% (OHW) de hidrolisado e 5,0 e 15,0% (OLW) mTG como valores limite. A análise ANOVA revelou que na região estudada houve um efeito significativo da concentração de mTG sobre o alongamento do couro. Em contraste, o hidrolisado de couro demonstrou uma influência baixa, mas significativa, na resistência à tração. Nenhum efeito significativo destes aditivos foi observado para o módulo de Young. O modelo matemático gerado para estimar os valores percentuais de alongamento foi validado, prevendo um valor próximo ao obtido no procedimento experimental. No geral, este trabalho demonstrou a aplicabilidade do hidrolisado de couro na minimização dos defeitos do couro.

**Palavras-chave:** *defeitos do couro, hidrolisado de couro, transglutaminase.*

# INDEX

Acknowledgements .....	ii
Abstract.....	iii
Resumo .....	iv
List of tables .....	vii
List of figures .....	ix
List of abbreviations and acronyms.....	xi
Chapter 1 .....	1
1. Introduction.....	2
1.1. Motivation and objectives.....	2
1.2. General Objective .....	3
1.3. Specific Objectives .....	3
Chapter 2 .....	4
2. Literature Review .....	5
2.1. Leather .....	5
2.2. Sustainability and tanning process.....	7
2.3. Leather processing .....	9
2.4. Leather defects .....	12
2.5. Leather defects correction.....	13
2.5.1. Transglutaminase.....	15
2.5.2. Commercial fillers .....	16
Chapter 3 .....	19
3. Methodology.....	20
3.1. Materials .....	20
3.2. Screening tests – Selection of additives.....	20
3.3. Characterization .....	22
3.3.1. Physical and mechanical characterization .....	22
3.3.2. Morphological characterization.....	23
3.3.3. Chemical characterization .....	23
3.3.4. Final validation.....	23
Chapter 4 .....	24
4. Results and Discussion .....	25
4.1. Preliminary screening tests .....	25
4.2. Design of experiments for the best combination .....	40

4.3. Final Validation .....	54
Chapter 5 .....	57
5. Conclusions and Future Works.....	58
5.1. Conclusions.....	58
5.2. Future works .....	59
References .....	60

## List of tables

Table 1. The average content of amino acids in type I collagen extracted from cattle hide (expressed as amino acids/1000 amino acids).....	14
Table 2. Level of variables for leather treatment with commercial fillers and WPB.....	21
Table 3. Experimental matrix of the two-level factorial design for expandable microspheres and WPB. ....	21
Table 4. Experimental matrix of the two-level factorial design for glass microspheres and WPB. ....	21
Table 5. Experimental matrix of the two-level factorial design for nanoclay particles and WPB. ....	21
Table 6. Level of variables for leather treatment with leather hydrolysate and mTG....	22
Table 7. Experimental matrix of the two-level factorial design for leather hydrolysate and mTG.....	22
Table 8. Samples of leather treated with expandable microspheres (flesh side).....	25
Table 9. Infrared spectral characteristics of control and treated leather samples.....	32
Table 10. Combination of additives delivered for organoleptic analysis, physical evaluation, and mechanical testing. ....	35
Table 11. Summary of the organoleptic analyses and physical evaluation of samples treated with the selected additives. ....	36
Table 12. Performance results of treated samples in flex resistance test results. ....	37
Table 13. SEM images of flesh side (up) and side view (down) of treated samples before and after the flex resistance test (with 300x magnification).....	38
Table 14. Experimental matrix of the rotational central composite design $2^2$ with 3 central points. ....	40
Table 15. Mechanical properties of treated leather according to the experimental matrix. ....	45
Table 16. ANOVA of additives influence over the maximum tensile strength considering a quadratic model.....	46
Table 17. ANOVA of additives influence over the maximum tensile strength considering a reduced linear model.....	46
Table 18. ANOVA of additives influence over the elongation percentage at maximum tension considering a quadratic model. ....	48



Table 19. ANOVA of additives influence over the elongation percentage at maximum stress considering a linear model.....	49
Table 20. ANOVA of additives influence over the Young's modulus considering a quadratic model. ....	51
Table 21. ANOVA of additives influence over the Young's modulus considering a reduced linear model. ....	52

## List of figures

Figure 1. Structure of collagen fibers, fibrils, triple helices of $\alpha$ -chains, aminoacids, and composition .....	5
Figure 2. Hide structure .....	6
Figure 3. Tanning interaction mechanisms between collagen and (a) chromium, (b) aluminum, (c) zirconium, and (d) tara (vegetable tannin) .....	7
Figure 4. Generic leather processing diagram .....	9
Figure 5. Rotary drums are employed in the soaking, liming, deliming, tanning, and dyeing stages .....	11
Figure 6. Defects of (a) scars, (b) material loss, and (c) cracks found in leather, each marked with an arrow .....	13
Figure 7. Main catalyzed reaction by microbial transglutaminase (mTG).....	15
Figure 8. Microscopic images (with 200x magnifications) of (a) nanoclay particles, (b) glass microspheres, and (c) expandable microspheres .....	17
Figure 9. Microscopic images of (a) flesh side and (b) grain side of leather samples (with 40x magnifications) .....	25
Figure 10. Microscopic analysis of flesh and grain side of leather samples (with 40x magnification): treated with 0.2% expandable microspheres and 20.0% WPB 40.0% WPB, respectively (a) and (b) for the flesh side, and (c) and (d) for the grain side.....	26
Figure 11. (a) Remanent liquid of the leather treatment with 0.7% glass microspheres and 20.0% WPB. Microscopic analysis (20x and 40x magnification for the flesh and grain sides, respectively) of samples treated with 20.0% WPB and 0.7% and 1.0% glass microspheres, respectively (b) and (c) for the flesh side, and (d) and (e) for the grain side .....	27
Figure 12. Microscopic analysis (with 20x magnification) of leather samples treated with 20.0% WPB and 1.0% and 4.0% nanoclay, respectively (a) and (b) for the flesh side, and (c) and (d) for the grain side .....	28
Figure 13. Microscopic analysis of leather samples (with 40x magnification) treated with 10.0% mTG and 25.0% and 50.0%, respectively (a) and (b) for the flesh side and (c) and (d) for the grain side .....	29

Figure 14. Microscopic analysis of leather samples (with 40x magnification) treated with 15.0% mTG and 25.0% and 50.0%, respectively (a) and (b) for the flesh side and (c) and (d) for the grain side .....	29
Figure 15. FTIR spectra of both sides of untreated leather (Control) and all treated samples .....	30
Figure 16. FTIR spectra of both sides of untreated leather (Control) and treated sample .....	31
Figure 17. Second-derivative spectra of flesh side of control and treated sample .....	33
Figure 18. Second-derivative spectra of grain side of control and treated sample.....	34
Figure 19. Distribution of tensile strength values recorded for each run .....	41
Figure 20. Distribution of elongation percentage values recorded for each run .....	42
Figure 21. SEM images (with 500x magnification) of the flesh side of treated samples (a) before and (b) after mechanical stretching .....	43
Figure 22. Stress/strain curve of untreated leather samples .....	43
Figure 23. Distribution of Young's modulus values recorded for each run.....	44
Figure 24. Relation between experimental and estimated values based on the reduced linear model for tensile strength .....	47
Figure 25. Generated response surface of the effect of the factors over the tensile strength inside the studied region based on the reduced linear model .....	47
Figure 26. Relation between experimental and estimated values based on the linear model for elongation percentage .....	50
Figure 27. Generated response surface of the effect of the factors over the elongation percentage inside the studied region based on the linear model .....	50
Figure 28. Relation between experimental and estimated values based on the reduced linear model for Young's modulus.....	52
Figure 29. Generated response surface of the effect of the factors over the Young's modulus inside the studied region based on the reduced linear model .....	53
Figure 30. Stress/strain curve of all samples treated with 40.0% leather hydrolysate and 15.0% mTG .....	55
Figure 31. SEM analysis of the flesh side fibers (a) before and (a) after mechanical stretching .....	55
Figure 32. SEM analysis of the grain side fibers (a) before and (a) after mechanical stretching .....	56

## **List of abbreviations and acronyms**

LH	leather hydrolysate
mTG	microbial transglutaminase
OLW	over leather weight
OHW	over hydrolysate weight
PB	polyurethane binders
WPB	waterborne polyurethane binder

Chapter 1

# **Introduction**

# 1. Introduction

## 1.1. Motivation and objectives

In 2015, the Portuguese government, alongside countries of the European Union and the United Nations, decided to take a step towards a sustainable future by adopting a strategy based on sustainability principles, centering on promoting the model of reducing, reusing, and recycling residues, contributing to the preservation of the environment and at the same time decreasing their impact on climate change (Escoto-Palacios et al., 2016; European Commission, 2020). In 2020 this plan was reinforced by the European Commission to accelerate the progression to greener industries through valorizing and utilizing residues to obtain value-added products of industrial interest (Kanagaraj et al., 2015; Pereira, 2021).

The leather industry was one of the industries affected by this new course of action. According to the literature, an average of 20% of a metric ton of wet salted hides is converted to leather. In contrast, the remanent is discarded as waste throughout the process, thus, contributing to an increase in the environmental impact of the leather industries and leading to numerous studies aiming at finding new approaches for leather tannage and leather waste applications (Dixit et al., 2015; Kanagaraj et al., 2006; Masilamani et al., 2016). Several literature sources showed advances in the search for novel technologies and tanning agents with lower environmental impact and appealing characteristics while promising findings in strategies to manage solid leather waste rose by its use in the production of value-added products (Altun & Yas, 2013; Pathan et al., 2019; Sivakumar & Mohan, 2020).

Despite these advances toward greener technologies, finished leather scraps still represent a meaningful percentage of leather waste (Marconi et al., 2020; Teferi, 2021). The term scraps refer to leftover leather remaining after the final cutting step in leather manufacturing, being labeled as low-quality leather due to defects on their surface and low structural integrity caused by mechanical stress during processing, resulting in insufficient aesthetic appealing attributes and inferior mechanical properties to meet quality standards (Basaran et al., 2012; Prabakar et al., 2016).

Improve the product's quality and mechanical properties are some of the principles of sustainability, with the leather research field focusing on implementing these principles into the production process to obtain more durable and fitter goods (Fan et al., 2019; O. Mohamed et al., 2018; Vieira Kopp et al., 2021). Adding fillers such as micro and nanoparticles in the finishing steps of leather enhances mechanical properties like plasticity, elasticity, and resistance. Moreover, aesthetically refined leather is attainable using polymeric resins like polyurethane-based binders (Kaygusuz et al., 2017; Olle et al., 2014; Prabakar et al., 2016).

Studies about using additives like collagen hydrolysates and nanoparticles to improve the mechanical properties of leather have been conducted over the past years. However, literature concerning the minimization of superficial and structural defects like material loss in low-quality leather products through the addition of fillers such as collagen hydrolysates and microparticles (e.g., nanoclay, expandable and borosilicated

microspheres) is sparse, giving room to new approaches on leather finishing improvement.

## 1.2. General Objective

The current work aims to obtain a leather with improved mechanical properties as a consequence of the reduction of structural and superficial defects employing by-products obtained from solid leather residues (leather hydrolysate) and fillers based on commercial expandable, rigid, or elastic low-density microparticles.

## 1.3. Specific Objectives

To achieve the stated general objective, the work establishes the following specific objectives:

- Conduct a morphological, chemical, and physical characterization of the leather samples;
- Establish new leather treatments with the defined fillers with particular emphasis on the ones using the leather hydrolysate;
- Evaluate the performance of organic and inorganic fillers, binders, and leather hydrolysates in the reduction of leather defects (screening tests);
- Perform specific tests according to the end users' requirements. This step will be conducted in cooperation with CTIC (Portuguese Leather Industry Technological Centre) and CTCP (Portuguese Footwear Technological Center);
- Evaluate the effect of the concentration of additives that proved to be most effective in the screening tests on the leather mechanical properties (tensile strength, elongation percentage, and Young modulus);
- Perform validation tests for the most promising additives concentrations under the studied region.

The following document is divided into five chapters, where the **first chapter** introduces the studied topic with a summarized justification and set objectives for the development of this research.

The **second chapter** reveals the current state of the art of leather processing and treatment, focusing on improving the leather with defects with views on sustainability.

The **third chapter** describes the techniques, protocols and conditions that were employed to carry out the leather treatments and its evaluation and analysis methods employed before and after the treatments.

In the **fourth chapter** are shown the results of all the experimental treatments carried out along with the respective comparison and discussion with similar works developed in related fields of the scientific community.

Finally, the **fifth chapter** presents a brief conclusion focusing on the most relevant information and providing other studies and perspectives to be considered for further development of this work.

## Chapter 2

# Literature Review



## 2. Literature Review

### 2.1. Leather

Leather is a natural-based material derived from animal hides and skins. It is known for sustaining harsh environmental conditions and microbial degradation and has remarkable mechanical properties (flexibility, thermal stability, plasticity, elasticity, and durability). These properties are mainly provided by collagen proteins, the main leather constituent (T. Covington, 2009; Sizeland et al., 2013). There are many types of collagens; the inter and intramolecular bonds between amino acids, the molecular composition, and the protein's final structure are some of the factors considered to make the differentiation (Shoulders & Raines, 2009). Regarding leather, type I collagen is the main constituent, presenting a helical structure supported by three parallel polypeptides of two  $\alpha_1$  and one  $\alpha_2$  chain assembled almost entirely by Proline (Pro), Hydroxyproline (Hyp), and Glycine (Gly) and a lower amount of different amino acids in a repeating sequence of Gly-X-Y where X and Y are mostly Pro and Hyp, respectively (Gelse et al., 2003; Wells et al., 2013).

These tripeptide chains are held together mainly through hydrogen bonds among the polypeptide functional groups (amino groups of glycine residues of one chain and the carbonyl group of the adjacent chain at the X position) and water molecules located between the amino acid chains (Kramer et al., 2000; Yang, 2008). Because of the charge distribution throughout the protein, stacks of four to eight collagen units are grouped to form microfibrils. The arrangement of these stacks forms a fibril, which establishes cross-links with other fibrils via covalent bonds, interlocking into bundles and forming collagen fibers (Escoto-Palacios et al., 2016; Mancopes & Gutierrez, 2009). The described structure can be seen in Figure 1.

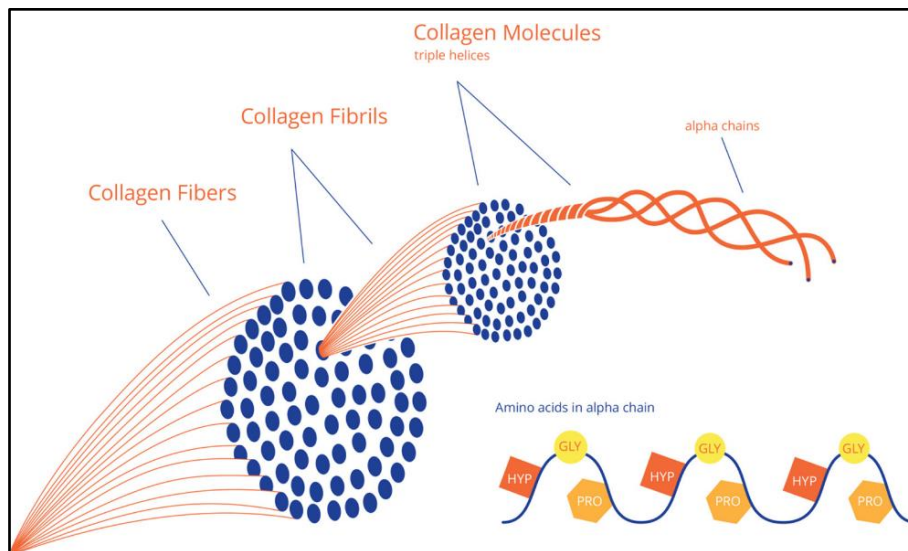


Figure 1. Structure of collagen fibers, fibrils, triple helices of  $\alpha$ -chains, aminoacids, and composition.  
Source: Adapted from Nijhuis et al. (2019).

How collagen fibers are distributed throughout the hide and skin of animals varies, presenting two distinct layers of different collagen arrangements. The outer layer, which is the first one, is named the grain layer. It contains hair follicles and is highly packed of interwoven fine collagen fibers, making it practically a solid surface (Z. Li et al., 2009;

O’leary & Attenburrow, 1996). The second layer is the corium layer, where collagen fiber bundles grow thicker as they expand away from the grain layer. The boundary between layers is not uniform, showing a transition zone. This region has relatively small collagen fibers and other structural components like elastin, fat, and other non-collagenous components (T. Covington, 2009; Prabakar et al., 2016). In Figure 2 it can be seen the described structure of the hide.

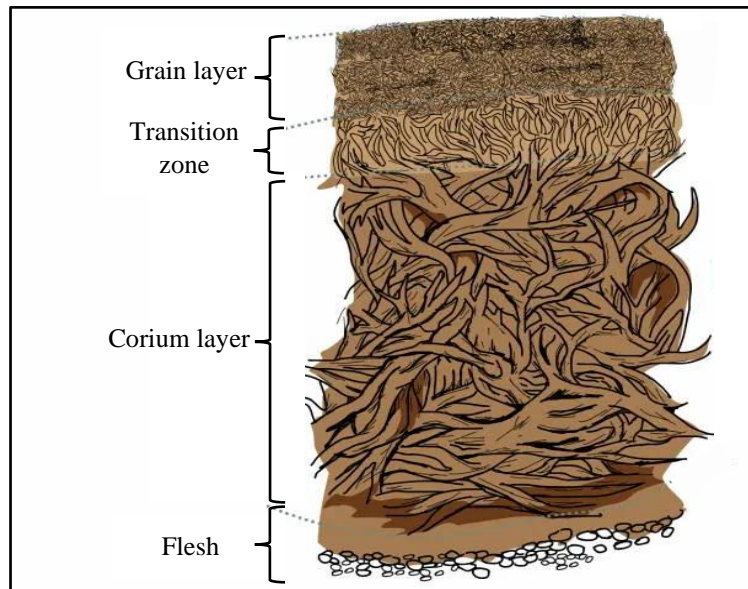


Figure 2. Hide structure. Source: Adapted from The Leather Satchel (2020).

Leather production is based on the reaction involving functional groups of collagen proteins and tanning agents such as vegetable tannins (polyphenols), mineral salts (chromium, titanium, aluminum salts), and aldehyde tannings (formaldehyde and glutaraldehyde), to name a few (A. Covington & Wise, 2020; Maina et al., 2019). Water molecules are displaced from their intermolecular location alongside the polypeptide chains to allow cross-linking between the amine and the carboxyl groups of the protein with the tanning agents, stabilizing the structure against chemical and microbial degradation, increasing heat resistance as well as mechanical properties (Escoto-Palacios et al., 2016; Goldschmidt & Streitberger, 2007). A schematic representation of some tanning interaction mechanisms can be seen in Figure 3.

The utilization of chromium salts in the tanning process is preferred over other tanning agents as it is cheaper, highly versatile, and results in greater mechanical properties, higher thermostability, and pleasant leather aesthetics (Lyu et al., 2018; Maina et al., 2019). The drawback of this method is the reported presence of chromium (III) ions and its oxidized form, chromium (VI), in considerable amounts in sludges and wastewater of tanneries, and even in leather articles (Deselnicu & Crudu, 2012; Ozgunay et al., 2007). These components compromise human health and environmental constituents like bacteria and water organisms since they are highly toxic, presenting a carcinogenic character (Hedberg, 2020; Rosu et al., 2018).

## 2.2. Sustainability and tanning process

In 2012 the European Chemical Agency (ECHA) stated that chromium salts, among other chemicals, are deemed hazardous for humans and the environment, and labeled them as Substances of Very High Concern (SVHC), restraining their usage to a minimum level in the production of leather articles designed to interact by any means with human skin (Dixit et al., 2015; European Chemical Agency (ECHA), 2012; Shi et al., 2016). These limitations, together with the current transition of the EU to more sustainable, greener, and environmentally amicable companies based on circular economy strategies, led the leather industry to expand its frontiers into testing new tanning agents, reevaluating old ones, and upgrading and adapting their methods to achieve these objectives (A. Covington & Wise, 2020; European Commission, 2015).

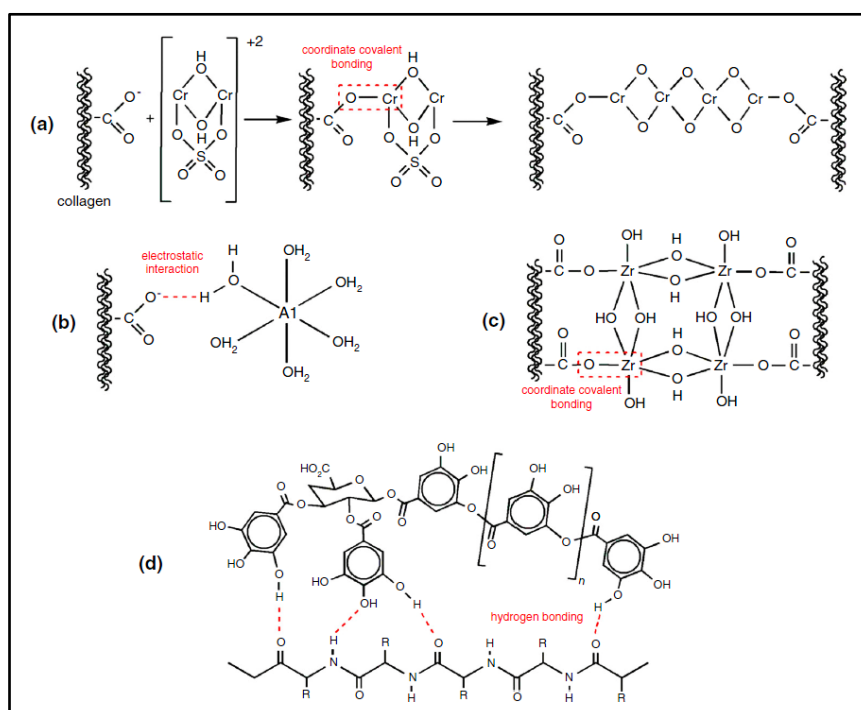


Figure 3. Tanning interaction mechanisms between collagen and (a) chromium, (b) aluminum, (c) zirconium, and (d) tara (vegetable tannin). Source: Modified from Onem et al. (2017).

Reducing the dosage of chromium salts in tanning was pursued by Baozhen & Jing (2015) when they tested the application of microbial transglutaminases (mTG) as a pre-tanning agent and posterior chrome tannage with 4% of the salt, resulting in a shrinkage temperature higher than 100 °C. In another study, Cai et al. (2015) proposed a new tanning method called inverse chrome tanning, where sheepskin was tanned with 3% (w/w) of aluminum-zirconium complex as the leading tanning agent and doses of  $Cr_2O_3$  around 1% (w/w) as a re-tanning agent, obtaining desirable mechanical and aesthetic properties (Baozhen & Jing, 2015; Cai et al., 2015).

Chrome-free tannage, commonly denominated wet-white tannage, comprises all tanning agents that do not include chromium in any form in the tanning of leather. Many alternatives were investigated in the search for compounds suitable for tanning and able to attain considerable mechanical properties and pleasant sensorial characteristics (Haroun et al., 2009; Wu et al., 2020).

An example of wet-white tannage is evidenced in the study conducted by Afsar & Sekeroglu (2008), where they proved that leather with higher shrinkage temperature could be obtained using 20% valonia extracts modified with 5% NaSH as a tanning agent and 5% (w/w) of oxazolidine as a pre-tanning agent rather than only valonia extract in the leather tannage. Furthermore, Yahia et al. (2019) concluded that a similar trend occurs when comparing the higher shrinkage temperature of leather tanned with a mix of 20% quebracho and 4% (w/w) oxazolidine against an inferior value reached in leather tanned with quebracho alone (Afsar & Sekeroglu, 2008; Yahia et al., 2019).

On the other hand, the combination of vegetable tannings, laponite nanoclay and aluminum salts in concentrations of 10%, 1%, and 3% (dry-basis), respectively, done by Shi et al. (2021) introduces significant hydrothermal improvement to the leather with a shrinkage temperature above 95 °C. Besides, the aesthetic appearance of the resultant leather is noteworthy, according to the authors. It was described by Lu et al. (2009) that the employment of nano-silicates as a tanning agent in combination with oxazolidine as a pre-tanner in the tannage of goat skin led to a higher resistance to mold and comparable thermal stability to chrome-tanned leather by using 5% (w/w) of nano-silicate and 2% (w/w) of oxazolidine.

It is essential to note that not only mechanical and esthetic characteristics were praised in leather under the cited conditions. Likewise, the collateral environmental impact of the experimental procedures was considerably lower when looking at measurements of the levels of total solids, chemical, and biochemical oxygen demand, free formaldehyde, and chromium (VI) content in comparison with chrome-tanned leather (Cai et al., 2015; Lu et al., 2009; Shi et al., 2021; Yahia et al., 2019).

Leather processing nowadays is achievable regardless of the chosen method for tanning. However, all of them follow a similar base sequence of standardized operations that can be grouped into 3 stages: pre-tanning, tanning, and post-tanning, as it is represented in the diagram of Figure 4 (IL&FS Ecosmart Limited, 2009; Maina et al., 2019). During these stages, the hide is subjected to various physicochemical changes, causing great mechanical stress over the structure of the leather. According to the literature, in tanneries, around 20% yield is achieved from a metric ton of wet salted hide, discarding the rest throughout the process, especially at the end, where the cutting step takes place (Kanagaraj et al., 2006; Teferi, 2021).

To further understand the modifications and refinements made to the hide from the initial state in the tannery until its final form at the exit and the influence of physicochemical elements have on the hide in the process to obtain a material meeting the market standards with appealing qualities and competitive mechanical properties it is necessary to review the conditions and operations involve in the process of leather manufacturing.



Figure 4. Generic leather processing diagram. Source: Own design.

### 2.3. Leather processing

Pre-tanning operations consist of storage, soaking, dehairing, liming, fleshing, splitting, de-liming, bating, degreasing, and pickling. The process starts with storing the hide, generally made by coating its surface with sodium chloride salt to dehydrate it and make it less susceptible to microbial decomposition (T. Covington, 2009). When leather processing starts, salted hides are soaked with cold water in rotatory drums to remove the salt and rehydrate the hide without damaging it while at the same time removing undesired elements like blood, flesh, and dust present in the material (Goldschmidt & Streitberger, 2007; Sivakumar et al., 2019).

After soaking, often the hair, fat, and other non-collagenous components are still attached to the hide and must be removed so dehairing and liming operations take place and are generally effectuated simultaneously by immersion of the hide in a lime and sulfide solution and stirred in rotary drums (IL&FS Ecosmart Limited, 2009). A critical aspect of this process is that a high pH causes the hydrolysis of non-collagenous proteins like albumins and globulins in the hide. In contrast, the charge distribution throughout the collagen proteins is destabilized. It causes swelling of the fibers and separation of fibrils bundles, resulting in a lower rigidity of the hide and greater accessibility to collagen, which favors a deeper penetration of ions and molecules into the hide in the subsequent steps (Covington & Wise, 2020; Maxwell et al., 2006).

Fleshing is carried out to remove the remaining flesh by mechanical means using rotary scraping rolls, adding more collagen availability. Following fleshing, the hide is adjusted in thickness with a blade by splitting it horizontally into two layers using a blade, where the top layer (grain) will become leather (INESCOP, 2012). At this point, delimiting is done by ammonium salts addition to decrease the pH of the hide from values around 12 to near 8, so in the next stage of bating and degreasing, proteolytic and lipolytic enzymes like proteases and lipases can degrade more effectively non-structural proteins and fat, increasing the level of exposure of the collagenous network (T. Covington, 2009).

The last operation in pre-tanning is pickling, where the pH is adjusted to acidic, so suitable conditions are met for the hide tannage. The acidification of the pelt enhances the reactivity of the functional groups of the peptides as a consequence of the increment in the positive charge of the amino group. In contrast, the negative charge is reduced in the carboxyl groups, which favors the tanning reaction (K. Li et al., 2009). Usually, sulfuric, hydrochloric, and acetic acid or a mixture of both are used to lower the pH to the necessary value for the chosen tanning method. Other chemicals involved in this process are sodium chloride salts to prevent the swelling of collagen fibers (Maina et al., 2019).

The tanning is the irreversible physicochemical transformation of the collagen proteins of the hide due to the reaction of the carboxyl and amine groups with tannic acids or tannins, resulting in a material with significantly improved stability and mechanical resistance, reducing the risk of putrefaction caused by microorganism (Watt, 1906). With the advances in science and technology, it was shown that tanning could be done with different compounds that demonstrated the same ability to react with collagen and provide the hide with similar characteristics (Lu et al., 2009; Maina et al., 2019; Shi et al., 2021).

Several methods were developed according to the selected tanning agent. Currently, the most common and economic practice is chrome tanning, using salts of chromium like elemental chromium (III) sulfate and chromium (III) oxide (Goldschmidt & Streitberger, 2007; Jiang et al., 2016). However, as described previously, chrome tanning has decreased in popularity due to its potential risk to society. Therefore, a diversity of tanning compounds has been proposed, studied, and applied as alternatives to chrome tanning; among them, vegetable tanning, as the first implemented tannage method, displayed significant growth over the past years, remarking its mechanical characteristics and the lower environmental impact and toxicity of its residues (Covington & Wise, 2020; Koloka & Moreki, 2011).

The tannage of hides involves the operation of wooden or metallic drums (shown in Figure 5), where the hides are introduced together with a chemical bath containing the chosen tanning agents. After this, the drums rotate, stirring and mixing the hides with the chemicals so tanning can occur (Tannery Projects, 2022). Big comb-shape shelves or pegs situated on the internal walls of the drums stretch and drag the pelts, promoting a synergic effect with the rotation of the drums, so a better mixing, a higher openness of the collagen matrix, and a deeper penetration of chemicals are obtained (T. Covington, 2009; INESCOP, 2012).

Post-tanning treatments are executed to grant the leather its final aesthetic appearance, distinctive characteristics, and mechanical properties, and according to the type of tannage adopted, it varies; however, processes such as sammying, shaving, deacidification, re-tanning, dyeing, fat-liquoring, drying, finishing, and cutting are processes involved in most tanneries (Hansen et al., 2021; Maina et al., 2019).



Figure 5. Rotary drums are employed in the soaking, liming, deliming, tanning, and dyeing stages.  
Source: Tannery Projects (2022).

After tannage, the excess moisture is removed from the leather by sammying it, then split, if necessary, to the desired thickness and shaved to acquire an even surface (IL&FS Ecosmart Limited, 2009). The next step is to deacidify the leather to keep the charge distribution throughout the material uniform. Re-tanning strengthens the bonds formed in the previous tanning and increases the thermal stability of leather by adding chemicals like oxazolidine, glutaraldehyde, or other tannins (Choudhury et al., 2007; Maina et al., 2019).

The dyeing of leather can be done along with the re-tanning by introducing the re-tanning components and the selected dyes into drums; on the other hand, it can also be done after re-tanning if needed. The dyes are chosen according to the final properties and characteristics preferred in the leather. They can be classified as acid, basic, direct, mordant, premetallized, reactive, and sulfur, regarding their structure and conditions in which they are applied (Covington, 2009).

The resultant leather is fat-liquored to prevent the collagen fibers from sticking to each other in a disorganized fashion after the excess water in the collagen matrix is removed in the subsequent drying process (Maina et al., 2019). Fat-liquoring benefits uniformity in fiber distribution, and enhances mechanical properties like tensile strength, elasticity, and softness. Materials like vegetable, mineral, synthetic oils, emulsions, and animal fat liquors might be employed in this process, depending on the final properties of the leather (Prabakar et al., 2016).

The remanent water is evaporated in the drying step, leaving around 30% humidity on the leather, so collagen fibers' viscoelastic properties are not altered negatively. The least expensive drying system consists in hanging the leather in drying chambers with natural air blown with fans through heating batteries. Nevertheless, other technologies like vacuum drying, paste drying, and secoterm drying are also implemented for the same end (INESCOP, 2012; Jeyapalina, 2004).

At this stage, the leather is known as “crust leather”, and its processing nearly ends. Yet, several strategies are applicable to improve its quality and define the characteristics and mechanical properties of the material (Borges Agustini et al., 2018). These strategies can be sorted according to the applied technique, the finishing effect, and the employed main finishing material since, typically, multiple components of different natures are employed to achieve the intended final performance in the leather (Basaran et al., 2012; Goldschmidt & Streitberger, 2007).

Generally, there are two significant groups regarding finishing materials: fillers and additives like pigments, nanoparticles, and nanocomposites. Binders consist of waxes, proteins, and synthetic polymers. Among the latter group, acrylic, butadiene, and polyurethane-based polymeric binders are most commonly used (Elsayed et al., 2018; Fan et al., 2019; O. A. Mohamed et al., 2009). Polyurethane binders (PB) are highly valued among coating materials; they maintain their performance and simultaneously withstand harsh conditions such as high temperatures and long-term outdoor exposure (Borges Agustini et al., 2018; S. Sundar et al., 2006).

Finally, leather is passed on to the last stage, known as cutting, where pieces of leather are selected and cut out according to the type of industry they will be processed in, which can be footwear, garment, gloves, leather goods, furniture, and upholstery (Barbanera et al., 2020; CTC, 2003). Each one requires specific leather characteristics; for instance, footwear industries rely on strong yet malleable materials, so the leather sent for this purpose must comply with such specifications (Solomon, 2021).

#### 2.4. Leather defects

A census made by the Centre Technique Cuir Chaussure Marroquinerie (CTC) in 2003 recorded that in leather products industries, the cutting ratios of finished leather can be estimated in a range of 25 to 60% each, highlighting that in the best cases, around 40% of the leather surface is used in the production of high-quality items, discarding the rest. The same report describes that the footwear industry is the main leather-consuming sector and, consequently, responsible for the largest leather waste generation. More recently, Marques et al. (2017) indicated that leather shoes occupy the most significant percentage of footwear products made in Portugal and that the leather waste originated from this sector is an environmental concern. Consequently, Marques and collaborators pointed out that if this industry would not engage in greener practices nor focus their procedures on circular economy principles, they should develop sustainable waste management and treatment processes rather than the current landfilling or incineration.

These residues consist mainly of scraps, leftover leather with superficial and structural defects caused by different factors like barbwire and parasitic diseases (scars, lice, skin disease, light flecks, and others) before its induction to the slaughterhouse, or by mechanical stress to which the leather is subjected during its processing (scratches, pinholes, material loss, grain looseness, and cracking), negatively impacting on the surface and structural integrity of the leather. The presence of these defects leads to its downgrading concerning industry standards, which reduces considerably their value in



the market (Basaran et al., 2012; CTC, 2003; Kahsay et al., 2015). Some leather defects are shown in Figure 6.

An observation made by Buehler (2006) suggested that elastic and fracture properties of collagen fibrils and fibers depend on the energetic effects of forces and the direction in which they are applied. Afterward, he concluded that some of the main factors that play a significant role in the deformation mechanics of collagen are the length of collagen molecules and the strength of their intermolecular interactions, highlighting how the weakest link in a collagen fibril can compromise the whole integrity of the fibril, and subsequently, the fiber (Buehler, 2006). On a macroscopic scale, it can be stated that each collagen fiber sustains a percentage of the administrated force under tension, so all the fibers act as a collective resistance (Fratzl et al., 1997).

Defects in leather can be translated into an absence of collagen fibers in the leather fabric. This alters the loading capacity of the collagen fibers surrounding the area where the defect is located, leading to an uneven stress distribution throughout the material and, subsequently, a poorer performance (Nalyanya, Rop, Onyuka, Birech, Wambulwa, et al., 2018). Liu et al. (2009) evidenced that mechanical properties were altered when they compared tensile strength, elongation percentage, and toughness of faulty leather with tight leather. The authors suggested the addition of fillers as a corrective measure for looseness in leather.



Figure 6. Defects of (a) scars, (b) material loss, and (c) cracks found in leather, each marked with an arrow. Source: Photos taken by the author.

In view of quality improvement, appearance, and mechanical properties of discarded scraps of leather by the minimization of their surface and structural defects and simultaneously reducing the quantity of leather scraps destined to waste, several methods have been proposed in the last decades, from tanning agents in tanning and re-tanning stages to inorganic and organic fillers and binders during post-tanning processes (Taylor et al., 2009; Tian, 2020).

## 2.5. Leather defects correction

Since solid leather waste is rich in collagen, its recuperation is an established practice in the industry and achievable through different methods. Moreover, the fields for its application in producing value-added products have grown over time (Brown, 2001; Ding et al., 2022; Jiang et al., 2016). One of its applications consists in hydrolyzing it for reuse as an additive in post-tanning stages to improve leather quality because their components of lower molecular weight (proline, glycine, glutamic acid, and lysine, to name a few,

presented in Table 1) possess high solubility, dispersibility, and capacity to form stable bonds with the potential to increase the thermal stability of leather (Denis et al., 2008; Dilek et al., 2019; Pahlawan et al., 2019).

Returning the proteins that once were part of the collagen matrix of the hide into the leather as reinforcement elements are one of the means to implement a sustainable process and can be done with the help of exogenous cross-linkers; these compounds are introduced in the system to act as a medium to form a bond between amino acids and collagen molecules by covalent bonds through their functional groups (COOH-, NH<sub>2</sub>-, OH-, CONH-), fixing them in place and further increasing the cohesion, stability, and strength of the network formed (Velmurugan et al., 2014).

Table 1. The average content of amino acids in type I collagen extracted from cattle hide (expressed as amino acids/1000 amino acids).

Amino Acid	Collagen		
	Li et al. (2013)	Kittiphattanabawon et al. (2015)	Rýglová et al. (2021)
Alanine	128.4	119	113
Arginine	51.0	51	50.5
Aspartic acid + asparagines	45.7	45	48
Cystine	0	0	1
Glutamic acid + glutamine	75.9	75	75
Glycine	330.6	330	315
Histidine	5.3	5	11.5
Hydroxylysine	7.7	7	np
Hydroxyproline	95.1	94	94.5
Isoleucine	11.4	11	14.5
Leucine	23.4	23	25.5
Lysine	26.5	26	28
Methionine	6.1	6	5
Phenylalanine	3.3	3	13.5
Proline	121.5	121	127
Serine	33.2	39	34.5
Threonine	18.4	18	16
Tryptophan	np	3	np
Tyrosine	3.7	3	7
Valine	21.5	21	22

np = not presented by the author.

Source: Data collected from values presented in the literature (Kittiphattanabawon et al., 2015; Z. R. Li et al., 2013; Rýglová et al., 2021).

Cross-linking agents may be classified according to their nature in metallic complexes, organic molecules, and physical treatment (irradiation), and the election of these relays, primordially, on the desired properties obtained in the leather and reaction

capacity towards collagen (INESCOP, 2012; Nishad Fathima et al., 2003; Wong et al., 2015). According to literature, organic compounds have been studied for their employment as cross-linking agents in biopolymers-based films like gelatin, hydrogels, and natural and artificial tissues, all of which share the building blocks of collagen as part of their structure (Cheng et al., 2019).

### 2.5.1. Transglutaminase

Novel cross-linking approaches embrace biotechnology, where enzymes such as transglutaminases (TG, protein-glutamine-glutamyltransferase, or EC 2.3.2.13) step forward as an innovative solution proposal (Baozhen & Jing, 2015). Initially, transglutaminases were proposed for use in food processing. Since these enzymes were found in mammalian insides (liver, blood), their extraction and purification were only possible in low quantities through expensive processes. Therefore, their application in the industry was not a viable option until 1989, when microbial transglutaminase (mTG) was successfully isolated from strains of *Streptoverticillium* sp (Ando et al., 1989; Lastowka et al., 2005).

This enzyme eases the polymerization of proteins by catalyzing an acyl-transfer reaction where  $\gamma$ -carboxamide groups of peptide-bounds glutamine residues act as acyl donors and  $\epsilon$ -amino groups of lysine residues as acyl acceptors, forming intra and intermolecular cross-links of  $\epsilon$ -( $\gamma$ -glutamyl) lysine bonds, represented in Figure 7 (Giosafatto et al., 2020; Polaina & MacCabe, 2007). Reports establish that collagen proteins act as an essential substrate for mTG cross-linkage, although collagen must be previously hydrolyzed so the enzyme may perform more efficiently (Cheng et al., 2019).

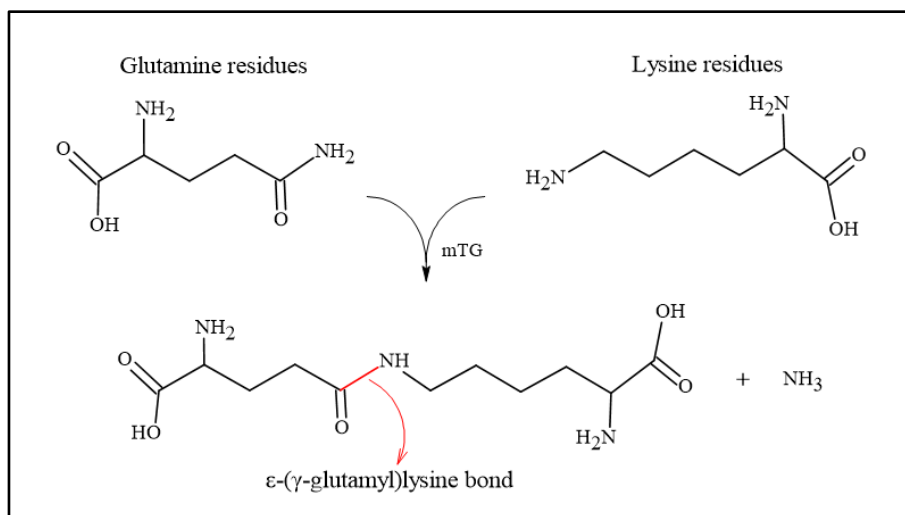


Figure 7. Main catalyzed reaction by microbial transglutaminase (mTG). Source: Own elaboration.

Hydrolyzing the discarded leather scraps generated during their processing results in a sustainable option for waste management and a feedstock for new products. It also provides a rich source of denatured collagen, which is essential for forming mTG-catalyzed cross-linking bonds between collagen amino acids. Stachel et al. (2010) worked on identifying cross-linking sites within the triple helical region of collagen molecules that provide favorable segments of mTG cross-linking. They found that using amounts between 1 and 500 active units of mTG per gram of collagen at 60 °C for 30 minutes

could result in the incorporation of a maximum of 5.4 mol isodipeptide cross-links per collagen monomer (Stachel et al., 2010).

The linkage established by mTG has proven great enzymatic and physical resistance; this is shown in the studies of Baozhen et al. (2015) and Lastowka et al. (2005), where the former recorded an increase in the shrinkage temperature of cowhide leather processed with mTG and, and the latter tested the enzymatic degradation of collagen fibrils treated with mTG, both concluding that the enzyme is a promising cross-linking agent. The work done by Taylor and collaborators in 2006 and 2007 showcased how gelatin from bovine skin (which shares a similar composition to hydrolyzed collagen) has the potential to act as an effective filler in leather processing. They demonstrated that these biopolymers polymerized with mTG when distributed evenly throughout the leather, bounding firmly to the fibers, and not easily removed in the subsequent stages of leather processing (Taylor et al., 2006, 2007)

Attempts to develop a self-cross-linking collagen fibril hydrogel for medical purposes were conducted by Jiang et al. (2019), working with dosages between 10 to 80 Units of mTG per gram of collagen at neutral pH. The results of their research proved to be promising since the obtained hydrogel evidenced that the incorporation of mTG not only was able to catalyze inter and intramolecular covalent cross-linking among collagen molecules, but also promoted the self-aggregation of said molecules into aligned collagen fibrils, mimicking the structure and biofunctionality of biological tissue, and even improving the thermal stability of the resultant material (Jiang et al., 2019).

Employing leather hydrolysate and chemical cross-linkers represents one of the strategies that can be used to reinforce and upgrade the leather. Nevertheless, other compounds, such as organic and inorganic composites, also present interesting capabilities as filler agents (Fan et al., 2019). Hence, utilizing micro and nanoparticles represents an appealing approach for leather filling material. According to their composition, structure, and affinity towards collagen, these filling agents will fasten to collagen fibers enhancing specific mechanical properties in the leather (O. Mohamed et al., 2018; Tian et al., 2018).

### 2.5.2. *Commercial fillers*

Inorganic fillers such as nanoclay (Figure 8. a) drew the attention of the leather scientific community, given the reported enhancement achieved on mechanical properties in polymer composites that incorporated these materials (Alexandre & Dubois, 2000; Jaisankar et al., 2013; Sanchez-Olivares et al., 2014). Generally, clay particles consist of layers of aluminosilicate sheets stacked one over another with a spacing between each other (known as interlayer or c-spacing). The sheets-like layers vary in length in the order of nanometers, yet on average, every sheet possesses 1 nm in thickness. Covalent bonds tie together the aluminosilicate layers while Van der Waals maintains the sheets piled up (Y. Chen et al., 2011; Luckham & Rossi, 1999; Prabakar et al., 2016).

Due to their size, the nanoclay particles can penetrate interfibrillar leather spaces and form part of the collagen matrix, sharing the load transfer received by the leather when submitted under stress (Y. Chen et al., 2011). This property was one of the factors that Prabakar et al. (2016) took into consideration when they treated loosened cattle wet-blue leather with an oil-water emulsion containing nanoclay particles. The authors describe

the value of 3% (w/w) of nanoclay as the optimum concentration given the improvement achieved in the material's handle, tensile, and tear strength. Additionally, an apparent filling and even distribution over the leather grain-corium section were obtained.

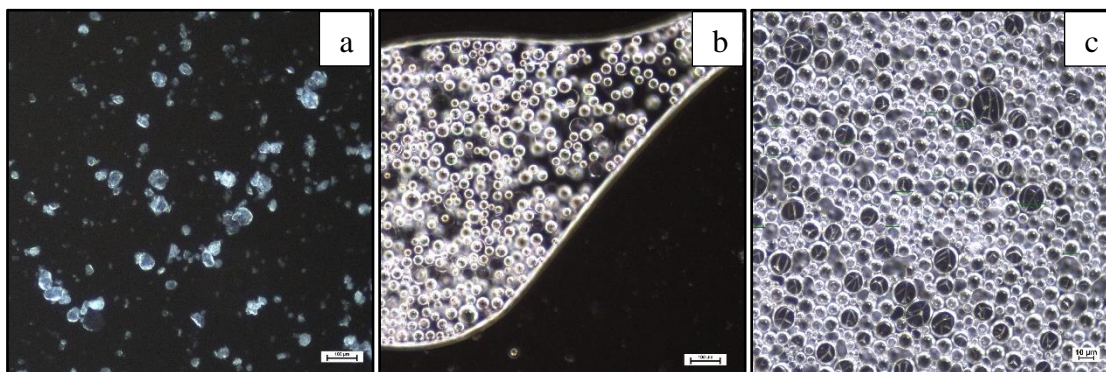


Figure 8. Microscopic images (with 200x magnifications) of (a) nanoclay particles, (b) glass microspheres, and (c) expandable microspheres. Source: Photographs taken by the author.

Another inorganic filler considered for leather improvement is glass microspheres (also known as glass beads). Since these micron-size soda-lime-borosilicated hollow beads (presented in Figure 8. b) are designed with a high strength-to-weight ratio and low density. The polymeric composites incorporating these glass beads have improved stability, resistance, and lightness (Koricho et al., 2015). A study described the strength and aesthetic continuity achieved when glass microspheres were employed as filling agents in leather recovery (Nieuwenhuizen, 1998).

On the other hand, advances in polymer science are constantly redefining boundaries with novel applications of polymeric composites, where remarkable development have been made in microencapsulation technology (Lensen et al., 2008; Winey & Vaia, 2007). According to the literature, these particulate composites can be employed in a variety of manners, one of them being light weighted filler agents. The integration of hollow microspheres (shown in Figure 8. c) in elastomeric composites significantly enhances tear resistance, plasticity, hardness, and other properties due to the characteristics of polymers composing the particles (Shorter, 2014).

The microparticles are formed by encapsulating a blowing agent (hydrocarbons like isobutane or isopentane) with a blend of monomers of methyl methacrylate, vinylidene chloride and acrylonitrile. The blended monomers' thermoplastic properties and the hydrocarbon's intern pressure lead these microspheres to expand when heated at temperatures above 80 °C (Fredlund, 2011). Currently, the incorporation of these microparticles is an implemented practice in the biofabrication of leather materials in dosages around 10% of collagen weight, providing superior strength and uniformity when compared to natural leather (Purcell et al., 2017)

Different polymeric binders are usually employed to reinforce the fastening of the fillers added to the leather. Among these, acrylic and polyurethane resins are currently the most employed in leather finishing applications. Acrylic binders provide leather with enhanced elasticity and flexibility in a wide range of temperatures. In contrast, PB can improve not only leather's elasticity and flexibility, but also resistance to solvents, abrasion, and mechanical strength, to name a few characteristics (Tracton, 2006). Currently, the usage of waterborne polyurethane binders (WPB) is replacing their

counterpart solvent base since they offer lower hazardous conditions for workers and reliable performance (Madbouly, 2021; Tian, 2020).

Several alternatives are proposed for discarded faulty leather, mainly the production of other goods based on the recovery of collagen, from value-added composites, and fertilizers, to its application in films, pharmaceutical, and medical industries (V. J. Sundar et al., 2011; Teferi, 2021). However, the literature about leather quality improvement by minimizing leather's structural and superficial defects by applying cross-linking agents and fillers to avoid leather disposal is still under development.

## Chapter 3

# Methodology

### 3. Methodology

#### 3.1. Materials

The samples of wet-white crust leather with a thickness of  $1.1 \pm 0.1$  mm and wet-white leather hydrolysate with a protein concentration of 609.31 g/L were provided by the Portuguese Leather Industry Technological Centre (CTIC) within the context of the Mobilizing project GreenShoes 4.0 (POCI-01-0247-FEDER-046082). A microbial transglutaminase preparation from Ajinomoto (110 active units/g) was acquired for the leather treatment. The expandable microspheres Expancel WE 20, with a media of 25  $\mu\text{m}$  in diameter, were purchased from Akzo Nobel, the glass microspheres Glass Bubbles iM16K from 3M with a diameter around 20  $\mu\text{m}$ , and the nanoclay particles Cloisite-20 from BYK with a medium size of 52  $\mu\text{m}$ . The Vecosol Binder U317 SN from Veco with 30% of solids was employed as the water-based polyurethane binder.

#### 3.2. Screening tests – Selection of additives

The selection of the additives to be incorporated in the leather to minimize its superficial and structural defects was assessed, firstly through a series of screening tests, evaluating the affinity of the additives on different concentrations towards the leather following a two-level factorial design  $2^2$  where each commercial filler (nanoclay particles, expandable and glass microspheres) was tested with the WPB, with the coding shown in Table 2 and structured in Table 3, Table 4 and Table 5, respectively for expandable microspheres, glass microspheres, and nanoclay particles. As for the leather hydrolysate and mTG, the same experimental design was applied with the values presented in Table 6 and planification established in Table 7.

For leather treatment with commercial fillers and WPB, the samples were cut into pieces of 11,5x11,5  $\text{cm}^2$  and soaked in Erlenmeyer flasks of 1000 mL with 200 mL of water for 1 hour at 30 °C and 150 rpm using a water bath with stirring (Julabo SW 22, Seelbach, Germany). After washing, the samples were retrieved from the flasks and introduced into other 1000 mL Erlenmeyer flasks containing 200 mL of a solution with the respective dose of the selected commercial filler and binder. The flasks were then stirred and placed in the water bath for 1 hour at 30 °C and 150 rpm. Finished the established time, the samples were removed from their flasks and dried in an environment of  $20 \pm 2$  °C and  $40 \pm 2\%$  relative humidity for 1 day (Prabakar et al., 2016; Purcell et al., 2017).

Similarly, the leather samples to be treated with the leather hydrolysate and mTG were also cut into pieces of 11,5x11,5  $\text{cm}^2$  for soaking in Erlenmeyer flasks of 1000 mL with 230 mL of water for 1 hour in a water bath at 30 °C and 150 rpm. After this time, the leather samples were removed from the flasks and introduced into other 1000 mL Erlenmeyer flasks with the corresponding 230 mL of the neutralized leather hydrolysate and cross-linking agent solution. Then, they were stirred and set into a water bath at 50 °C and 150 rpm for 1 hour. After 1 hour, the leather samples were taken from their flasks and left to dry in an environment of  $40 \pm 2\%$  relative humidity and  $20 \pm 2$  °C for 1 day (Bertazzo et al., 2011; Cheng et al., 2019).



Table 2. Level of variables for leather treatment with commercial fillers and WPB.

Factors	Level of variables	
	-1	1
Expandable microspheres (OLW %)	0.2	1
Glass microspheres (OLW %)	0.7	1
Nanoclay particles (OLW %)	1	4
Polyurethane binder (WPB) (OLW %)	20	40

OLW %: Over leather weight percentage.

Table 3. Experimental matrix of the two-level factorial design for expandable microspheres and WPB.

Assay	Coded variables		Real variables	
	Expandable microspheres	WPB	Expandable microspheres (OLW %)	WPB (OLW %)
1	1	1	1	40
2	1	-1	1	20
3	-1	1	0.2	40
4	-1	-1	0.2	20

Table 4. Experimental matrix of the two-level factorial design for glass microspheres and WPB.

Assay	Coded variables		Real variables	
	Glass microspheres	WPB	Glass microspheres (OLW %)	WPB (OLW %)
1	1	1	1	40
2	1	-1	1	20
3	-1	1	0.7	40
4	-1	-1	0.7	20

Table 5. Experimental matrix of the two-level factorial design for nanoclay particles and WPB.

Assay	Coded variables		Real variables	
	Nanoclay particles	WPB	Nanoclay particles (OLW %)	WPB (OLW %)
1	1	1	4	40
2	1	-1	4	20
3	-1	1	1	40
4	-1	-1	1	20

Table 6. Level of variables for leather treatment with leather hydrolysate and mTG.

Factors	Level of variables	
	-1	1
Leather hydrolysate (OLW %)	25	50
Microbial Transglutaminase (mTG) (OHW %)	10	15

OHW %: Over hydrolysate weight percentage.

Table 7. Experimental matrix of the two-level factorial design for leather hydrolysate and mTG.

Assay	Coded variables		Real variables	
	Leather hydrolysate	mTG	Leather hydrolysate (OLW %)	mTG (OHW %)
1	-1	-1	25	10
2	1	-1	50	10
3	-1	1	25	15
4	1	1	50	15

The combination showing the best performance on the screening tests was further studied using a rotational central composite design  $2^2$  with 3 central points in hopes to find the best combination within the studied range of additives to establish the influence of the study variables over the leather's mechanical properties, rendering predictive models that can be implemented for further optimization if such models are suitable and reproducible. The statistical analysis of the influence of the variables was carried out using the software Design-Expert® v.11.1.2.0. An analysis of variance (ANOVA) and a quadratic response surface method with a significance level of  $p < 0.05$  was applied to analyze the obtained data and find the most favorable conditions for leather's mechanical properties improvement and defects minimization.

### 3.3. Characterization

#### 3.3.1. Physical and mechanical characterization

Leather samples before and after treatment were conditioned over a period of 48 hours in an atmosphere of  $23 \pm 2$  °C and relative humidity of  $50 \pm 5\%$  in accordance with the standard ISO 2419:2012. Tensile strength tests were carried out based on ISO 3376:2020 standards acquiring tensile strength, elongation percentage at maximum tension and Young modulus (E) as properties of the samples. The Young's modulus of elastic deformation was determined as described by Ma & Lu (2008) using eq (1). The tests were conducted in seven samples with a universal tensile tester Autograph AGS-10kNX from Shimadzu (Kyoto, Japan). For data statistical analysis, it was considered the average and standard deviation of all obtained measurements.

$$E \text{ (MPa)} = \frac{\frac{\text{load}}{\text{width} \cdot \text{thickness}}}{\frac{\text{displacement}}{\text{length}}} \quad (1)$$

### *3.3.2. Morphological characterization*

The morphological analysis of collagen fiber and fibrils arrangement before and after treatment was conducted by optical microscopy with an optical microscope (Nikon Eclipse 50i) attached to a camera (Nikon Digital Sight), and if needed, by Scanning Electron Microscopy (SEM) using a Phenom Pro microscope from Phenom-World (Eindhoven, Netherlands). Carbon sheets were employed to fix the samples for analysis. The Software NIS-Elements BR was used for the image analysis obtained with optical microscopy.

### *3.3.3. Chemical characterization*

The presence of functional groups, their inter and intramolecular bonds (and reaction with cross-linkers when applied) before and after treatment were analyzed by Fourier-Transform Infrared Spectroscopy (FTIR) employing an MB 3000 (Montreal QC, Canada) model FTIR from ABB Inc. The collection of the spectra was set in a range of 550 to 4000  $\text{cm}^{-1}$  at a resolution of 16  $\text{cm}^{-1}$  and an average of 32 scans. The software Horizon MB v.3.4 was used to process the resulting spectra.

### *3.3.4. Final validation*

Aiming to validate the samples for the leather sector, the best solutions were reproduced at a large scale (firstly using an A4 size level) and characterized according to specific CTIC and CTCP procedures. The treatment of the samples was done by CTIC according to the formulation and procedure IPB.

## Chapter 4

# **Results and Discussion**

## 4. Results and Discussion

### 4.1. Preliminary screening tests

A series of preliminary screening tests were conducted to determine the combination of fillers and cross-linkers that shows the most significant improvements on the surface and structural integrity of the leather for further optimization. It is important to point out that the size of the microparticles is bigger than the interfibrillar spaces in the grain side (order of nanometers) of the leather; therefore, the optical examination began with the examination of the flesh and grain sides of the samples, distinguished in Figure 9.

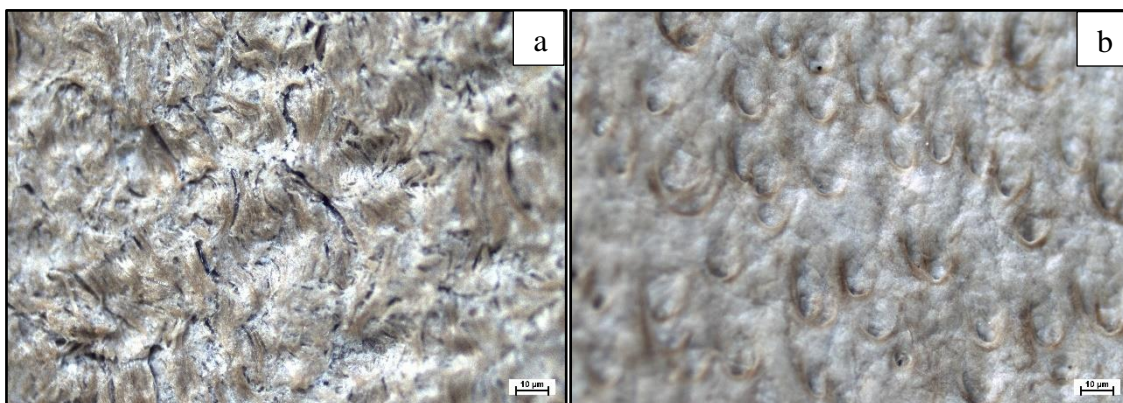
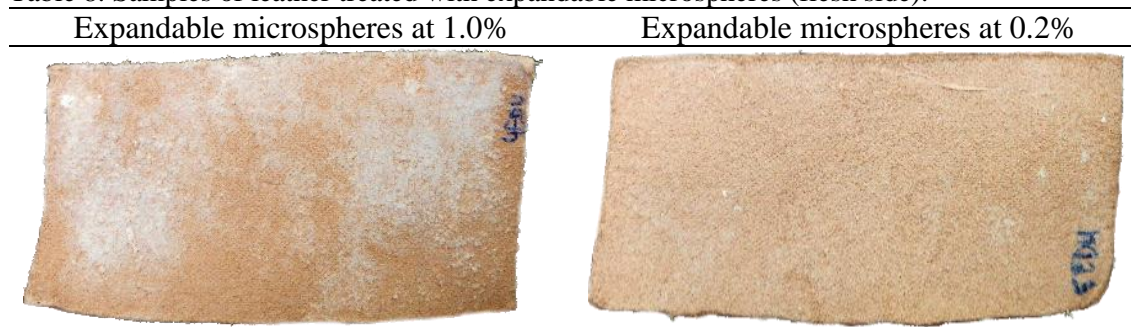


Figure 9. Microscopic images of (a) flesh side and (b) grain side of leather samples (with 40x magnifications).

The analysis began with the samples treated with the combinations of expandable microspheres and WPB according to the values in Table 3. The incorporation of expandable microspheres without binder on the samples was also tested for comparison purposes. Table 8 gathers the images of the resultant samples where the microspheres on the leather surface are visible to the naked eye when using a concentration of 1.0%, while in 0.2%, it is barely apparent. Since the leather with 1.0% of expandable microspheres results to be neither appealing nor aesthetic, it was discarded for further analysis.

Table 8. Samples of leather treated with expandable microspheres (flesh side).



Two WPB concentrations (20.0 and 40.0%), maintaining 0.2% of microspheres for each assay, were examined by optical microscopy. It was observed that both presented rather similar results concerning the distribution of the binder and filler in the flesh side, with a slightly higher quantity of spheres for the 40.0% WPB sample (visible in Figure 10). The grain side demonstrated a much higher concentration of microparticles distributed on its surface. A change in the rigidity of the sample was detected, being the

one with 40.0% noticeably higher than the one with 20.0%. Such stiffness resulted in an undesired feature for the leather and the determinant factor for discarding it for further mechanical evaluation.

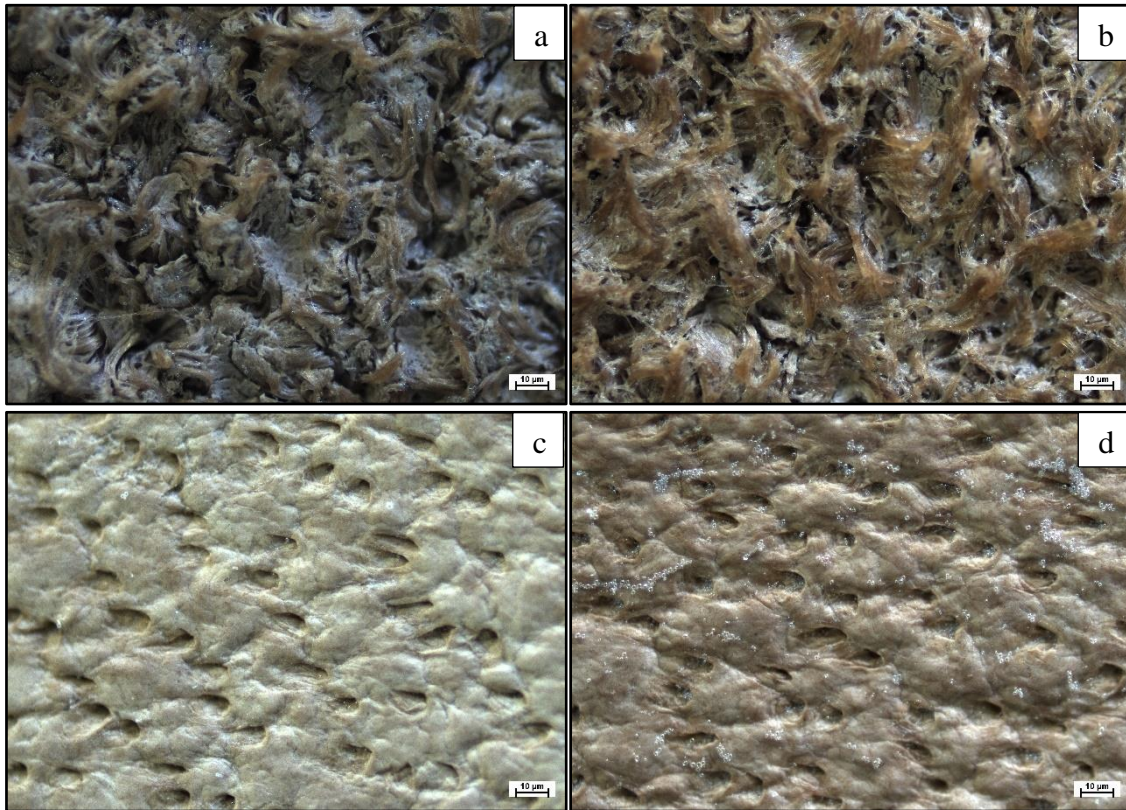


Figure 10. Microscopic analysis of flesh and grain side of leather samples (with 40x magnification): treated with 0.2% expandable microspheres and 20.0% WPB and 40.0% WPB, respectively (a) and (b) for the flesh side, and (c) and (d) for the grain side.

The analysis continued with the application of glass microspheres and binder as established in Table 4. During the treatment, it was observed that the beads did not exhibit great affinity towards the leather (see Figure 11), leaving a significant amount of microparticles (white traces) in the remanent liquid. In the microscopic analysis, no significant difference was found between microsphere distribution in the flesh side of samples using 0.7% and 1.0% of microparticle concentration. Yet, the grain side shows a relatively higher concentration.

Tian et al. (2018) described how the shape and surface of the glass beads may negatively influence the interfacial adhesion between the particles and polyurethane resins (Tian et al., 2018). An interesting characteristic that samples with 40.0% WPB presented was rigidity, which was significantly higher when compared to the samples with 20.0%. Therefore, the lowest concentration of the additives (0.7% glass microspheres and 20.0% WPB) was chosen to continue with their mechanical analysis.

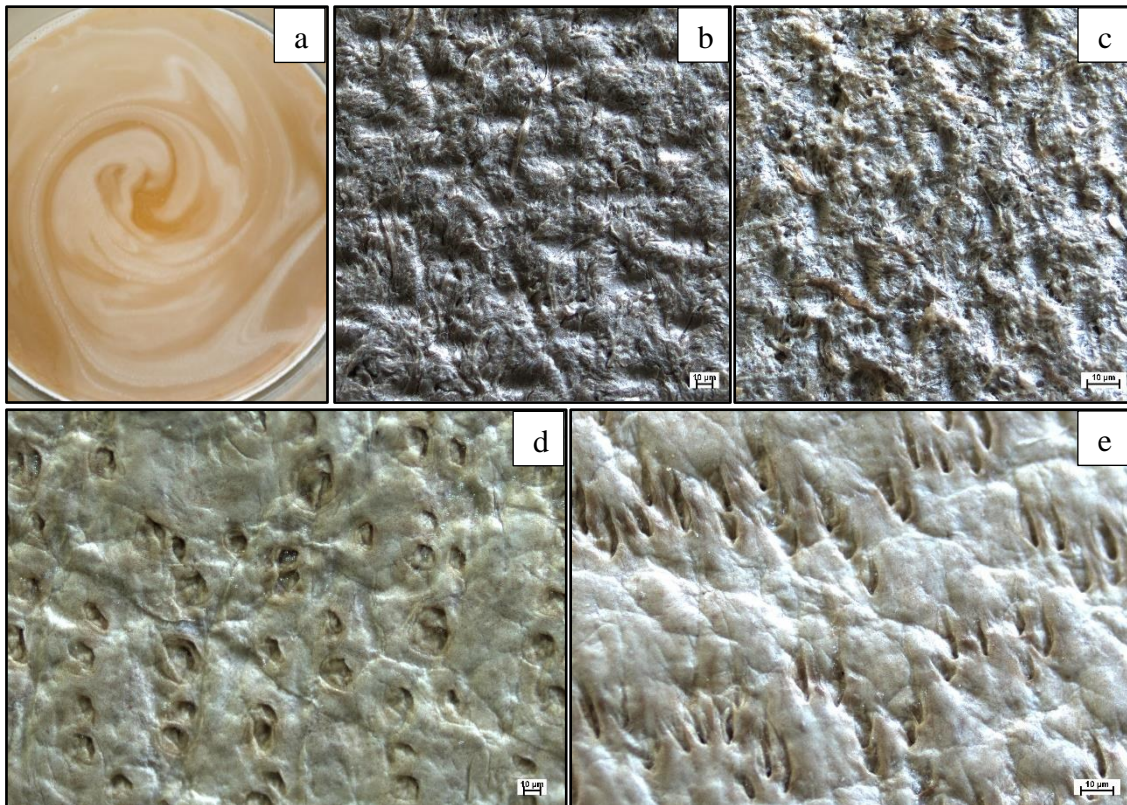


Figure 11. (a) Remanent liquid of the leather treatment with 0.7% glass microspheres and 20.0% WPB. Microscopic analysis (20x and 40x magnification for the flesh and grain sides, respectively) of samples treated with 20.0% WPB and 0.7% and 1.0% glass microspheres, respectively (b) and (c) for the flesh side, and (d) and (e) for the grain side.

Moving forward with the screening, incorporating nanoclay particles with the binder was tested. Given the low solubility of the nanoclay in water, a surfactant (Tween 80) was added to the solution to increase its solubility. A 4/3 ratio of nanoclay/Tween 80 was used before mixing with the binder. It has been noticed that the rigidity of all samples treated with 40.0% WPB, regardless of the used filler, was considerably higher than the one with 20.0%; therefore, the treatment with 40.0% of the binder was discarded for further examination.

The remaining samples were examined with an optical microscope (see Figure 12). Considering the flesh side, it was observed that when using 4.0% nanoclay, the binder and filler manage to access the intrafibrillar spaces (space between collagen fibers), separating them into individual fibers and reaching greater surface area coverage. In contrast, with 1.0% nanoclay the fibers stuck in bundles, most likely an effect of the WPB, isolating nanoclay groups over some fiber bundles and displaying a poor distribution throughout the surface, thus presenting a poor coverage of the superficial area. On the grain side, the presence of the nanoparticles is hardly visible at 1.0%, while at 4.0% a greater concentration is evident. The distribution of the binder and the filler also appears more homogeneous with 4.0% nanoclay, hence, this concentration was selected for further analysis.

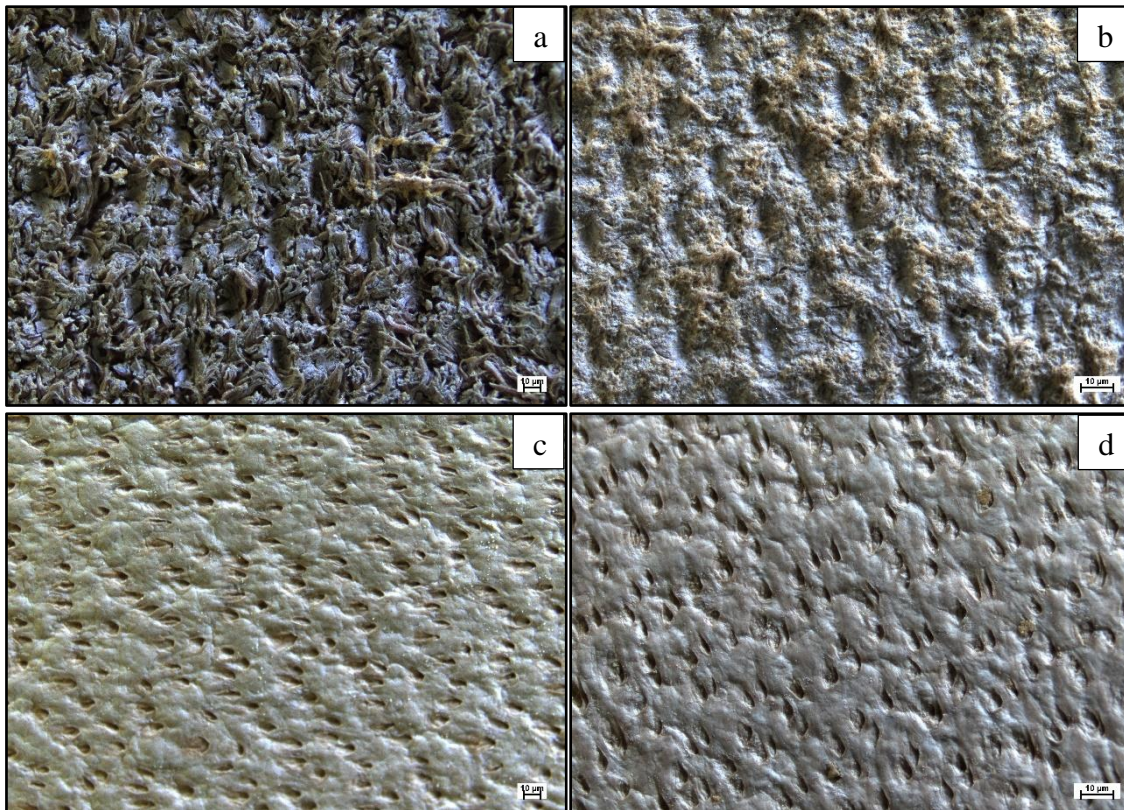


Figure 12. Microscopic analysis (with 20x magnification) of leather samples treated with 20.0% WPB and 1.0% and 4.0% nanoclay, respectively (a) and (b) for the flesh side, and (c) and (d) for the grain side.

The screening tests continued with the analysis of samples treated with wet-white leather hydrolysate and mTG under the contents established in the previous chapter (Table 7). When handling the samples, a lightly higher rigidity was noticed in samples using the higher leather hydrolysate concentration (50.0% OLW) and mTG (15.0% OHW). When analyzed by optical microscopy (Figure 13 and 14) the structure of the fibers at the flesh side seems to be messier after the incorporation of leather hydrolysate and mTG at any of the considered concentrations. On the other hand, the grain side appears to be unaltered. When the amount of leather hydrolysate increases, a coat-like film is formed over both sides of the sample.

Chemical characterization was performed by FTIR to verify the formation of cross-linking bonds in the leather. The following analysis is based on the sample treated with 25.0% leather hydrolysate and 10.0% mTG, considering that all treated samples presented similar spectra (see in Figure 15). In Figure 16, the vibration assignments of the analyzed spectra are disclosed. The change in the vibration's intensity (peaks) and wavenumbers magnitude reveals if the bonds were changed in any manner. According to the literature, to confirm if cross-links were formed due to the presence of mTG, the most important regions of the spectrum to check are the ones of amide A, amide B, amide I, amide II, and amide III (Jiang et al., 2019; Staroszczyk et al., 2012).



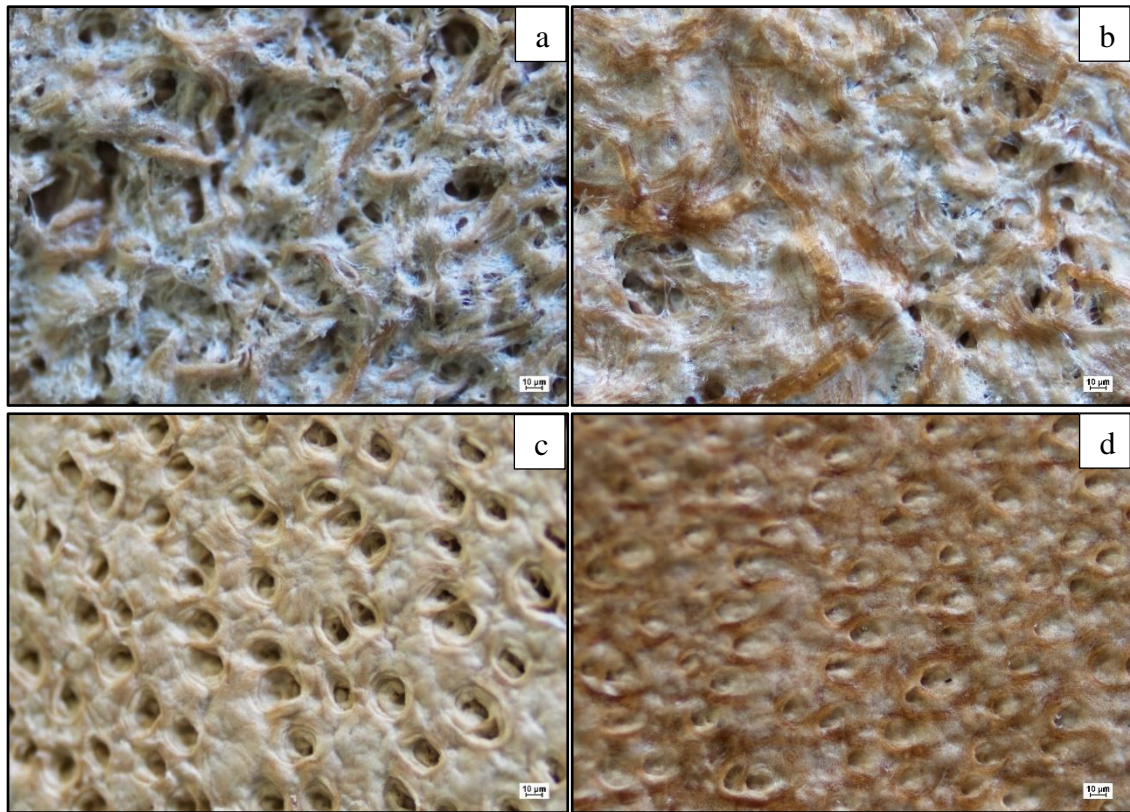


Figure 13. Microscopic analysis of leather samples (with 40x magnification) treated with 10.0% mTG and 25.0% and 50.0%, respectively (a) and (b) for the flesh side and (c) and (d) for the grain side.

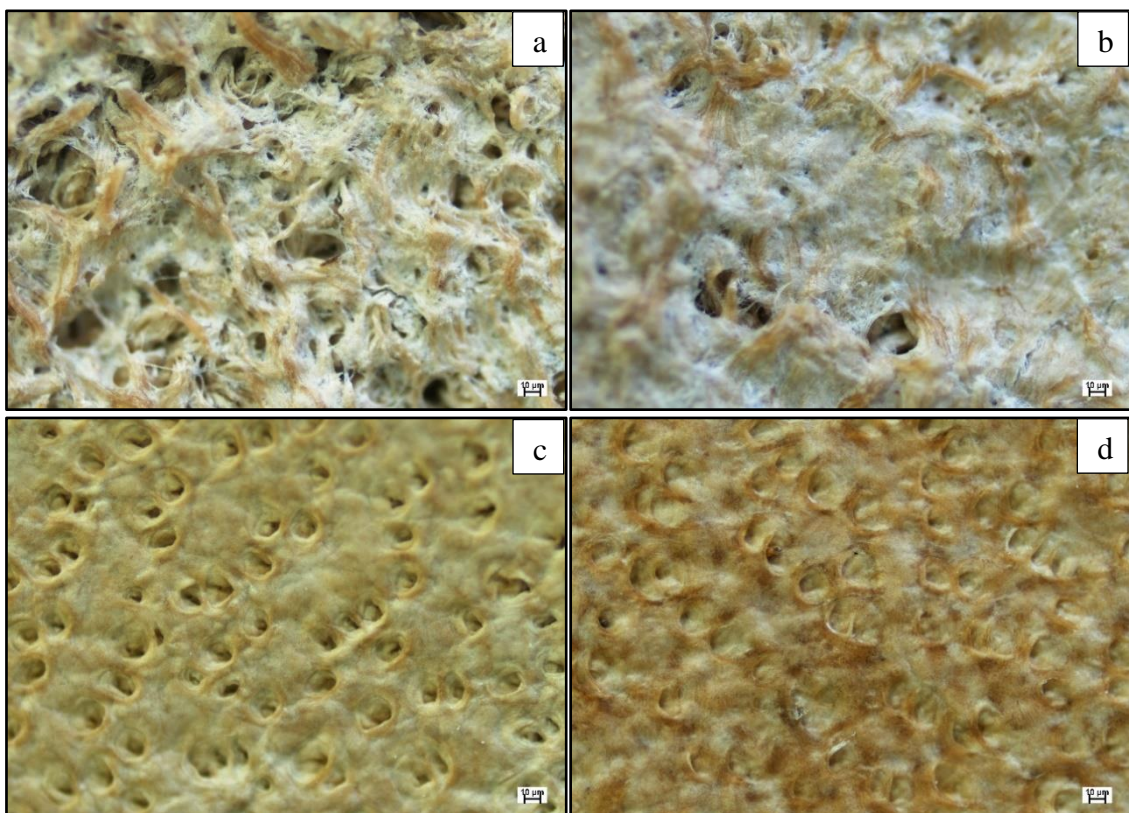


Figure 14. Microscopic analysis of leather samples (with 40x magnification) treated with 15.0% mTG and 25.0% and 50.0%, respectively (a) and (b) for the flesh side and (c) and (d) for the grain side.

The regions of these amides are spread mostly on the sides of the spectrum. Amide A and B are normally located in the range of 3400 to 3000  $\text{cm}^{-1}$ . They are associated with the stretching vibrations of the hydrogen bonding of -OH ( $\nu_{\text{OH}}$ ) and -NH ( $\nu_{\text{NH}}$ ) groups with a carbonyl group of the peptide chain of collagen (Amirrah et al., 2022; Namba, 2020). On the opposite side, the amide I band is found between the frequencies of 1600 and 1800  $\text{cm}^{-1}$  showing the vibrations caused by the stretching of -C=O groups ( $\nu_{\text{C=O}}$ ) of amides in collagen's backbone structure (Riaz et al., 2018).

In the region of 1550 to 1300  $\text{cm}^{-1}$  the vibrations from the amide II band are exposed, which are characterized by the bending of -NH ( $\delta_{\text{NH}}$ ) groups and stretching vibrations of -CN groups ( $\nu_{\text{C-N}}$ ), and lastly, rounding the frequencies from 1250 to 1100  $\text{cm}^{-1}$ , the amide III bands represented by  $\delta_{\text{NH}}$ ,  $\nu_{\text{C-N}}$  and wagging vibrations of the -CH<sub>2</sub> groups ( $\omega_{\text{CH}_2}$ ) of glycine backbone and proline side chains are perceptible (Jiang et al., 2019; Sanden et al., 2019).

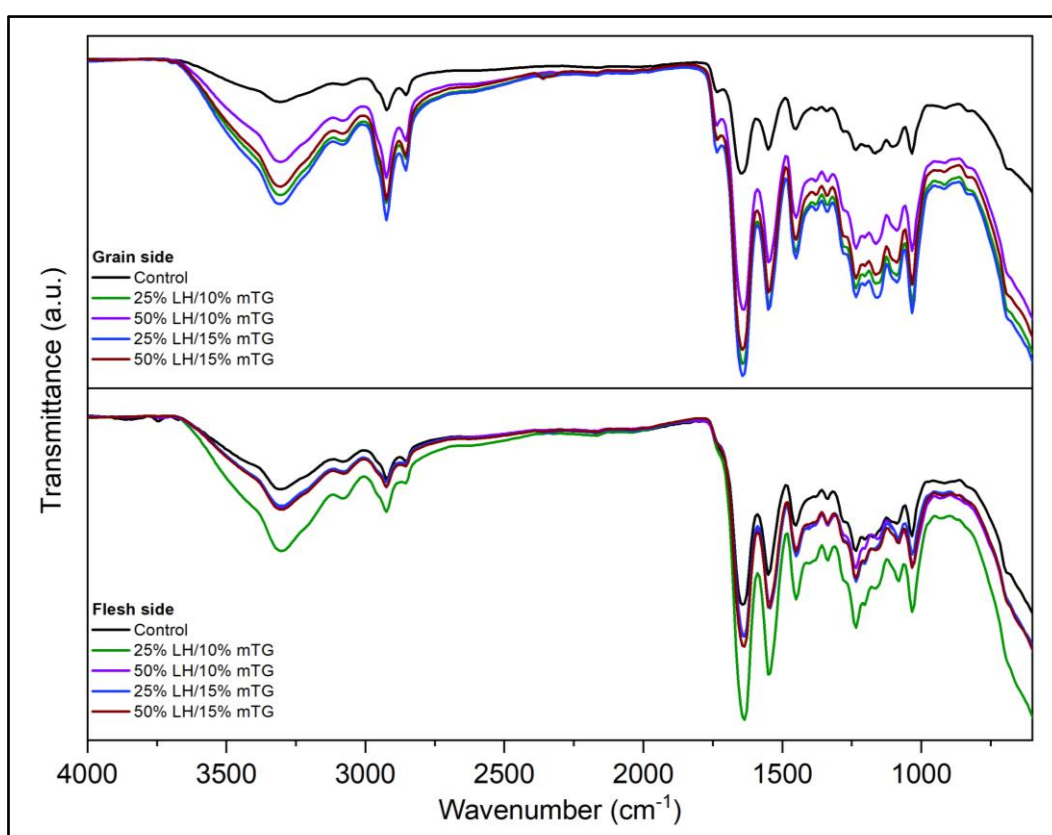


Figure 15. FTIR spectra of both sides of untreated leather (Control) and all treated samples.

The growth of all the amide bands intensity (amide A in 3308  $\text{cm}^{-1}$ , amide B in 3078  $\text{cm}^{-1}$ , amide I in 1642  $\text{cm}^{-1}$ , amide II in 1550  $\text{cm}^{-1}$  and amide III in 1234  $\text{cm}^{-1}$ ) in Figure 16 can be interpreted as an increase in the concentration of compounds that share the same chemical structure of the untreated leather sample (from now forward defined as Control), which is mainly collagen. Given the nature of the leather hydrolysate that was employed for the treatment (which derives from the leather that is being treated) is logical to assume that the proteins and amino acids incorporated share the same functional groups.

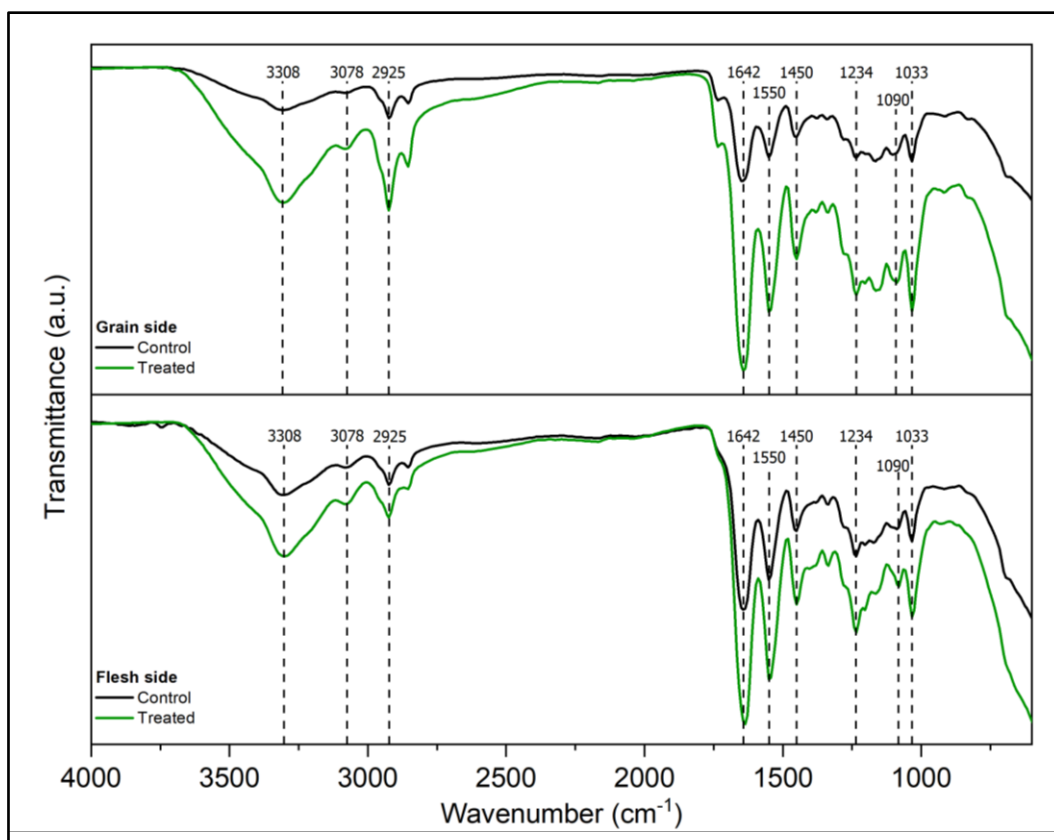


Figure 16. FTIR spectra of both sides of untreated leather (Control) and treated sample.

Besides the peaks in the amide bands, other regions also presented a noticeably higher percentage of transmittance. For instance, at  $2925\text{ cm}^{-1}$ , already reported by authors like Riaz et al. (2018) and Rabotyagova et al. (2008) as the anti-symmetrical stretching vibrations of the  $-\text{CH}_2$  component ( $\nu_{\text{asCH}_2}$ ) of glycine backbone and proline side chain of collagen molecules, while Sanden et al. (2019) specified that at  $1450\text{ cm}^{-1}$  is found the symmetrical bending vibrations of the same component ( $\delta_{\text{sCH}_2}$ ) (Rabotyagova et al., 2008; Riaz et al., 2018; Sanden et al., 2019).

The evident intensity rising at  $1090$ , and  $1033\text{ cm}^{-1}$  is rather interesting, given that this frequency is normally assigned to C-OH stretching vibrations of carbohydrates residues ( $\nu_{\text{C-OH}}$ ) associated collagen residues (Kittiphattanabawon et al., 2015). It could also be due to the detection of vibrations of functional groups of different amino acids that share a common range of wavenumbers, like the stretching vibrations of  $-\text{COC}$  groups ( $\nu_{\text{C-O}}$ ) of serine around  $1030\text{ cm}^{-1}$ , bending vibrations of hydrogen-bonded  $-\text{COH}$  groups ( $\delta_{\text{COH}}$ ) of aspartic and glutamic acid from  $1058$  to  $1540\text{ cm}^{-1}$ , or even  $\nu_{\text{C-N}}$  of histidine between  $1100$  and  $1090\text{ cm}^{-1}$ , all of which appear in higher quantities probably because these compounds were released during the leather hydrolysis and later stuck on the collagen's matrix of the sample (Barth, 2007; Riaz et al., 2018).

The subtle changes in the chemical structure of the leather components can be more evident applying the second-derivative procedure. This procedure is normally used to aid in visualizing secondary structures often hidden behind overlapped peaks in the FTIR spectrum (Namba, 2020; Zou & Ma, 2014). Given the initial spectrum presented in Figure 16, in the amide regions, there might exist overlapped peaks that are not visible to the naked eye; therefore, an analysis of the second derivative of the spectra of both sides

(flesh and grain side) of the sample was conducted. The list of the wavenumbers and the corresponding identified band assignment identified on the second-derivative analysis of the sample spectra are presented in Table 9.

Table 9. Infrared spectral characteristics of control and treated leather samples.

Region	Wavenumber (cm <sup>-1</sup> )				Band assignment
	Flesh side		Grain side		
	Control	Treated	Control	Treated	
Amide A	3309	3309	3309	3309	$\nu_{\text{NH}}$ , $\nu_{\text{OH}}$
	3201	3201	3201	3201	$\nu_{\text{NH}}$
Amide B	3075	3075	3075	3075	$\nu_{\text{C-N}}$
	2939	2939	2938	2938	$\nu_{\text{asCH}_2}$
	2910	2910	2908	2908	
Amide I	1650	1650	1650	1650	$\nu_{\text{C=O}}$ , $\nu_{\text{NH}}$
Amide II	1542	1532	1543	1534	$\nu_{\text{C-N}}$ , $\delta_{\text{NH}}$
	1427	1419	1427	1427	$\nu_{\text{sC=O}}$ , $\delta_{\text{sCH}_2}$
	1335	1356	1334	1334	$\omega_{\text{CH}_2}$
Amide III	1234	1234	1249	1242	$\nu_{\text{C-N}}$ , $\delta_{\text{NH}}$
	1202	1202	1195	1195	$\omega_{\text{CH}_2}$ , $\delta_{\text{COH}}$
	1134	1134	1134	1134	$\nu_{\text{C-O}}$ , $\nu_{\text{C-OH}}$
	1050	1041	1050	1050	$\nu_{\text{C-O}}$

Examining the spectrum flesh side's second-derivative (Figure 17), the peak pointed out at 3308 cm<sup>-1</sup> in the amide A region of the FTIR spectra is a product of the overlapping of the peaks at 3309 and 3201 cm<sup>-1</sup>, where the  $\nu_{\text{OH}}$  and  $\nu_{\text{NH}}$  are slightly better distinguishable. The intensity at the former wavenumbers increases in both peaks, indicating an augmentation in -NH groups bounding. This supposition is further reinforced by the rise in the peak at the amide B band (now at 3075 cm<sup>-1</sup>), which denotes higher activity regarding  $\nu_{\text{C-N}}$ . The interaction between -CN groups with the backbone structure of collagen seems to be stronger given the transmittance increase at 2939 and 2910 cm<sup>-1</sup>, which can be interpreted as the formation of hydrogen bonds between amide groups and collagen molecules.

The former peak in the amide I band at 1642 cm<sup>-1</sup> is now located at 1650 cm<sup>-1</sup> and displays an intensity growth, suggesting more carboxamide interactions of  $\nu_{\text{C=O}}$  and  $\nu_{\text{NH}}$ . This is verified in the amide II band, where the former peak (initially at 1550 cm<sup>-1</sup> but relocated at 1542 cm<sup>-1</sup> in the second-derivative spectra) has now been enhanced and shifted 10 cm<sup>-1</sup> towards a lower wavenumber magnitude, denoting greater interactions of  $\nu_{\text{C-N}}$  and  $\delta_{\text{NH}}$ . A similar shift is found in the following peak at 1481 cm<sup>-1</sup>, that after the treatment, it has decreased even further and reached its end at 1473 cm<sup>-1</sup>, possibly due to the interactions that carbonyl groups had in the cross-linking reaction.

The peak previously identified at 1450 cm<sup>-1</sup> has shifted to 1427 cm<sup>-1</sup>, later dropping 8 cm<sup>-1</sup> from its original location with higher intensity. A shift towards a higher wavenumber is noticeable from 1335 to 1356 cm<sup>-1</sup>, slightly increasing its former intensity and bringing the two last bands closer, suggesting a higher degree of collagen chain arrangement due to interactions between  $\nu_{\text{sC=O}}$ ,  $\omega_{\text{CH}_2}$  and  $\delta_{\text{sCH}_2}$ . Finally, in the amide III bands,  $\nu_{\text{C-O}}$ ,  $\nu_{\text{C-N}}$ , and  $\delta_{\text{NH}}$  appear to have grown at 1234 and 1202 cm<sup>-1</sup> with an intensity

increase registered. The transmittance reduction that takes place at  $1134\text{ cm}^{-1}$  can be understood as an increase in the vibration caused by the  $-\text{CH}_2$  components of collagen molecules, hinting at a less arranged packing of the collagen fibers. Lastly, an intensity increase, and a wavenumber shift from  $1050\text{ cm}^{-1}$  to  $1041\text{ cm}^{-1}$  was registered.

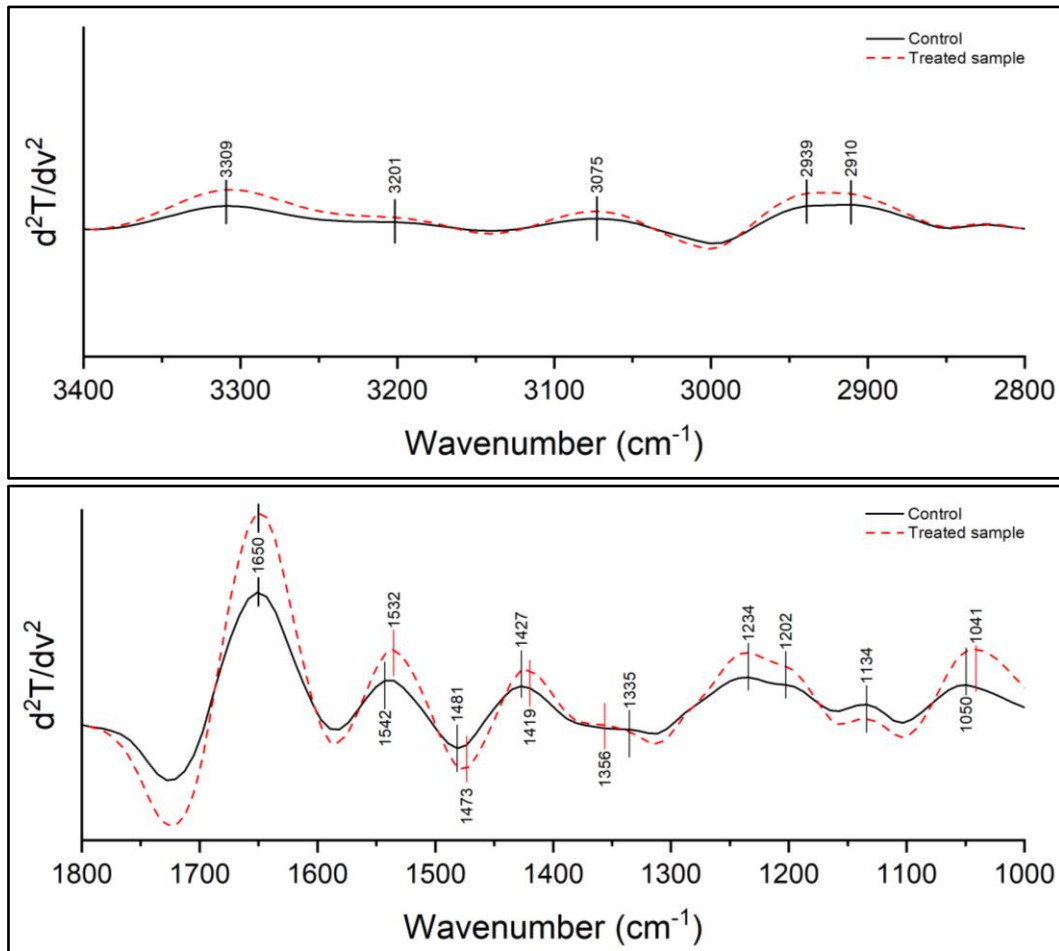


Figure 17. Second-derivative spectra of flesh side of control and treated sample.

Similar to the pattern displayed in the spectrum on the flesh side of the treated sample, the grain side (Figure 18) presents a much higher difference regarding peak intensity between the control and the treated samples. It is likely that given the size of collagen fibers on the grain side (much thinner when compared to the flesh side), the resultant superficial area available for reaction with mTG lead to much more intense development of cross-links.

When Staroszczyk et al. (2012) analyzed the effect of mTG on the structure of cod gelatin films, they noticed a similar pattern in the amide A, B, I, II, and III bands regarding peak intensity variations. However, these growths in the intensities were accompanied by shifts in the wavenumbers of the peaks in the amide A, B, and I bands towards lower magnitudes. The authors point out that as a consequence of mTG-catalyzed cross-linking, the intensity increment on the amide I band is expected to be much larger than on the amide II since the interactions of  $-\text{NH}_2$  free groups are reduced due to their change to  $-\text{NH}$  groups after the cross-linking, strengthening  $\nu_{\text{C=O}}$  and  $\nu_{\text{NH}}$  interactions (Staroszczyk et al., 2012).

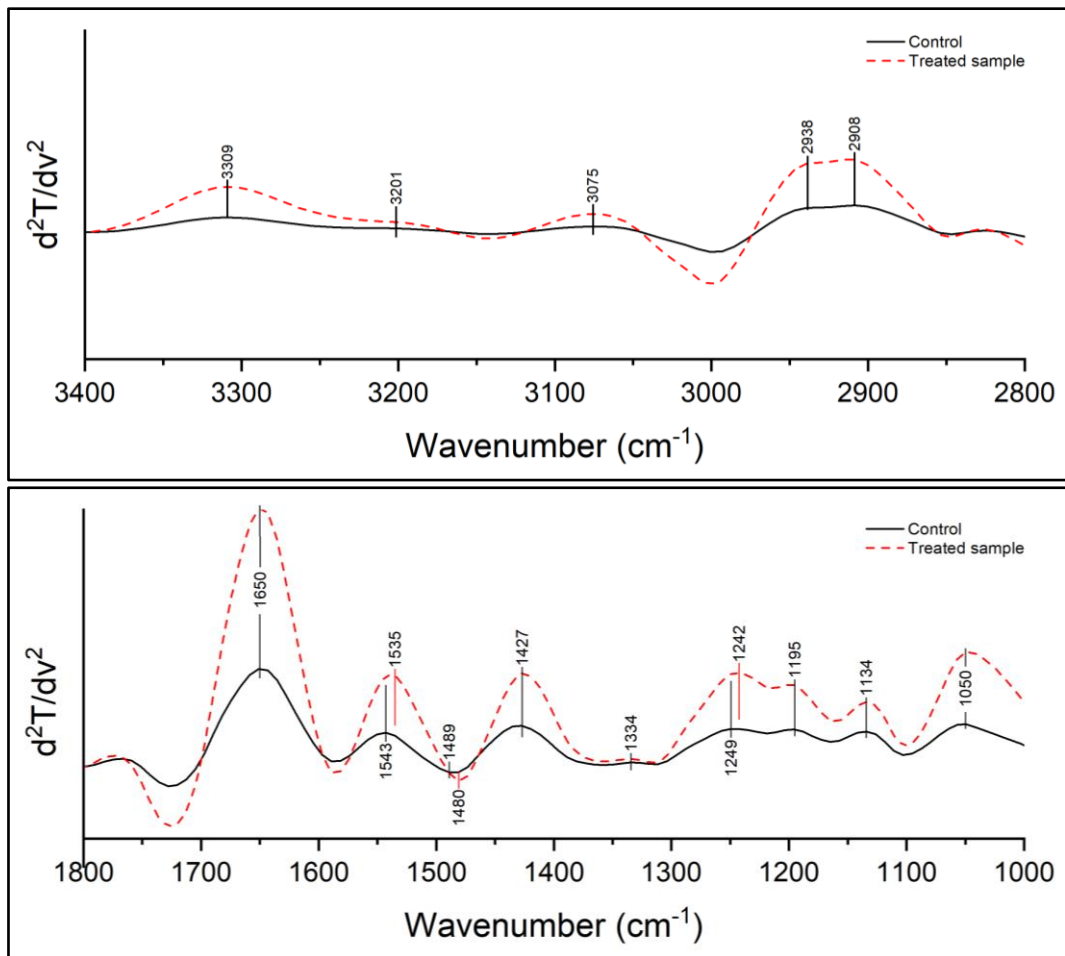


Figure 18. Second-derivative spectra of grain side of control and treated sample.

The study conducted by Jiang et al. (2019) reported a similar behavior in the amide A and B bands, which were widened after introducing mTG to a collagen solution at pH 7, indicating that this change could have been originated from the inter and intramolecular covalent bonds among collagen molecules. Further analyses confirmed this assumption, and they concluded that at these conditions (pH 7, 25 °C, 10 to 80 active units/g of acid-soluble collagen, and 6 hours of reaction), the production of collagen-based material with properties of self-aggregation of collagen is possible (Jiang et al., 2019).

The intensity variations observed by Cheng et al. (2019) are consistent with the ones presented in this work, where amide bands of FTIR spectra of collagen-based solutions are enhanced after the introduction of mTG. The authors highlighted that enzyme accessibility and collagens' structural integrity are important factors in the cross-linking efficiency of mTG (Cheng et al., 2019). On the other hand, Namba (2020) who developed chitosan-gelatin-based particles with enzyme (mTG) induced cross-linking, noticed in the FTIR analysis the increase of the peaks intensity in the amide regions, arguing that the reason for this growth is found in the formation of isopeptide bonds catalyzed by mTG (Namba, 2020).

Thus, the increment in all the amide peaks can be interpreted as a result of the successful incorporation of leather hydrolysate into the collagen matrix of the leather samples, where isopeptide bonds were formed by the effect of mTG. However, further studies are needed to confirm if the cross-links were established between the leather hydrolysate amino acids and the collagen fibers of the leather sample.

A series of analyses were carried out to end the screening test and select one combination of additives to deepen the study of its effect on leather properties. Four samples of leather, each one treated with the combination of additives C<sub>1</sub>, C<sub>2</sub>, C<sub>3</sub>, and C<sub>4</sub> (described in Table 10), were sent to the facilities of the Footwear Technological Centre of Portugal (CTCP in Portuguese) to perform organoleptic analyses and physical evaluation before and after processing (results detailed in Table 11), and mechanical testing of treated samples such as the flex resistance test in accordance with the specifications detailed in the standard ISO 5402-1:2017. SEM analysis was also conducted on the samples before and after the mechanical testing (presented in Table 13) to access the morphological changes distinguishable in leather.

Table 10. Combination of additives delivered for organoleptic analysis, physical evaluation, and mechanical testing.

<b>Combination</b>	<b>Filler</b>	<b>Binder</b>
C <sub>1</sub>	0.2% expandable microspheres	20.0% WPB
C <sub>2</sub>	0.7% glass microspheres	20.0% WPB
C <sub>3</sub>	4.0% nanoclay particles	20.0% WPB
C <sub>4</sub>	25.0% wet-white leather hydrolysate	10.0% mTG

The flex resistance test is normally employed to evaluate the durability of leather, particularly in the footwear industry. It evaluates the deterioration of the leather surface before and after repetitive flexing cycles that recreate a leather item's life cycle (Maina et al., 2019; Meyer et al., 2021). The results of the flex-resistant test are summarized in Table 12, where the grade indicates the visible presence of wrinkles and cracks, grading with 0 to a material free of cracks and wrinkles, grade of 2 or less to the presence of very small cracks and wrinkles in the grain layer, and grades higher than 2 for leathers considered not suitable or of insufficient quality for the footwear industry.

Analyzing the results in Table 11, it can be argued that the higher compaction of the leather in C<sub>1</sub>, C<sub>2</sub>, and C<sub>3</sub> treatments may have been caused by the hardening of collagen fibers due to the WPB coating, limiting the free movement of the fibers and wrapping the fibers and bundles of fibers, which increases the thickness of the material. In contrast, the rougher ending over the leather surface may result from an uneven dispersion of WPB. Furthermore, Correa Brito (2012) mentions that the lower the solid concentration in resins applied in leather coating processes, the higher the resin penetration into the leather matrix. It also describes how the treatment time could be an influencing factor in these types of treatment, indicating that with longer periods, a deeper penetration is achieved (Correa Brito, 2012). Considering these factors, it is possible that the WPB had not reach a deep penetration level under the set conditions for the treatment (observable in Table 13), causing a rougher feeling on the leather surface.

Table 11. Summary of the organoleptic analyses and physical evaluation of samples treated with the selected additives.

<b>Combination</b>	<b>Organoleptic analysis results</b>	<b>Physical measurements results</b>
C <sub>1</sub>	Slightly rougher to the touch and mildly more compact Small reduction of visible defects <sup>†</sup>	No significant dimensional changes Weight reduction of 17.5%
C <sub>2</sub>	Notably rougher to the touch and more compact Small reduction of visible defects <sup>†</sup>	Significant thickness increase and superficial area contraction Weight increase of 5.0%
C <sub>3</sub>	Notably rougher to the touch and more compact Small reduction of visible defects <sup>†</sup>	Significant thickness increase and superficial area contraction Weight increase of 7.4%
C <sub>4</sub>	Smother to touch Small reduction of visible defects <sup>†</sup>	Mildly thickness increase Weight reduction of 23.8%

<sup>†</sup> Defects such as scratches and scars on the leather surface.

In the case of C<sub>4</sub> treatment, the used temperature (50 °C) might be responsible for the leather thickness increase. Temperatures above 40 °C cause the destabilization of hydrogen bonds that maintain the helical structure of collagen molecules, leading to its gradual unfolding without getting cracked, distancing further the collagen molecules from each other (Cheng et al., 2019; Stachel et al., 2010). This opening allowed the penetration of the additives into the collagen structure, enhancing the reaction among the functional groups of the leather's collagen, free amino acids in solution, and mTG, thickening the final size of collagen molecules and, consequently, the fibers.

The smother sensation over the C<sub>4</sub> sample's surface was expected, considering that the addition of leather hydrolysate alone contributes to the filling effect on leather, enhancing the fullness of the produced leather (Dilek et al., 2019). Subjective evaluations performed by Taylor et al. (2010) in leather samples treated with a gelatin/whey protein isolate as the filler and mTG as the cross-linker agent, revealed an improvement in the fullness of the material, a property that is closely related to the smoothness (Taylor et al., 2010; Xiao et al., 2023).

In accordance with the objectives of this study, the minimization of leather defects can be achieved under the selected conditions and face to the results shown in Table 11; however, the degree of efficiency varies according to the treatment's main objective. If the end-user requires an improved yet lighter leather, C<sub>1</sub> and C<sub>4</sub> can be considered. Alternatively, if the leather is expected to be denser and rougher, then treatments C<sub>2</sub> and C<sub>3</sub> can be implemented. Although the application of the latter one may be considered problematic given that in the market, the value of a leather piece is established by many factors, some of them are useable area, area of defect, and sheet thickness, which all come into conflict with each other if C<sub>2</sub> and C<sub>3</sub> are integrated into the leather processing (S. Y. Chen et al., 2021; Jawahar et al., 2023).



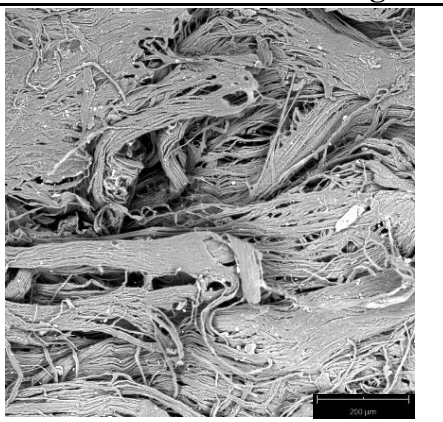
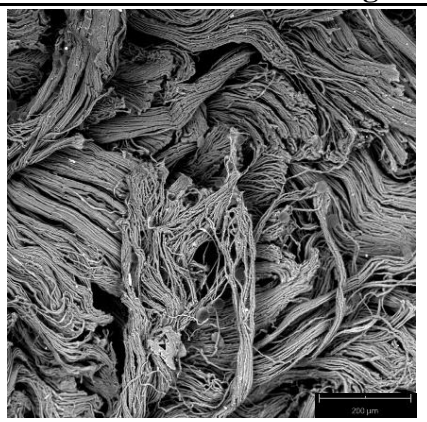
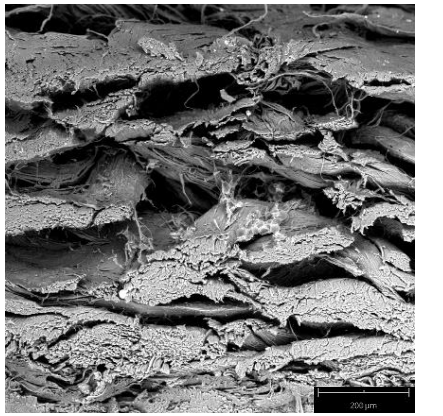
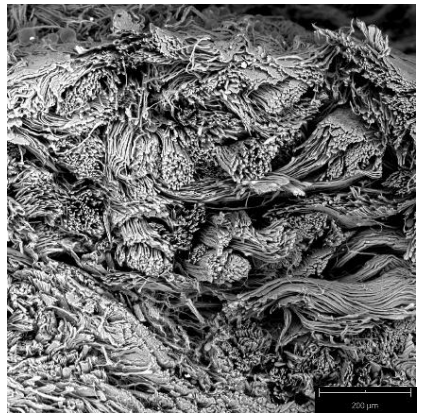
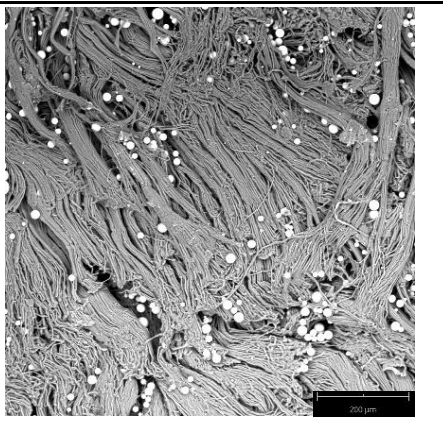
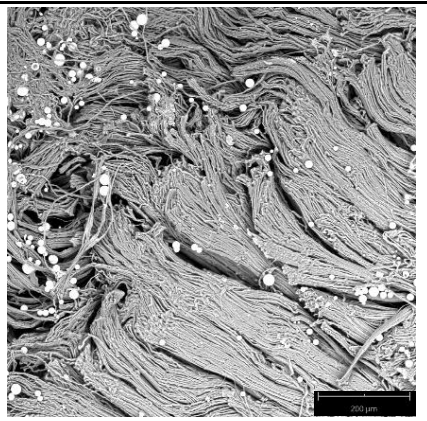
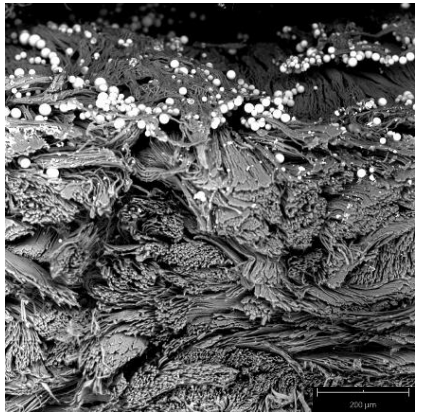
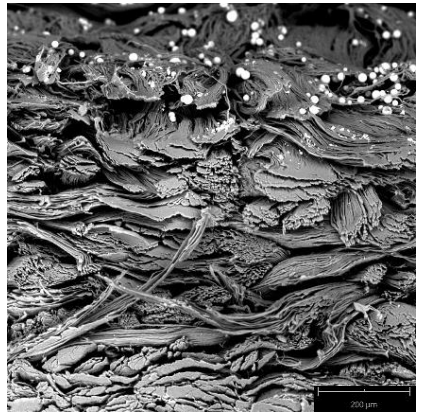
After comparing the results in Table 12, the sample treated with C<sub>4</sub> revealed a better performance than all the other combinations, demonstrating to be the most effective in superficial defect minimization (obtaining grade 1) and getting grade 2 after applying 100.000 flexing cycles. A common pattern was recognizable in the SEM images (presented in Table 13) taken after the flex resistance test when compared to their state before the test, consisting of a looseness of the fibers in all the samples, and a loss of filler material in cases C<sub>1</sub>, C<sub>2</sub>, and C<sub>3</sub>. The superficial area contraction reported on C<sub>2</sub> and C<sub>3</sub> treated samples is verified in the SEM images in Table 13, as it is distinguishable how the fibers and fiber bundles are much more compacted in comparison to C<sub>1</sub> and C<sub>4</sub>. The remarks made earlier support the mechanical test results, considering the information reported by Correa Brito (2012) and Tian et al. (2018).

Table 12. Performance results of treated samples in flex resistance test results.

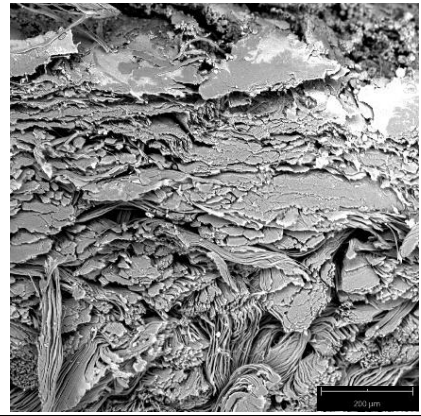
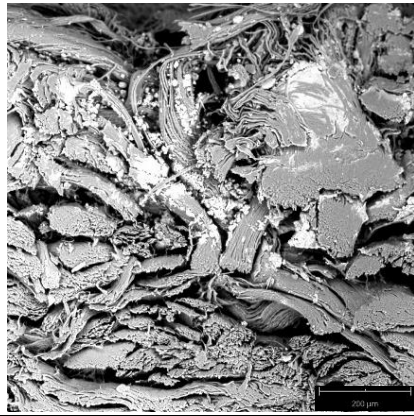
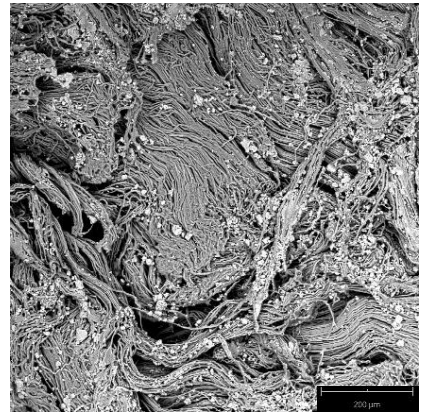
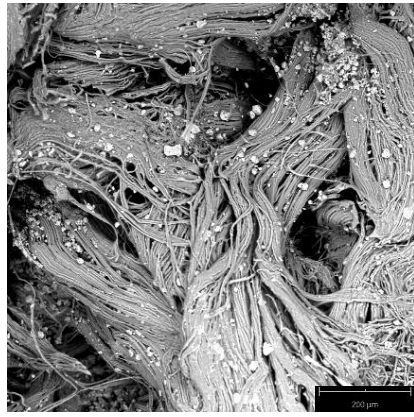
<b>Combination</b>	<b>C<sub>1</sub></b>	<b>C<sub>2</sub></b>	<b>C<sub>3</sub></b>	<b>C<sub>4</sub></b>
Initial Wrinkle level	Grade 2	Grade 2	Grade 3	Grade 1
Wrinkle level after 100.000 cycles	Grade 3	Grade 3	Grade 4	Grade 2

The distribution of nanoclay particles throughout the corium layer of the leather, as perceptible in Table 13, resembles the description made by Prabakar et al. (2016) after analyzing TEM images of leather treated with 3.0% (w/w) of Cloisite Na<sup>+</sup> nanoclay. They mentioned how the particles tend to assemble around groups of fiber bundles as seen in the images of C<sub>3</sub> in Table 13 (Prabakar et al., 2016). The work of Sanchez-Olivares et al. (2014) suggested that at concentrations between 3.0 and 6.0% (w/w), nanoparticles of Cloisite Na<sup>+</sup> may produce stiffer products since they tend to occupy interfibrillar spaces in the collagen matrix of the leather, reinforcing it (Sanchez-Olivares et al., 2014).

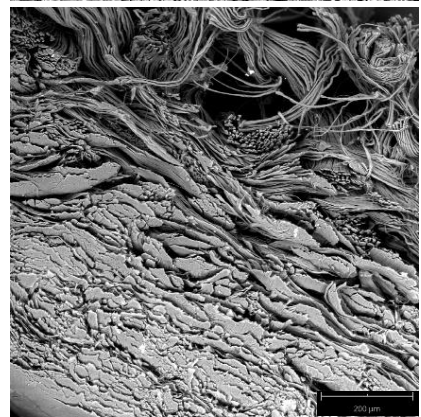
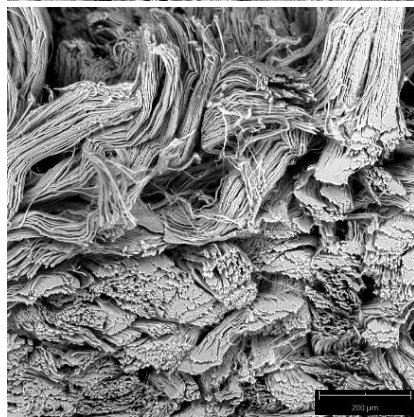
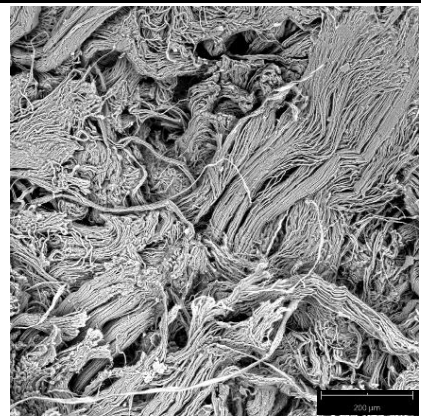
Table 13. SEM images of flesh side (up) and side view (down) of treated samples before and after the flex resistance test (with 300x magnification).

Combination	Before mechanical testing	After mechanical testing
C <sub>1</sub>		
		
C <sub>2</sub>		
		

C<sub>3</sub>



C<sub>4</sub>



#### 4.2. Design of experiments for the best combination

After analyzing the preliminary studies, the combination showing the best performance was chosen for a deeper study by employing a rotational central composite design  $2^2$  with 3 central points. Particularizing, the final results of the screening test indicated that combination C<sub>4</sub>, i.e., the one using leather hydrolysate and mTG, is the most favorable by minimizing the leather's superficial defects and proving a lesser level of attrition after mechanical testing. To continue with the evaluation of the effects of the additives on the leather defects, the variables of the study were redefined in a range of values that include the previously analyzed ones, in the hope of determining the most favorable amount of each additive for their incorporation in leather treatment at a larger scale. The percentages of leather hydrolysate per gram of leather and the percentage of mTG per gram of hydrolysate were selected in a range of 15.0 to 45.0% and 5.0 to 15.0%, respectively.

Quantitative methods were employed to aid in the leather's defects minimization measurements, setting as the response variables the maximum tensile strength (MPa), elongation percentage at maximum stress (%), and Young's modulus (MPa). These parameters are associated with the quality of the leather allowing to assess if an improvement was achieved in the leather's integrity (Liu et al., 2009; Ma & Lu, 2008; Nalyanya, Rop, Onyuka, Birech, & Sasia, 2018). Other parameters such as thickness, fiber diameter, and orientation index were considered as constant.

The experimental procedure followed is detailed in section 3.2. of this work, and the experimental matrix is shown in Table 14. The mechanical properties of the treated samples were measured according to the methodology described in section 3.3.1. and are presented in Table 15.

Table 14. Experimental matrix of the rotational central composite design  $2^2$  with 3 central points.

Assay	Coded values		Real values	
	Leather Hydrolysate	mTG	Leather Hydrolysate (% OLW)	mTG (% OHW)
1	-1	-1	15	5
2	1	-1	45	5
3	-1	1	15	15
4	1	1	45	15
5	- $\alpha$	0	8.786	10
6	+ $\alpha$	0	51.213	10
7	0	- $\alpha$	30	2.928
8	0	+ $\alpha$	30	17.071
9	0	0	30	10
10	0	0	30	10
11	0	0	30	10

OLW= Over Leather Weight; OHW= Over Hydrolysate Weight; Value of  $\alpha = 1.41421$

The average values of the mechanical properties of untreated leather correspond to a maximum tensile strength of  $18.63 \pm 1.79$  MPa, an elongation percentage at maximum tension of  $37.53 \pm 3.63\%$ , and Young's modulus of  $58.07 \pm 7.24$  MPa. In the selected study region, the elongation percentage is the response that proves to be improved the most, with the highest achieved value (60.31%) with 30.00% of leather hydrolysate and 17.07% of mTG, while the maximum tensile strength achieved was of 17.09 MPa after adding 51.21% of leather hydrolysate and 10.00% of mTG. The Young's modulus's lowest recorded value was 32.73 MPa, while the highest was 59.14 MPa.

It is important to point out that the standard deviation of each run was considerably high. This is understandable considering that leather is a natural material without a fixed composition. Other factors like its anisotropic nature, its chemical composition (linked to the chemical treatment selected for its processing), and the type, and severity of the defect on the structure and surface of the material, among other factors might affect the mechanical properties of the material (Ali et al., 2020; Z. Li et al., 2009; Sizeland et al., 2015). Figures 19, 20, and 23 show the divergence from a normal distribution of values obtained in measuring the mechanical properties in each run. In said figures, the HT initials (hydrolysate + mTG) represent each assay condition.

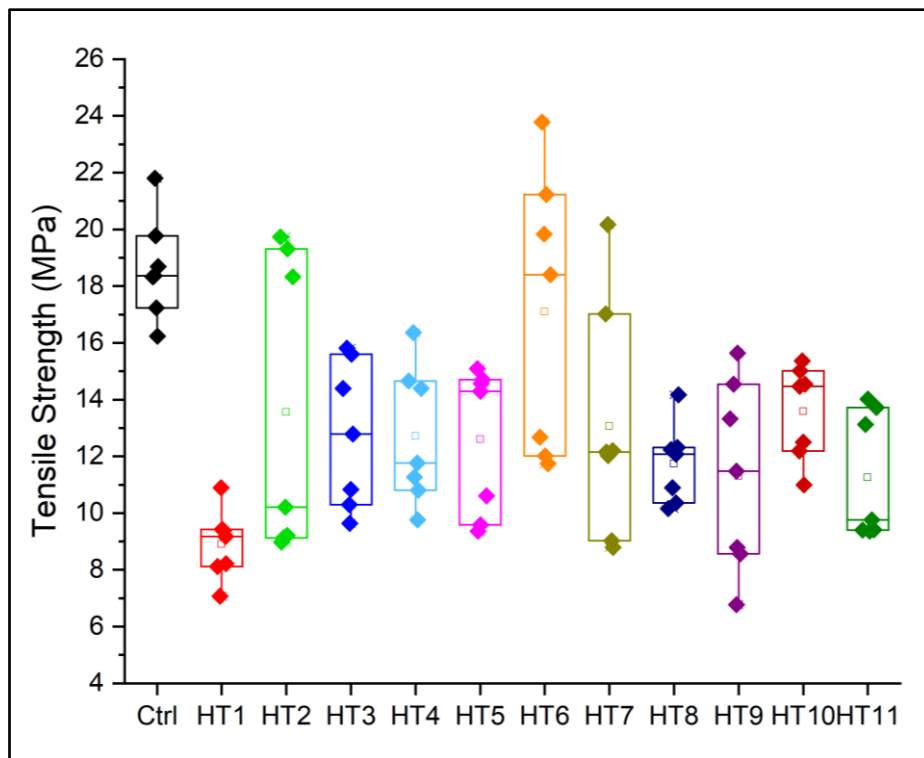


Figure 19. Distribution of tensile strength values recorded for each run.

When Wells et al. (2013) studied the correlation between collagen fibril diameter, degree of alignment, and leather strength, they found that there is a relationship between the fibril diameter of bovine leather and its tear strength (related to the tensile strength). Furthermore, they concluded that in highly aligned fibrils, the diameter of fibers is more significant in their final strength, yet in tissues with no fibril alignment, the influence of the degree of alignment is greater than the fibril's diameter on the strength of the material. The authors also implied that the animal's age may play a role in fibril's diameter

distribution on bovine leather since this factor was related to the variations of their tear strength recordings (Wells et al., 2013).

The slight thickness increase mentioned in Table 11 can translate into richer and more compact fibrils and fiber bundle structures. Wells et al. (2016) reported that leather with tighter fiber packing tends to present a lower tensile strength. Additionally, they proved that an excessive fibril alignment can lead to a loose fiber packaging, which increases the tensile strength of the leather (Wells et al., 2016). Additionally, Sizeland et al. (2015) indicated that a change in fiber alignment is associated with a variation in the thickness of the leather, possibly affecting the material's tensile strength (Sizeland et al., 2015).

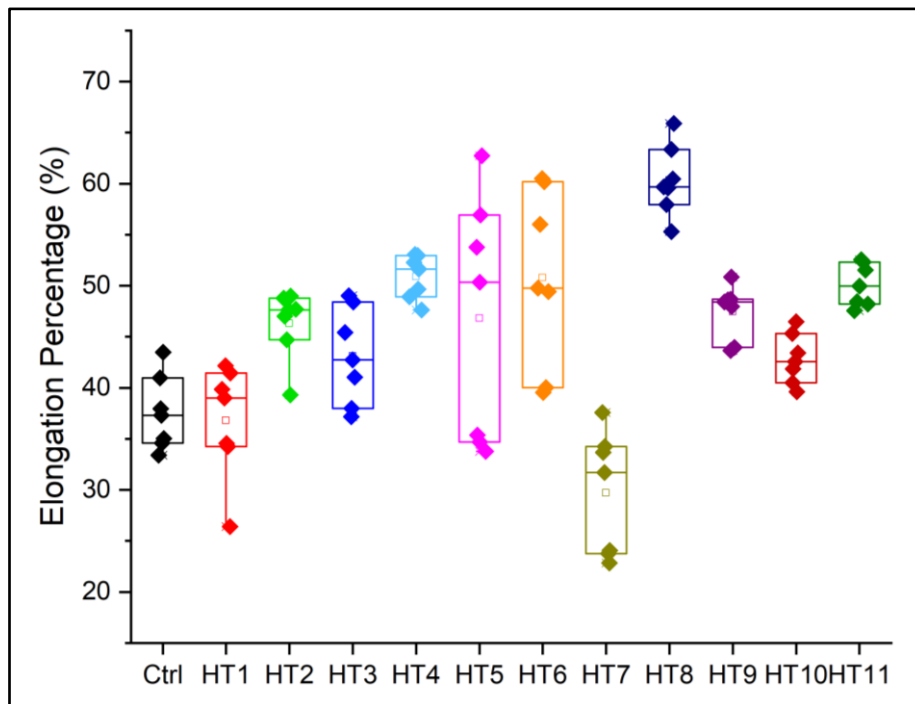


Figure 20. Distribution of elongation percentage values recorded for each run.

The degree to which fibers are aligned bears a relation with the elasticity of the fibers, and, subsequently, with the elongation percentage of leather. The way in which the collagen fibers are stretched was initially described by Fratzl et al. (1997), indicating how the stretching of leather can be divided into 2 phases, the straightening of the unaligned fibers, and then the stretching of all aligned fibers as well as the previously unaligned fibers (Fratzl et al., 1997). This stretching process was confirmed later on by Yang (2008) and Sizeland et al. (2015), adding that leathers submitted to cross-linking processes are likely to develop a decrease in the alignment of their fibers and a thickness increase, a change that is evident in Table 11 (Sizeland et al., 2015; Yang, 2008).

This stretching process is demonstrated in the SEM images taken of the samples before and after subjected to the tensile strength test presented in Figure 21. It can be seen how, before the stretching, there exist fibers and bundles of fibers with a certain degree of alignment, but most of them do not follow a specific direction, while after the stretching, the fibers and bundle of fibers are more straightened in the direction where the stress was applied.

One of the characteristics of collagen fibers is their viscoelastic nature, which allows them to stretch elastically under stress until the breakage point. Li et al. (2009) depicted how the layers of leather may assume different rheologic behaviors, associating the grain layer to the non-linear region of the leathers' tensile strength/elongation percentage graph (known as the strain/stress curve presented in Figure 22) given its similarity to a viscoelastic solid with high viscosity, while the corium layer (flesh side) is responsible for the linear region of the stress/strain curve since the fibers in this area resemble an elastic solid with low viscosity (Jeyapalina, 2004; Z. Li et al., 2009).

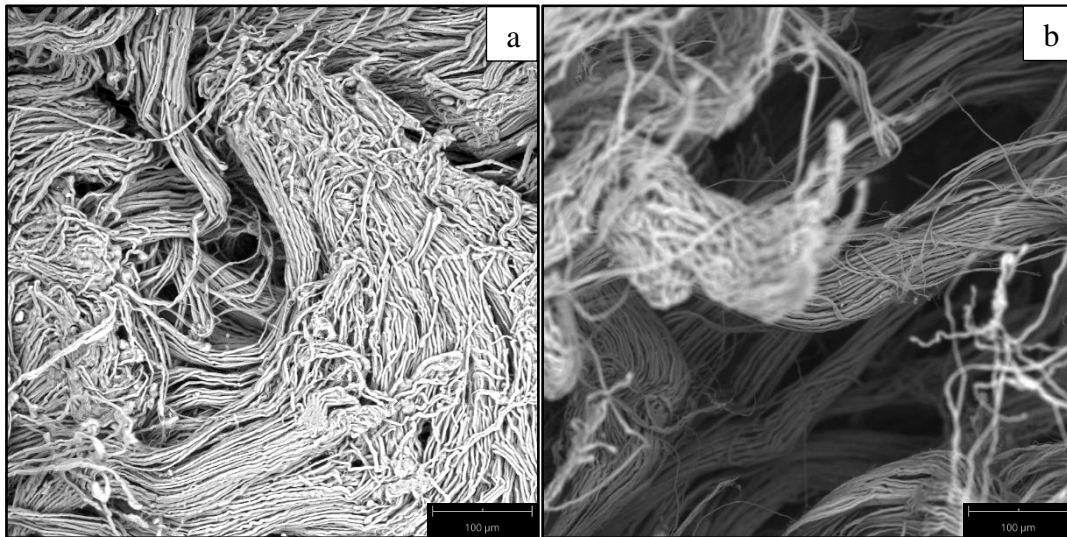


Figure 21. SEM images (with 500x magnification) of the flesh side of treated samples (a) before and (b) after mechanical stretching.

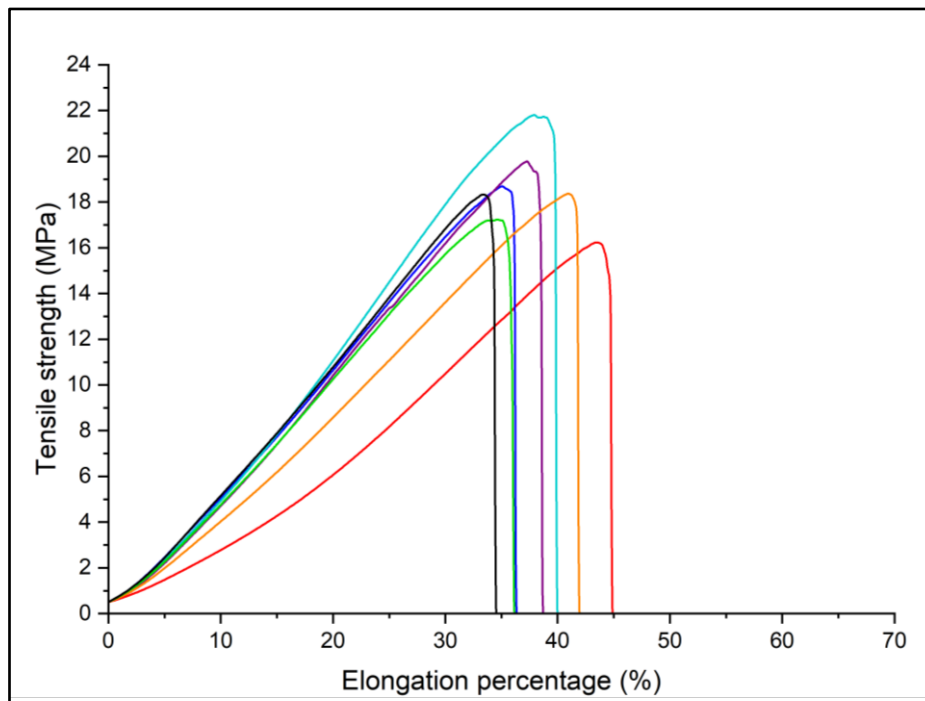


Figure 22. Stress/strain curve of untreated leather samples.

Young's modulus can be defined as the amount of force by area that is needed to produce an elastic deformation in a material. The elastic deformation of leather was described by Ma & Lu (2008) as a measure of the material rigidity, pointing out that the

lower the value of Young's modulus is, the more elastic the material becomes, indicating that a reversible deformation only requires small amounts of strength to reach a specific deformation percentage (Ma & Lu, 2008).

Among the factors that influence Young's modulus, the initial cross-section area of the material being put under stress and the force applied to it has been named. A variation in leather dimensions is likely to cause an impact on the measurement of tensile strength and Young's modulus values (Yang, 2008). This is reflected in the results obtained for the response variables, leading to an increase in systematic errors and affecting the final values of this work.

The divergence between the recorded values has been observed as something that frequently occurs in the measurement of mechanical properties of leather; therefore, it is reasonable to suggest that the variation in the response values presented in this work could also be explained if parameters such as fibril alignment, fibrils diameter, and overall dimensional changes were taken into account. Atmospheric factors such as humidity and temperature also affect the mechanical properties of leather, although, these were kept constant to the possible extent.

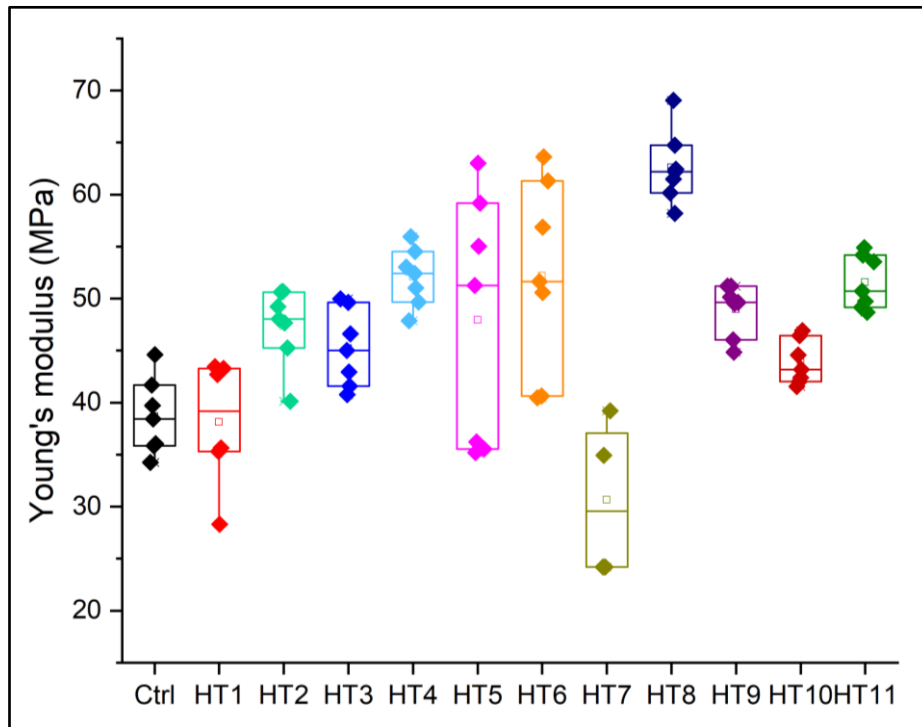


Figure 23. Distribution of Young's modulus values recorded for each run.

The addition of leather hydrolysate as a filler agent and mTG as a cross-linking agent was not found in the literature during this work's development; therefore, comparing the values obtained from the proposed leather treatment results is troublesome. Nevertheless, it has been found that leather hydrolysate was incorporated on collagen-based materials, as tanning or filler agents, with other cross-linkers. Moreover, mTG as a cross-linker has been employed with different filler agents. These studies will be used as a reference to discuss the results of this work.



Table 15. Mechanical properties of treated leather according to the experimental matrix.

Assay	Coded values		Real values				
	LH	mTG	LH (% OLW)	mTG (% OHW)	Tensile Strength (MPa)	Elongation Percentage (%)	Young's Modulus (MPa)
1	-1	-1	15	5	8.89 ± 1.22	36.80 ± 5.54	34.41 ± 7.11
2	1	-1	45	5	13.55 ± 5.24	46.29 ± 3.39	45.86 ± 13.17
3	-1	1	15	15	12.76 ± 2.57	43.10 ± 4.73	42.25 ± 2.15
4	1	1	45	15	12.72 ± 2.42	50.87 ± 2.14	37.06 ± 6.24
5	-α	0	8.786	10	12.60 ± 2.61	46.80 ± 12.00	40.12 ± 3.68
6	+α	0	51.213	10	17.09 ± 4.91	50.78 ± 8.71	48.62 ± 11.11
7	0	-α	30	2.928	13.05 ± 4.15	29.69 ± 6.00	59.14 ± 19.06
8	0	+α	30	17.071	11.74 ± 1.39	60.31 ± 3.46	34.56 ± 3.36
9	0	0	30	10	11.30 ± 3.36	47.44 ± 2.64	36.43 ± 6.33
10	0	0	30	10	13.58 ± 1.67	42.81 ± 2.46	43.60 ± 5.11
11	0	0	30	10	11.25 ± 2.23	50.07 ± 2.06	32.73 ± 3.36

LH= Leather hydrolysate.

After analyzing the values in Table 15, the lower the quantity of leather hydrolysate and mTG incorporated in the leather, the lower the tensile strength and elongation percentage values. Regarding Young's modulus values, a reduction seems to be attained under most of the considered conditions. An analysis of variance (ANOVA) of the effect of the added amounts of leather hydrolysate and mTG on the evaluated leather mechanical properties was conducted.

While examining the central point values of the response variables in Table 15, it has been noticed a considerable standard deviation among them, being small in the tensile strength variable (1.32), then higher in the elongation percentage (3.67), and finally greater in Young's modulus (5.52). These deviations indicate a lack of reproducibility of the experimental design under the selected conditions.

Table 16 revealed that among all the factors and their correlations, only the concentration of leather hydrolysate significantly influences the tensile strength of leather. As a result, this gave a quadratic model with a value of  $p > 0.05$ , which indicates that the model is not significant when calculating the tensile strength values inside the studied region. Thus, another ANOVA was conducted considering a linear approach by reducing unnecessary terms for the analysis (terms with  $p$  values much greater than 0.05).

Analyzing Table 17, it can be seen that a significantly reduced linear model is achieved considering only the percentage of leather hydrolysate per gram of leather weight as the influencing factor in the material's tensile strength. The model also demonstrates a not significant lack of fit; however, the new correlation coefficient ( $R^2$ ) is only 37.32%, while the predicted  $R^2$  is -13.72%. These parameters indicate that the resultant model is not recommended to predict values of tensile strength inside the studied region, yet the experimental values adjust with a 37.32% of precision to the values calculated with the mathematical model.

Table 16. ANOVA of additives influence over the maximum tensile strength considering a quadratic model.

<b>Factors</b>	<b>SS</b>	<b>DF</b>	<b>MS</b>	<b>F-value</b>	<b>p-value</b>	
<b>Model</b>	27.99	5	5.60	2.28	0.193	not significant
A-Leather hydrolysate	15.02	1	15.02	6.12	0.056	
B-Transglutaminase	0.172	1	0.172	0.070	0.801	
AB	5.54	1	5.54	2.26	0.193	
A <sup>2</sup>	5.55	1	5.55	2.26	0.193	
B <sup>2</sup>	0.307	1	0.307	0.125	0.739	
<b>Residual</b>	12.27	5	2.45			
Lack of Fit	8.74	3	2.91	1.65	0.3989	not significant
Pure Error	3.53	2	1.77			
<b>Total</b>	40.26	10				
<b>Std. Dev.</b>	1.57		<b>R<sup>2</sup></b>		0.6952	
<b>Mean</b>	12.60		<b>Adjusted R<sup>2</sup></b>		0.3905	
<b>C.V. %</b>	12.44		<b>Predicted R<sup>2</sup></b>		-0.7409	
			<b>Adeq Precision</b>		5.0620	

SS= Sum of Squares; DF= Degrees of Freedom; MS= Mean Square; Std. Dev.= Standard Deviation; Adeq= Adequate; C.V. %= Coefficient of Variation.

Table 17. ANOVA of additives influence over the maximum tensile strength considering a reduced linear model.

<b>Factors</b>	<b>SS</b>	<b>DF</b>	<b>MS</b>	<b>F-value</b>	<b>p-value</b>	
<b>Model</b>	15.02	1	15.02	5.36	0.0459	significant
A-Leather hydrolysate	15.02	1	15.02	5.36	0.0459	
<b>Residual</b>	25.24	9	2.80			
Lack of Fit	21.71	7	3.10	1.76	0.4099	not significant
Pure Error	3.53	2	1.77			
<b>Total</b>	40.26	10				
<b>Std. Dev.</b>	1.67		<b>R<sup>2</sup></b>		0.3732	
<b>Mean</b>	12.60		<b>Adjusted R<sup>2</sup></b>		0.3035	
<b>C.V. %</b>	13.29		<b>Predicted R<sup>2</sup></b>		-0.1372	
			<b>Adeq Precision</b>		5.4285	

SS= Sum of Squares; DF= Degrees of Freedom; MS= Mean Square; Std. Dev.= Standard Deviation; Adeq= Adequate; C.V. %= Coefficient of Variation.

In Figure 24 it can be verified the scarce correlation between the experimental values and the estimated values obtained from the reduced linear model from Table 17. The equation of the mentioned model is presented in Equation 2. The magnitude of the coefficient related to the leather hydrolysate variable (0.09) proves the reduced influence of leather hydrolysate (A in Equation 2) over the tensile strength inside the studied region.

The influence of the leather hydrolysate over the leather tensile strength is illustrated in the response surface presented in Figure 25.

$$TS \text{ (MPa)} = 9.85 + 0.09 A \quad (2)$$

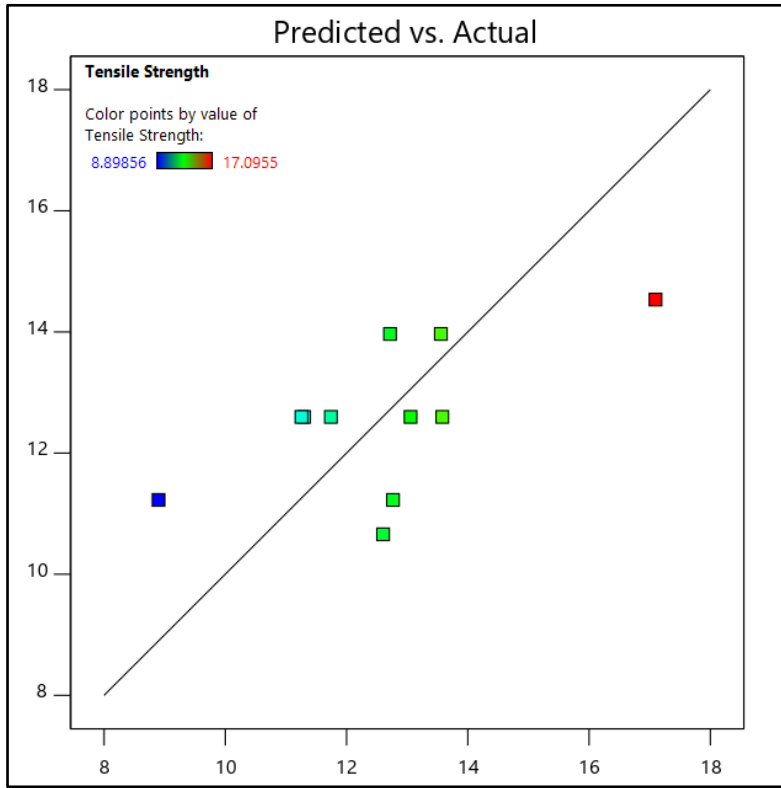


Figure 24. Relation between experimental and estimated values based on the reduced linear model for tensile strength.

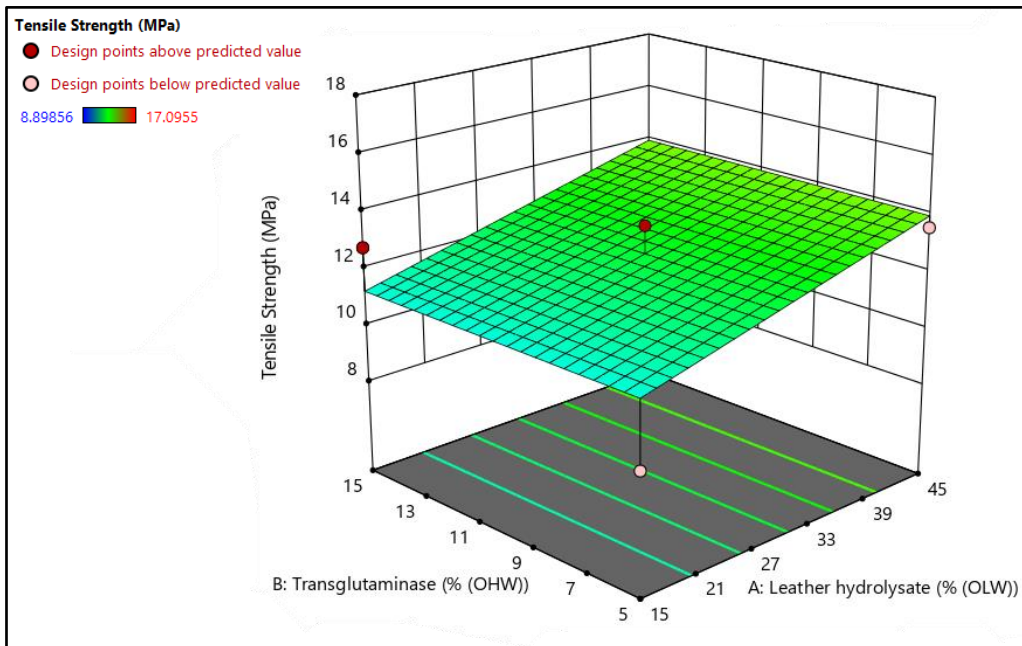


Figure 25. Generated response surface of the effect of the factors over the tensile strength inside the studied region based on the reduced linear model.

Taylor et al. (2010) analyzed if an improvement could be achieved in the mechanical properties of leather when treated with combinations of 5 to 7.5% (w/w) of gelatin and 1 to 2% (w/w) of whey protein isolate as fillers with 5% (w/w) of mTG as a cross-linking agent at pH 6.8. These additives were tested on different leather pieces, namely the butt, belly, and neck area, since, according to the literature, the fiber orientation and diameter vary. Their results indicated that the tensile strength was mildly improved in some areas, while the effect was the opposite in others. They concluded that no significant difference was found between their control pieces and test samples (Taylor et al., 2010).

Tensile strength was one parameter evaluated by Dilek et al. (2019) in their research focused on evaluating the capacity of leather hydrolysate when used as a tanning agent in dosages of 7, 10 and 15% (w/w). They noticed that with higher concentrations of leather hydrolysate, the tensile strength was enhanced by 55.26% of its initial value (leather without hydrolysate), attributing this improvement to the tendency of collagen hydrolysate to form stable bonds with collagen in the tanning process (Dilek et al., 2019).

The *p*-value of the quadratic model generated for the elongation percentage from the studied factors and the correlations in Table 18 proves to be not significant ( $p > 0.05$ ) for a 95% confidence level, indicating that this mathematical model is not suitable for estimating values inside the studied region. However, it points out the significant effect of the mTG concentration over the leather elongation percentage when the material is treated within the amounts studied in this work. A reduction of factors is needed to achieve a proper model to determine the response variable inside the studied region; thus, an ANOVA based on a lesser degree model was proposed.

Table 18. ANOVA of additives influence over the elongation percentage at maximum tension considering a quadratic model.

<b>Factors</b>	<b>SS</b>	<b>DF</b>	<b>MS</b>	<b>F-value</b>	<b><i>p</i>-value</b>
<b>Model</b>	450.81	5	90.16	2.38	0.1811 not significant
A-Leather hydrolysate	65.54	1	65.54	1.73	0.2452
B-Transglutaminase	367.04	1	367.04	9.71	0.0264
AB	0.7417	1	0.7417	0.0196	0.8941
A <sup>2</sup>	0.6908	1	0.6908	0.0183	0.8978
B <sup>2</sup>	13.49	1	13.49	0.3567	0.5764
<b>Residual</b>	189.09	5	37.82		
Lack of Fit	162.06	3	54.02	4.00	0.2066 not significant
Pure Error	27.03	2	13.51		
<b>Total</b>	639.90	10			
<b>Std. Dev.</b>	6.15		<b>R<sup>2</sup></b>		0.7045
<b>Mean</b>	45.91		<b>Adjusted R<sup>2</sup></b>		0.4090
<b>C.V. %</b>	13.40		<b>Predicted R<sup>2</sup></b>		-0.8960
			<b>Adeq Precision</b>		4.5531

SS= Sum of Squares; DF= Degrees of Freedom; MS= Mean Square; Std. Dev.= Standard Deviation; Adeq= Adequate; C.V. %= Coefficient of Variation.

The reduction of not significant terms in the quadratic model led to a significant linear model ( $p < 0.05$ ) with an acceptable lack of fit (see Table 19). The  $R^2$  was reduced from 70.45% to 67.60%, yet this value can still be considered appropriate. An improvement was noticed in the Adjusted  $R^2$  (59.50%). Even though there is still a not significant term (leather hydrolysate) in the mathematical model considering a confidence level of 95%, its removal does not significantly affect the statistical fitting afterward.

Table 19. ANOVA of additives influence over the elongation percentage at maximum stress considering a linear model.

<b>Factors</b>	<b>SS</b>	<b>DF</b>	<b>MS</b>	<b>F-value</b>	<b>p-value</b>	
<b>Model</b>	432.58	2	216.29	8.35	0.0110	significant
A-Leather hydrolysate	65.54	1	65.54	2.53	0.1504	
B-Transglutaminase	367.04	1	367.04	14.16	0.0055	
<b>Residual</b>	207.32	8	25.92			
Lack of Fit	180.30	6	30.05	2.22	0.3423	not significant
Pure Error	27.03	2	13.51			
<b>Total</b>	639.90	10				
<b>Std. Dev.</b>	5.09		<b>R<sup>2</sup></b>		0.6760	
<b>Mean</b>	45.91		<b>Adjusted R<sup>2</sup></b>		0.5950	
<b>C.V. %</b>	11.09		<b>Predicted R<sup>2</sup></b>		0.3042	
			<b>Adeq Precision</b>		7.2488	

SS= Sum of Squares; DF= Degrees of Freedom; MS= Mean Square; Std. Dev.= Standard Deviation; Adeq= Adequate; C.V. %= Coefficient of Variation.

The notable difference between the Predicted  $R^2$  and Adjusted  $R^2$  reveals that the model might satisfy the fitting between the experimental and theoretical values calculated considering the linear model. Yet, the prediction of values using said model only guarantees a 30.42% accuracy inside the studied region. The equation of the mathematical linear model is shown in equation 3, where the influence of the concentration of mTG is clearly significant over the elongation percentage of leather, supporting the data presented in Table 19.

$$EP (\%) = 26.64 + 0.19 A + 1.35 B \quad (3)$$

The correlation level between the experimental and estimated values of the elongation percentage calculated with the generated mathematical linear model is verified in Figure 26. It can be seen in the response surface (Figure 27) that the higher the amount of mTG incorporated in the treatment of leather, the higher is expected to be the elongation percentage.

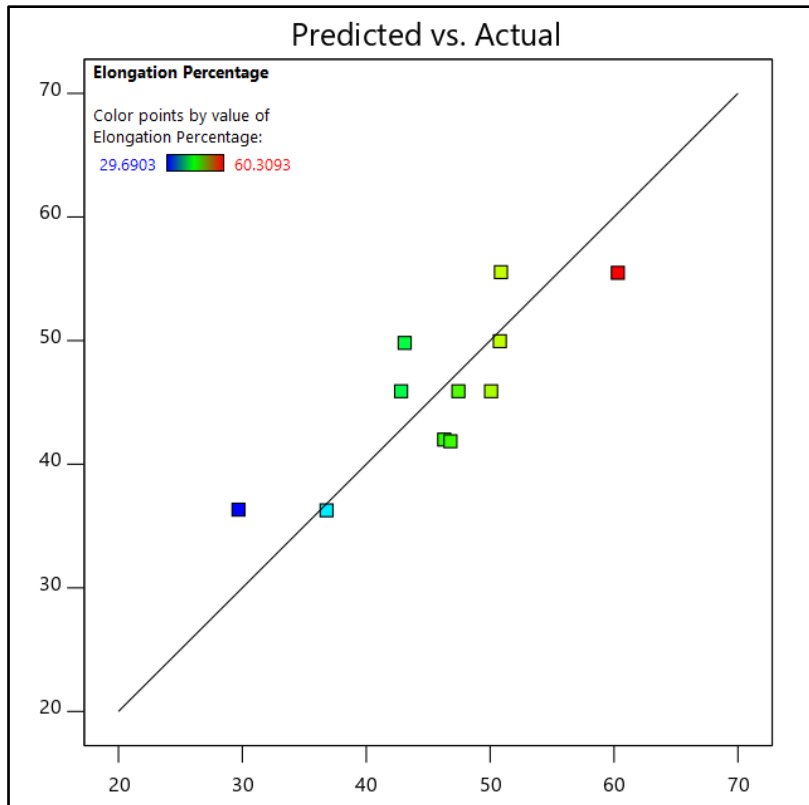


Figure 26. Relation between experimental and estimated values based on the linear model for elongation percentage.

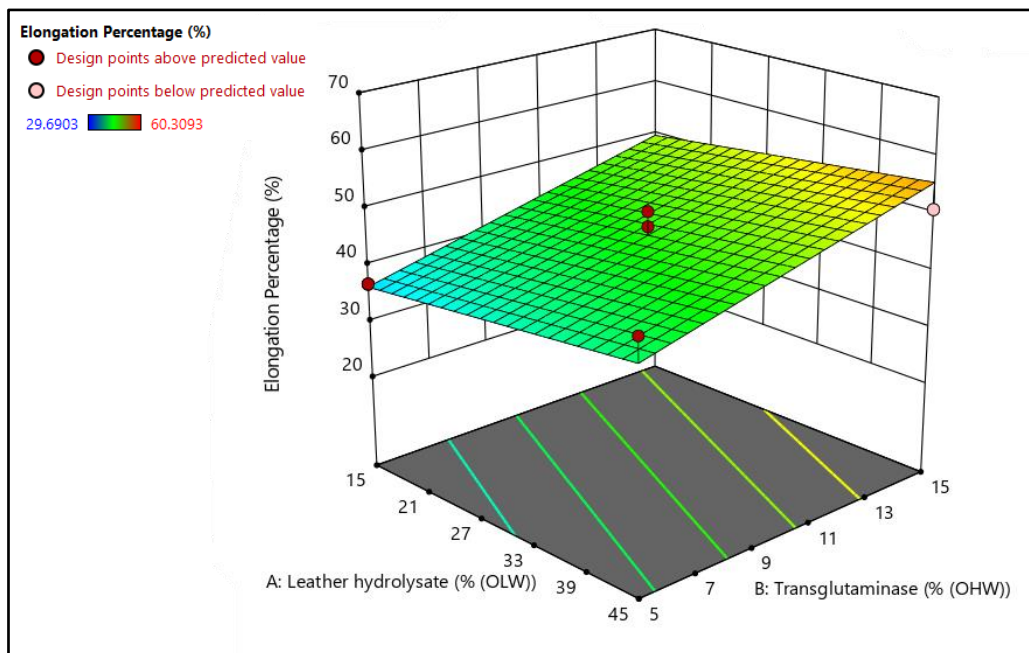


Figure 27. Generated response surface of the effect of the factors over the elongation percentage inside the studied region based on the linear model.

Afsar et al. (2010) incorporated leather hydrolysate as a retanning agent and oxazolidine as a cross-linker in leather treatment in view to improve its mechanical properties. Their findings revealed that a considerable improvement is attained with low quantities of the additives while increasing the amount of leather hydrolysate and the cross-linker results in a low elongation percentage (Afşar et al., 2010).

Films produced by Ocak (2018) using different concentrations of leather hydrolysate and chitosan were evaluated regarding their mechanical properties. It was observed that a reduction in the elongation percentage of the film occurs when the quantity of leather hydrolysate is reduced, and the chitosan concentration increased, explaining that the bonding of the studied additives created a compact and dense structure. In contrast, the film without chitosan presented a loosened structure, given that the interactions governing the film network were polymer-polymer, justifying the lack of elasticity in the films with chitosan (Ocak, 2018).

The increase in the elongation percentage after adding mTG into denaturalized collagen-based films formulated by Cheng et al. (2019) resembles the tendency obtained in this work. They reported how the film's elasticity and thermal stability improved (Cheng et al., 2019). The results of this work favor the claim that the cross-linking achieved led to a lower fiber arrangement, allowing them to have a greater range of motion, which increases the overall elongation percentage of leather (Sizeland et al., 2015; Wells et al., 2013, 2016).

The factors and their correlations demonstrated their lack of significance over the leather Young's modulus within the ranges established in this work. This generated a mathematical quadratic model with a  $p \gg 0.05$  in Table 20. Considering the presented data, a reduction of terms was made as an attempt to find a mathematical model to appropriately predict the response variable's values. Nonetheless, even with the reduction of the terms, no fitting model was achieved (Table 21). A change in the confidence level to 90% was also considered; however, this did not prove to be useful given that the new significance level of the factor and the model were higher than 10% ( $p > 0.1$ ).

Table 20. ANOVA of additives influence over the Young's modulus considering a quadratic model.

<b>Factors</b>	<b>SS</b>	<b>DF</b>	<b>MS</b>	<b>F-value</b>	<b>p-value</b>	
<b>Model</b>	335.08	5	67.02	1.23	0.4143	not significant
A-Leather hydrolysate	41.87	1	41.87	0.7659	0.4215	
B-Transglutaminase	159.53	1	159.53	2.92	0.1483	
AB	69.25	1	69.25	1.27	0.3115	
A <sup>2</sup>	21.79	1	21.79	0.3986	0.5556	
B <sup>2</sup>	57.97	1	57.97	1.06	0.3504	
<b>Residual</b>	273.36	5	54.67			
Lack of Fit	212.32	3	70.77	2.32	0.3155	not significant
Pure Error	61.04	2	30.52			
<b>Total</b>	608.45	10				
<b>Std. Dev.</b>	7.39		<b>R<sup>2</sup></b>		0.5507	
<b>Mean</b>	41.35		<b>Adjusted R<sup>2</sup></b>		0.1014	
<b>C.V. %</b>	17.88		<b>Predicted R<sup>2</sup></b>		-1.7072	
			<b>Adeq Precision</b>		3.1594	

SS= Sum of Squares; DF= Degrees of Freedom; MS= Mean Square; Std. Dev.= Standard Deviation; Adeq= Adequate; C.V. %= Coefficient of Variation.

Table 21. ANOVA of additives influence over the Young's modulus considering a reduced linear model.

Factors	SS	DF	MS	F-value	p-value	
<b>Model</b>	159.53	1	159.53	3.20	0.1073	not significant
B-Transglutaminase	159.53	1	159.53	3.20	0.1073	
<b>Residual</b>	448.91	9	49.88			
Lack of Fit	387.87	7	55.41	1.82	0.4004	not significant
Pure Error	61.04	2	30.52			
<b>Total</b>	608.45	10				
<b>Std. Dev.</b>	7.06		<b>R<sup>2</sup></b>		0.2622	
<b>Mean</b>	41.35		<b>Adjusted R<sup>2</sup></b>		0.1802	
<b>C.V. %</b>	17.08		<b>Predicted R<sup>2</sup></b>		-0.2386	
			<b>Adeq Precision</b>		4.1942	

SS= Sum of Squares; DF= Degrees of Freedom; MS= Mean Square; Std. Dev.= Standard Deviation; Adeq= Adequate; C.V. %= Coefficient of Variation.

The study factors' lack of influence is evidenced in the  $R^2$ , adjusted  $R^2$ , and predicted  $R^2$  values, resulting in eminent low values. This is displayed in the sparsity of points in Figure 28. The equation of the mathematical model is presented in equation 4. The generated response surface for Young's modulus is depicted in Figure 29.

$$YM \text{ (MPa)} = 50.27 - 0.89 A \quad (4)$$

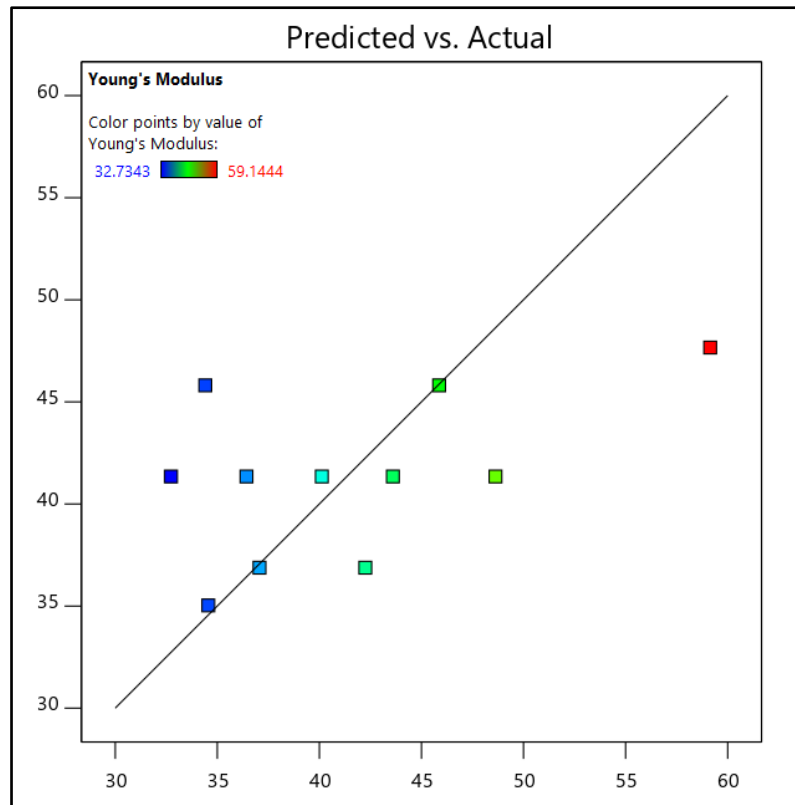


Figure 28. Relation between experimental and estimated values based on the reduced linear model for Young's modulus.



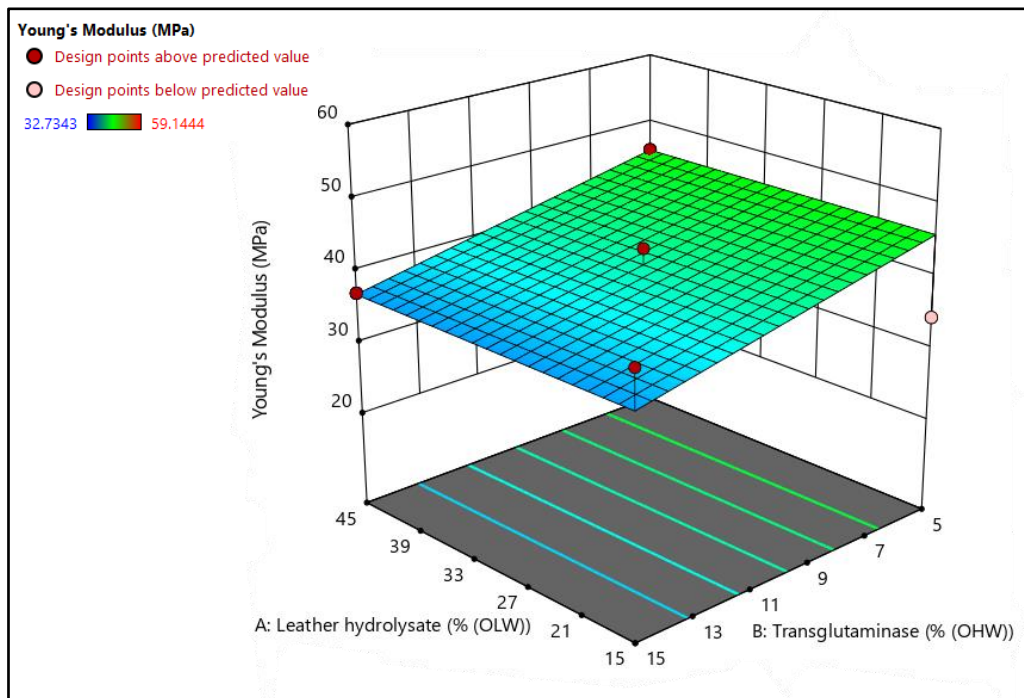


Figure 29. Generated response surface of the effect of the factors over the Young's modulus inside the studied region based on the reduced linear model.

In a study carried out by Taylor et al. (2009), the authors treated loose-grain hides by incorporating mTG to cross-link glutamine and lysine residues from casein and whey protein in a gel-like structure formed by gelatin that can penetrate the surface of leather. Their results indicated that Young's modulus of the treated leather significantly increased its value, whereas tensile strength and elongation percentage were not significantly influenced (Taylor et al., 2009). Findings reported by Liu et al. (2017) described that the elevated values of Young's modulus can be associated with a denser fibrous structure (Liu et al., 2017).

The incorporation of leather hydrolysate into the leather matrix may result in the formation of covalent bonds between the amino acids and collagen fiber as demonstrated by Dilek et al. (2019), however, this reaction is very unlikely to take place in crust leather given where the functional groups available in collagen molecules are much reduced after the tanning process, providing less reactive sites for the formation of covalent bonds between the leather hydrolysate components and leather's collagen fibers (Dilek et al., 2019).

On the other hand, adding mTG and leather hydrolysate to the leather has proven the formation of cross-links in the leather matrix. According to the literature, the cross-links formed by mTG in collagen-based tissues are reported to increase the material's overall leather stability, thermal resistance, and mechanical properties (Baozhen & Jing, 2015; Cheng et al., 2019). However, it is noteworthy to point out that collagen must first go through denaturalization to provide available cross-linking sites for the mTG to catalyze the bonding reaction (Stachel et al., 2010).

It is possible that the cross-links were not formed among the collagen fiber of leather, but rather among the leather hydrolysate amino acids, developing regions with a net-like structure with collagen fibrils trapped in between (not chemically bounded to the cross-links), producing a more compacted fiber network assemblance and, subsequently, the increase in the overall thickness of the leather. Such structure would not affect the rigidity of the collagen fibers in a significant manner, since no changes were made over the fiber's composition, explaining the lack of influence of leather hydrolysate and mTG in the Young's modulus of the treated leather. Yet, it could favor the stress transfer through the structure while creating a slight resistance to fibers' rearrangement, justifying the increase in the elongation percentage with the incorporation of leather hydrolysate and mTG and a thickness increase in the collagen matrix as a consequence.

### 4.3. Final Validation

According to the ANOVA conducted between the factors and each studied response variable, the elongation percentage was the only response variable with a mathematical model suitable to predict its value with accuracy to some extent. To verify this, a validation run was performed.

Given the superior mechanical performance of chrome-tanned leather described in the literature compared to other types of tanning, the values used for further comparison will be chrome-tanned leather (Bielak & Zielińska, 2022). According to industry standards, mechanical properties of leather, such as maximum tensile strength and elongation percentage at maximum stress, are expected to be higher than 15.0 MPa and 40.0%, respectively (Bertazzo et al., 2011; Meyer et al., 2021). Therefore, the concentration selected for the leather hydrolysate was 40.0% and 15.0% for mTG.

According to the mathematical model (eq. 2) the expected value for elongation percentage was  $54.59 \pm 5.09\%$ . The tensile strength and Young's modulus were also calculated, even though their mathematical models (eq. 3 and eq. 4) were considered unsuitable for predicting values inside the studied region. The models indicated a value of  $13.45 \pm 1.67$  MPa for tensile strength and  $36.88 \pm 7.06$  MPa for Young's modulus.

The test was conducted on 7 samples and the final values were calculated considering the average of all samples. The experimental elongation percentage was  $49.62 \pm 2.32\%$  while the tensile strength was  $17.46 \pm 0.65$  MPa and the Young's modulus was  $54.24 \pm 1.94$  MPa (verifiable in Figure 30). Considering the standard deviation of the theoretical elongation percentage, the obtained experimental value falls into the range of the expected value, validating the mathematical model proposed in this work. It can be said that within the range of values established in this work, the predictive mathematical model of elongation percentage can be taken into account to improve the elasticity of faulty leather.

Passing to the experimental tensile strength and the Young's modulus, the achieved values demonstrated the inaccuracy of the models, proving that said models are indeed not suitable for the estimation of tensile strength and Young's modulus values inside the studied region.

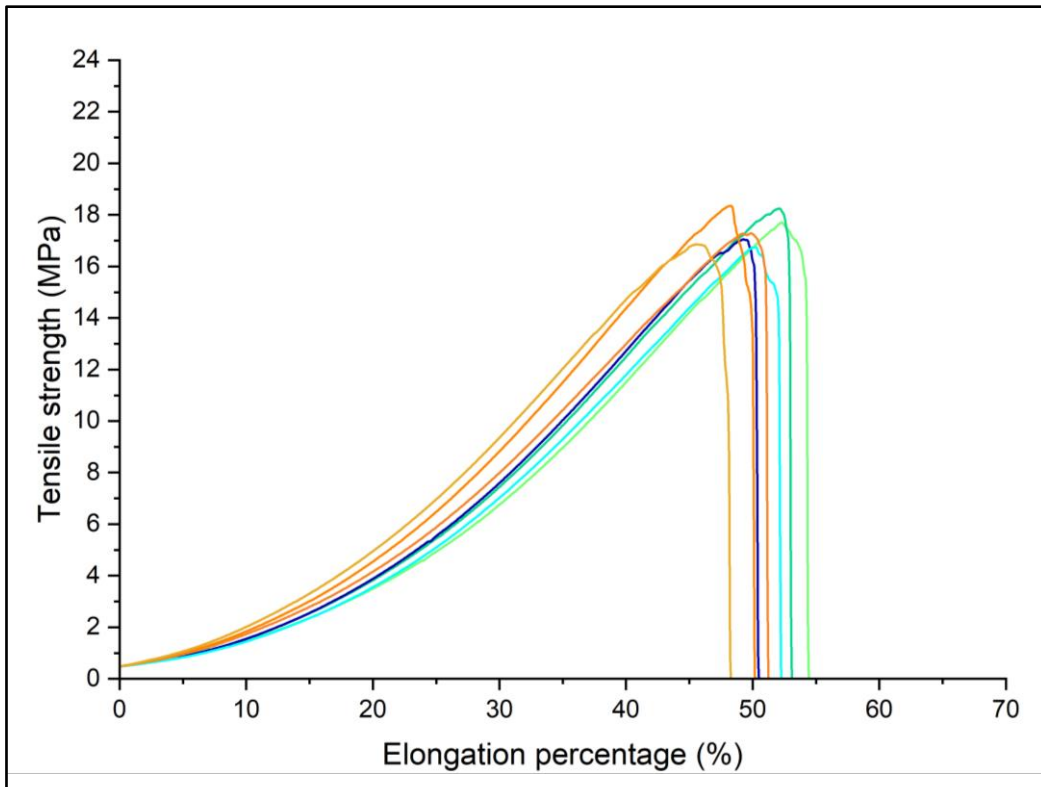


Figure 30. Stress/strain curve of all samples treated with 40.0% leather hydrolysate and 15.0% mTG.

Figures 31 and 32 show the fibers' state before and after breakage by stretching. The low degree of fiber alignment is visible on the flesh side before submission to tensile stress, supporting the idea of a greater elongation percentage due to fiber disorganization.

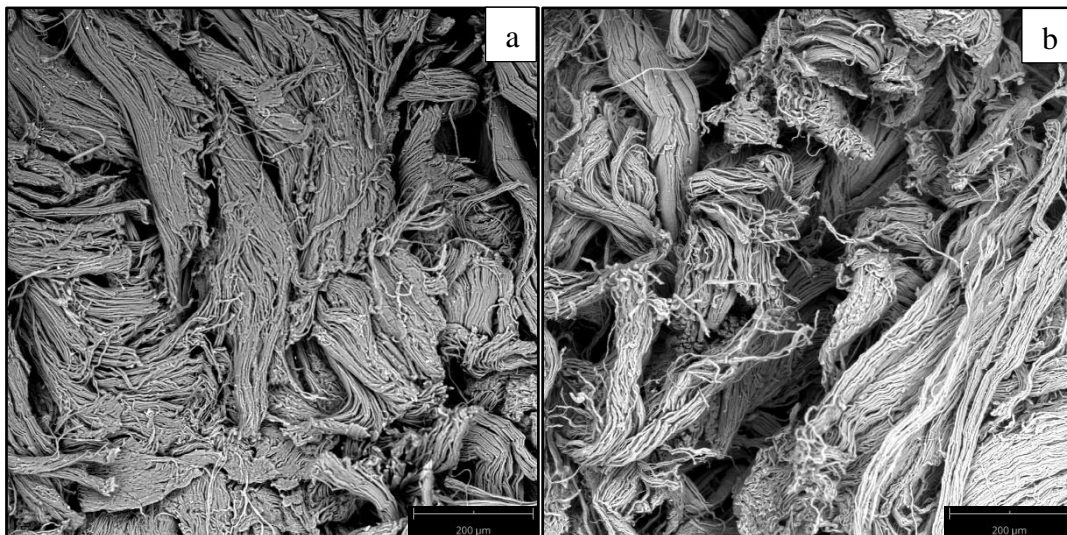


Figure 31. SEM analysis of the flesh side fibers (a) before and (a) after mechanical stretching.

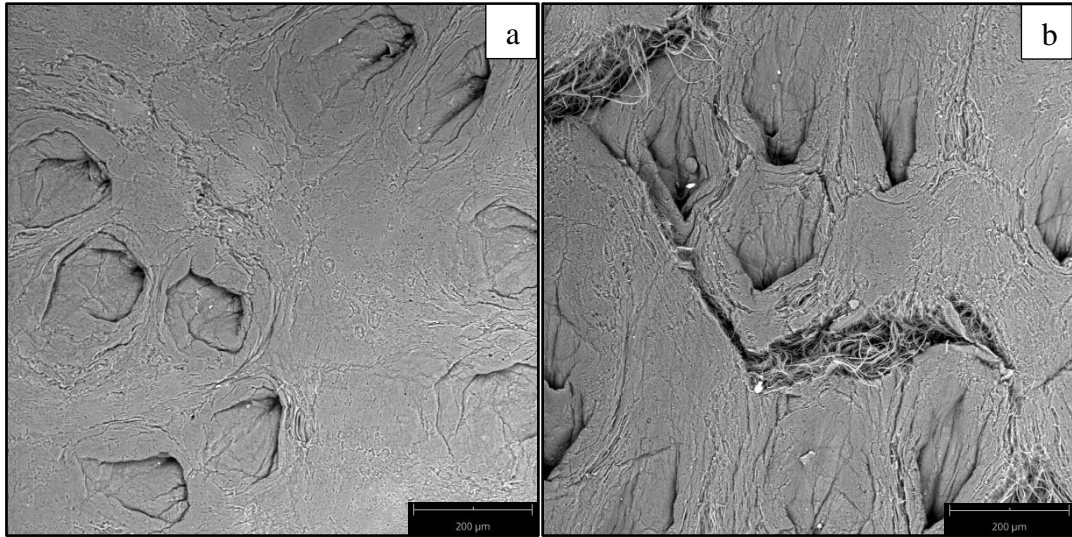


Figure 32. SEM analysis of the grain side fibers (a) before and (a) after mechanical stretching.

## Chapter 5

# **Conclusions and Future Works**

## 5. Conclusions and Future Works

### 5.1. Conclusions

The discard of low-quality leather represents an unnecessary and costly waste. This product can be treated by reinserting its constituent elements (leather hydrolysate) that can be obtained from materials disposed of throughout the leather processing. The diminishment of the downgrading factor of leather was set as the main objective of this work by employing by-products obtained from solid leather residues (leather hydrolysate) and fillers based on commercial expandable, rigid, or elastic low-density microparticles.

The reduction of superficial defects was achieved under the studied conditions in this work (0.2% expandable microspheres, 0.7% glass microspheres and 4.0% nanoclay particles, each combined with 20.0% WPB), highlighting the treatment of faulty leather at 50.0 °C for 1 hour and constant stirring with 25.0% (OHW) of leather hydrolysate and 10.0% (OLW) of mTG as the best combination of additives to obtain a lighter, smoother, and elastic leather without a significant dimensional variance.

To deepen the understanding of the effect that the concentration of the selected additives has on the leather properties, a design of experiments was followed, considering a rotational central composite design  $2^2$  with 3 central points as the best approach and defining the boundaries of the study region between 15.0 and 45.0% (OHW) for the leather hydrolysate and 5.0 to 15.0% (OLW) for mTG.

The statistical analysis of the results revealed a significant effect of the concentration of mTG over the elongation percentage of leather. In contrast, the leather hydrolysate demonstrated a weak yet significant influence over the tensile strength. No significant effect was found in the leather regarding Young's modulus. The validation of the mathematical model obtained for the prediction of values of elongation percentage inside the studied region was successful, obtaining an elongation percentage of 49.62%, which is higher than the minimum required for leather according to industry standards.

The minimization of leather defects was accomplished, yet the optimization of the treatment conditions and the effect of additive concentration is still under development. Therefore, a series of complementing research is suggested in the next section.

## 5.2. Future works

For future studies, it is recommended to develop work according to the following points:

- Conduct studies such as x-ray diffraction and differential scanning calorimetry (DSC) to determine the stability of the obtained leather samples and deepen the understanding of the effect of the studied factors on leather structure;
- Analyze the influence of temperature and reaction time of the mTG and leather hydrolysate treatment over the mechanical leather properties;
- Consider variables such as fiber diameter and orientation index to study the leather mechanical properties treated with mTG and leather hydrolysate;
- Evaluate other mechanical properties of leather that are also considered in its quality assessment, such as tear strength, stitch tearing strength, and water vapor permeability;
- Evaluate the compatibility of other cross-linking agents like oxazolidine E with leather hydrolysate and its effect on the leather mechanical properties and compare the obtained results with the ones of the present work.

## References

- Afşar, A., Aslan, A., Ocak, B., Hidrolizatları, K., Oksazolidinin, İ., İşletisinde Birlikte, D., Üzerine, K., Araştırma, B., & Gülümser, G. (2010). *A study on usability of collagen hydrolysate along with oxazolidine in leather processing*. <https://www.researchgate.net/publication/287548776>
- Afsar, A., & Sekeroglu, O. (2008). An investigation about the effect of oxazolidine on modified valonia extract tanning. *African Journal of Biotechnology*, 7(20), 3737–3742. <http://www.academicjournals.org/AJB>
- Alexandre, M., & Dubois, P. (2000). Polymer-layered silicate nanocomposites: preparation, properties and uses of a new class of materials. *Material Science and Engineering*, 28, 1–63.
- Ali, M. F., Kamal, M., & Islam, M. S. (2020). Comparative Study on Physical Properties of Different Types of Leather in Bangladesh. *Mahbub Kamal Journal of Engineering Research and Application Wwww.Ijera.Com*, 10, 55–63. <https://doi.org/10.9790/9622-1002035563>
- Altun, ehmus, & Yas, F. (2013). Biodiesel production from leather industry wastes as an alternative feedstock and its use in diesel engines. *Energy Exploration & Exploitation*, 31, 759–770.
- Amirrah, I. N., Lokanathan, Y., Zulkiflee, I., Wee, M. F. M. R., Motta, A., & Fauzi, M. B. (2022). A Comprehensive Review on Collagen Type I Development of Biomaterials for Tissue Engineering: From Biosynthesis to Bioscaffold. In *Biomedicines* (Vol. 10, Issue 9). MDPI. <https://doi.org/10.3390/biomedicines10092307>
- Ando, H., Adachi, M., Umeda, K., Matsuura, A., Nonaka, M., Uchio, R., Tanaka, H., & Motoki, M. (1989). Purification and characteristics of a novel transglutaminase derived from microorganisms. *Agricultural and Biological Chemistry*, 53(10), 2613–2617. <https://doi.org/10.1080/00021369.1989.10869735>
- Baozhen, C., & Jing, C. (2015). Microbial transglutaminases as pre-tanning agents in the leather industry. *Journal of the American Leather Chemists Association*, 110.
- Barbanera, M., Belloni, E., Buratti, C., Calabrò, G., Marconi, M., Merli, F., & Armentano, I. (2020). Recycled leather cutting waste-based boards: thermal, acoustic, hygrothermal and ignitability properties. *Journal of Material Cycles and Waste Management*, 22(5), 1339–1351. <https://doi.org/10.1007/s10163-020-01024-3>
- Barth, A. (2007). Infrared spectroscopy of proteins. In *Biochimica et Biophysica Acta - Bioenergetics* (Vol. 1767, Issue 9, pp. 1073–1101). <https://doi.org/10.1016/j.bbabi.2007.06.004>
- Basaran, B., Yorgancioglu, A., & Onem, E. (2012). A novel approach in leather finishing: Surface modification with flock fibers. *Textile Research Journal*, 82(15), 1509–1516. <https://doi.org/10.1177/0040517512449048>



- Bertazzo, M., Roig, M., Segarra, V., Bertazzo, M., Martínez, M. A., Ferrer, J., & Raspi, C. (2011). *Chrome-free leather, tanned with oxazolidine*. <https://www.researchgate.net/publication/283673203>
- Bielak, E., & Zielińska, G. (2022). Comparison and assessment of selected parameters of chrome-free and chrome-tanned leather. *Leather and Footwear Journal*, 22(1), 3–16. <https://doi.org/10.24264/lfj.22.1.1>
- Borges Agustini, C., Winter, C., RS, M. E., & Gutierrez, M. (2018). Behavior of Polymer Films and its Blends for Leather Finishing. *Trends in Textile Engineering & Fashion Technology*, 1(4). <https://doi.org/10.31031/tteft.2018.01.000518>
- Brown, E. (2001). Modified collagen hydrolysate, potential for use as a filler for leather. *Journal of the American Leather Chemists Association*, 96, 262–267. <https://www.researchgate.net/publication/282694853>
- Buehler, M. J. (2006). Nature designs tough collagen: Explaining the nanostructure of collagen fibrils. *PNAS*, 103(33), 12285–12290. [www.pnas.org/cgi/doi/10.1073/pnas.0603216103](http://www.pnas.org/cgi/doi/10.1073/pnas.0603216103)
- Cai, S., Zeng, Y., Zhang, W., Wang, N., & Shi, B. (2015). Inverse Chrome Tanning Technology Based on Wet White Tanned by Al-Zr Complex Tanning Agent. *Journal of the American Leather Chemists Association*, 110.
- Chen, S. Y., Cheng, Y. C., Yang, W. L., & Wang, M. Y. (2021). Surface Defect Detection of Wet-Blue Leather Using Hyperspectral Imaging. *IEEE Access*, 9, 127685–127702. <https://doi.org/10.1109/ACCESS.2021.3112133>
- Chen, Y., Fan, H., & Shi, B. (2011). Nanotechnologies for leather manufacturing: a review. *Journal of the American Leather Chemists Association*, 106, 260–273.
- Cheng, S., Wang, W., Li, Y., Gao, G., Zhang, K., Zhou, J., & Wu, Z. (2019). Cross-linking and film-forming properties of transglutaminase-modified collagen fibers tailored by denaturation temperature. *Food Chemistry*, 271, 527–535. <https://doi.org/10.1016/j.foodchem.2018.07.223>
- Choudhury, S. D., DasGupta, S., & Norris, G. E. (2007). Unravelling the mechanism of the interactions of oxazolidine A and E with collagens in ovine skin. *International Journal of Biological Macromolecules*, 40(4), 351–361. <https://doi.org/10.1016/j.ijbiomac.2006.09.003>
- Correa Brito, L. E. (2012). *Obtención de cuero flor rectificada con la utilización de 3 niveles de ligantes de impregnación para calzado*. Escuela Superior Politécnica de Chimborazo.
- Covington, A., & Wise, W. (2020). Current trends in leather science. *Journal of Leather Science and Engineering*, 2(1). <https://doi.org/10.1186/s42825-020-00041-0>
- Covington, T. (2009). *Tanning chemistry: the science of leather*. Royal Society of Chemistry.
- CTC. (2003). *Wastes generated in the leather products industry*.

- Denis, A., Brambati, N., Dessauvages, B., Guedj, S., Ridoux, C., Meffre, N., & Autier, C. (2008). Molecular weight determination of hydrolyzed collagens. *Food Hydrocolloids*, 22(6), 989–994. <https://doi.org/10.1016/j.foodhyd.2007.05.016>
- Deselnicu, V., & Crudu, M. (2012). *Synthetic organic tanning system*.
- Dilek, Y., Basaran, B., Sancakli, A., Oral Bitlisli, B., & Yorgancioglu, A. (2019). Evaluation of Collagen Hydrolysate on the Performance Properties of Different Wet-White Tanned Leathers. *Society of Leather Technologists and Chemists*, 103, 129–134.
- Ding, X., Wei, B., Dai, R., Chen, H., & Shan, Z. (2022). Effect of collagen hydrolysate obtained from leather waste on the setting, hydration and crystallization process of gypsum. *Journal of Industrial and Engineering Chemistry*, 110, 158–167. <https://doi.org/10.1016/j.jiec.2022.02.047>
- Dixit, S., Yadav, A., Dwivedi, P. D., & Das, M. (2015). Toxic hazards of leather industry and technologies to combat threat: A review. In *Journal of Cleaner Production* (Vol. 87, Issue C, pp. 39–49). Elsevier Ltd. <https://doi.org/10.1016/j.jclepro.2014.10.017>
- European Chemical Agency (ECHA). (2012). *Background document to the Opinion on the Annex XV dossier proposing restrictions on Chromium VI in leather articles*.
- Elsayed, H., Attia, R., Mohamed, O., Haroun, A., & El-Sayed, N. (2018). Preparation of polyurethane silicon oxide nanomaterials as a binder in leather finishing. *Fibers and Polymers*, 19(4), 832–842. <https://doi.org/10.1007/s12221-018-7979-4>
- Escoto-Palacios, J. M., Pérez-Limiñana, M. Á., & Arán-Ais, F. (2016). *From leather waste to functional leather* (I. T. del C. y C. INESCOP, Ed.).
- European Commission. (2015). *Cerrar el círculo: un plan de acción de la UE para la economía circular*.
- European Commission. (2020). *European Commission 2020 - New circular economy action plan*.
- Fan, Q., Ma, J., & Xu, Q. (2019). Insights into functional polymer-based organic-inorganic nanocomposites as leather finishes. *Journal of Leather Science and Engineering*, 1(1). <https://doi.org/10.1186/s42825-019-0005-9>
- Fratzl, P., Misof, K., Zizak, I., Rapp, G., Amenitsch, H., & Bernstorff, S. (1997). Fibrillar Structure and Mechanical Properties of Collagen. *Journal of Structural Biology*, 122, 119–122.
- Fredlund, J. (2011). *Synthesis of Thermo Expandable Microspheres*. KTH Chemical Science and Engineering.
- Gelse, K., Pöschl, E., & Aigner, T. (2003). Collagens - Structure, function, and biosynthesis. *Advanced Drug Delivery Reviews*, 55(12), 1531–1546. <https://doi.org/10.1016/j.addr.2003.08.002>
- Giosafatto, C. V. L., Fusco, A., Al-Asmar, A., & Mariniello, L. (2020). Microbial transglutaminase as a tool to improve the features of hydrocolloid-based bioplastics.

*International Journal of Molecular Sciences*, 21(10).  
<https://doi.org/10.3390/ijms21103656>

Goldschmidt, A., & Streitberger, H.-J. (2007). *Pocket book for the leather technologists*.

Hansen, É., de Aquim, P. M., & Gutterres, M. (2021). Environmental assessment of water, chemicals and effluents in leather post-tanning process: A review. *Environmental Impact Assessment Review*, 89.  
<https://doi.org/10.1016/j.eiar.2021.106597>

Haroun, M., Khristova, P., Covington, A. D., Gurshi, A., & Covington, D. (2009). Potential of vegetable tanning materials and basic aluminum sulphate in Sudanese leather industry. In *Article in Journal of Engineering Science and Technology* (Vol. 4, Issue 1). <https://www.researchgate.net/publication/49593918>

Hedberg, Y. S. (2020). Chromium and leather: a review on the chemistry of relevance for allergic contact dermatitis to chromium. *Journal of Leather Science and Engineering*, 2(1). <https://doi.org/10.1186/s42825-020-00027-y>

IL&FS Ecosmart Limited. (2009). *Technical EIA guidance manual for leather/skin/hide processing industry*.

INESCOP. (2012). *Manual for oxazolidine tanned leather*.

Jaisankar, S. N., Ramalingam, S., Subramani, H., Mohan, R., Saravanan, P., Samanta, D., & Mandal, A. B. (2013). Cloisite-G-methacrylic acid copolymer nanocomposites by graft from method for leather processing. *Industrial and Engineering Chemistry Research*, 52(4), 1379–1387. <https://doi.org/10.1021/ie300290g>

Jawahar, M., Anbarasi, L. J., & Geetha, S. (2023). Vision based leather defect detection: a survey. *Multimedia Tools and Applications*, 82(1), 989–1015.  
<https://doi.org/10.1007/s11042-022-13308-x>

Jeyapalina, S. (2004). *Studies on the hydro-thermal and viscoelastic properties of leather*.

Jiang, H., Liu, J., & Han, W. (2016). The status and developments of leather solid waste treatment: A mini-review. *Waste Management and Research*, 34(5), 399–408.  
<https://doi.org/10.1177/0734242X16633772>

Jiang, H., Zheng, M., Liu, X., Zhang, S., Wang, X., Chen, Y., Hou, M., & Zhu, J. (2019). Feasibility study of tissue transglutaminase for self-catalytic cross-linking of self-assembled collagen fibril hydrogel and its promising application in wound healing promotion. *ACS Omega*, 4(7), 12606–12615.  
<https://doi.org/10.1021/acsomega.9b01274>

Kahsay, T., Negash, G., Hagos, Y., & Hadush, B. (2015). Pre-slaughter, slaughter and post-slaughter defects of skins and hides at the Sheba Tannery and Leather Industry, Tigray region, northern Ethiopia. *Onderstepoort Journal of Veterinary Research*, 82(1).  
<https://doi.org/10.4102/OJVR.V82I1.931>

- Kanagaraj, J., Senthilvelan, T., Panda, R. C., & Kavitha, S. (2015). Eco-friendly waste management strategies for greener environment towards sustainable development in leather industry: A comprehensive review. In *Journal of Cleaner Production* (Vol. 89, pp. 1–17). Elsevier Ltd. <https://doi.org/10.1016/j.jclepro.2014.11.013>
- Kanagaraj, J., Velappan, K. C., Chandra Babu, N. K., & Sadulla, S. (2006). Solid wastes generation in the leather industry and its utilization for cleaner environment □ A review. In *Journal of Scientific & Industrial Research* (Vol. 65).
- Kaygusuz, M. K., Meyer, M., & Aslan, A. (2017). The Effect of TiO<sub>2</sub>-SiO<sub>2</sub> nanocomposite on the performance characteristics of leather. *Materials Research*, 20(4), 1103–1110. <https://doi.org/10.1590/1980-5373-MR-2017-0180>
- Kittiphattanabawon, P., Nalinanon, S., Benjakul, S., & Kishimura, H. (2015). Characteristics of pepsin-solubilised collagen from the skin of splendid squid (*Loligo formosana*). *Journal of Chemistry*, 2015. <https://doi.org/10.1155/2015/482354>
- Koloka, O., & Moreki. (2011). Tanning hides and skins using vegetable tanning agents in Hukuntsi sub-district, Botswana. *Journal of Agricultural Technology*, 7(4), 915–922. <http://www.ijat-aatsea.com>
- Koricho, E. G., Khomenko, A., Haq, M., Drzal, L. T., Belingardi, G., & Martorana, B. (2015). Effect of hybrid (micro- and nano-) fillers on impact response of GFRP composite. *Composite Structures*, 134, 789–798. <https://doi.org/10.1016/j.compstruct.2015.08.106>
- Kramer, R. Z., Venugopal, M. G., Bella, J., Mayville, P., Brodsky, B., & Berman, H. M. (2000). Staggered molecular packing in crystals of a collagen-like peptide with a single charged pair. *Journal of Molecular Biology*, 301(5), 1191–1205. <https://doi.org/10.1006/jmbi.2000.4017>
- Lastowka, Andrew., Maffia, G. J., & Brown, E. M. (2005). A comparison of chemical, physical and enzymatic cross-linking of bovine type I collagen fibrils. *Journal of the American Leather Chemists Association*, 100, 196–202.
- Lensen, D., Vriezema, D. M., & van Hest, J. C. M. (2008). Polymeric microcapsules for synthetic applications. *Macromolecular Bioscience*, 8(11), 991–1005. <https://doi.org/10.1002/mabi.200800112>
- Li, K., Chen, H., Wang, Y., Shan, Z., Yang, J., & Brutto, P. (2009). A salt-free pickling regime for hides and skins using oxazolidine. *Journal of Cleaner Production*, 17(17), 1603–1606. <https://doi.org/10.1016/j.jclepro.2009.06.004>
- Li, Z., Paudecerf, D., & Yang, J. (2009). Mechanical behaviour of natural cow leather in tension. *Acta Mechanica Solida Sinica*, 22(1), 37–44. [https://doi.org/10.1016/S0894-9166\(09\)60088-4](https://doi.org/10.1016/S0894-9166(09)60088-4)
- Li, Z. R., Wang, B., Chi, C. feng, Zhang, Q. H., Gong, Y. dan, Tang, J. J., Luo, H. yu, & Ding, G. fang. (2013). Isolation and characterization of acid soluble collagens and pepsin soluble collagens from the skin and bone of Spanish mackerel (*Scomberomorus niphonius*). *Food Hydrocolloids*, 31(1), 103–113. <https://doi.org/10.1016/j.foodhyd.2012.10.001>

- Liu, C.-K., Latona, N. P., & Brady, M. (2017). The Prediction of Leather Mechanical Properties from Airborne Ultrasonic Testing of Hides. *Journal of the American Leather Chemists Association*, 112.
- Liu, C.-Kung., Latona, N. P., Lee, Joseph., & Cooke, P. H. (2009). Microscopic observations of leather looseness and its effects on mechanical properties. *Journal of American Leather Chemists Association*, 104, 230–236. <https://www.researchgate.net/publication/43286062>
- Lu, Y., Chen, Y., Fan, H., Peng, B., & Shi, B. (2009). A Novel Nano-SiO<sub>2</sub> Tannage for Making Chrome-Free Leather.
- Luckham, P. F., & Rossi, S. (1999). The colloidal and rheological properties of bentonite suspensions. *Advances in Colloid and Interface Science*, 82, 43–92.
- Lyu, B., Chang, R., Gao, D., & Ma, J. (2018). Chromium Footprint Reduction: Nanocomposites as Efficient Pretanning Agents for Cowhide Shoe Upper Leather. *ACS Sustainable Chemistry and Engineering*, 6(4), 5413–5423. <https://doi.org/10.1021/acssuschemeng.8b00233>
- Ma, J., & Lu, H. (2008). Elasticity studies on leather retanned with various types of acrylic polymers. *Journal of the American Leather Chemists Association*, 103, 363–369.
- Madbouly, S. A. (2021). Waterborne polyurethane dispersions and thin films: Biodegradation and antimicrobial behaviors. *Molecules*, 26(4). <https://doi.org/10.3390/molecules26040961>
- Maina, P., Ollengo, M. A., & Nthiga, E. W. (2019). Trends in leather processing: A Review. *International Journal of Scientific and Research Publications (IJSRP)*, 9(12), p9626. <https://doi.org/10.29322/ijsrp.9.12.2019.p9626>
- Mancopes, F., & Gutteres, M. (2009). *Modificação da estrutura do colagênio durante o processamento de couro*. [www.enq.ufrgs.br/oktoberforum](http://www.enq.ufrgs.br/oktoberforum)
- Marconi, M., Barbanera, M., Calabrò, G., & Baffo, I. (2020). Reuse of leather scraps for insulation panels: Technical and environmental feasibility evaluation. *Procedia CIRP*, 90, 55–60. <https://doi.org/10.1016/j.procir.2020.01.053>
- Masilamani, D., Madhan, B., Shanmugam, G., Palanivel, S., & Narayan, B. (2016). Extraction of collagen from raw trimming wastes of tannery: A waste to wealth approach. *Journal of Cleaner Production*, 113, 338–344. <https://doi.org/10.1016/j.jclepro.2015.11.087>
- Maxwell, C. A., Wess, T. J., & Kennedy, C. J. (2006). X-ray diffraction study into the effects of liming on the structure of collagen. *Biomacromolecules*, 7(8), 2321–2326. <https://doi.org/10.1021/bm060250t>
- Meyer, M., Dietrich, S., Schulz, H., & Mondschein, A. (2021). Comparison of the technical performance of leather, artificial leather, and trendy alternatives. *Coatings*, 11(2), 1–15. <https://doi.org/10.3390/coatings11020226>

- Mohamed, O. A., Moustafa, A. B., Mehawed, M. A., & El-Sayed, N. H. (2009). Styrene and butyl methacrylate copolymers and their application in leather finishing. *Journal of Applied Polymer Science*, *111*(3), 1488–1495. <https://doi.org/10.1002/app.29022>
- Mohamed, O., Elsayed, H., Attia, R., Haroun, A., & El-Sayed, N. (2018). Preparation of acrylic silicon dioxide nanoparticles as a binder for leather finishing. *Advances in Polymer Technology*, *37*(8), 3276–3286. <https://doi.org/10.1002/adv.22112>
- Nalyanya, K. M., Rop, R. K., Onyuka, A., Birech, Z., & Sasia, A. (2018). Effect of crusting operations on the physical properties of leather. *Leather and Footwear Journal*, *18*(4), 283–294. <https://doi.org/10.24264/lfj.18.4.4>
- Nalyanya, K. M., Rop, R., Onyuka, A., Birech, Z., Wambulwa, M. C., & Sasia, A. (2018). Synergistic effect of Aloe barbadensis miller and Carrageenan on the mechanical performance of leather. *Journal of AQEIC*, *69*(3), 59–68. <https://www.researchgate.net/publication/338968096>
- Namba, D. (2020). *Microencapsulation involving chitosan enzyme-induced crosslinking*. Polytechnic Institute of Bragança.
- Nieuwenhuizen, L. (1998). Synthetic fill materials for skin, leather, and furs. *Journal of the American Institute for Conservation*, *37*(1), 135–145. <https://doi.org/10.1179/019713698806082976>
- Nishad Fathima, N., Balaraman, M., Raghava Rao, J., & Unni Nair, B. (2003). Effect of zirconium(IV) complexes on the thermal and enzymatic stability of type I collagen. *Journal of Inorganic Biochemistry*, *95*(1), 47–54. [https://doi.org/10.1016/S0162-0134\(03\)00071-0](https://doi.org/10.1016/S0162-0134(03)00071-0)
- Ocak, B. (2018). Film-forming ability of collagen hydrolysate extracted from leather solid wastes with chitosan. *Environmental Science and Pollution Research*, *25*(5), 4643–4655. <https://doi.org/10.1007/s11356-017-0843-z>
- O’leary, D. N., & Attenburrow, G. E. (1996). Differences in strength between the grain and corium layers of leather. *Journal of Materials Science*, *31*, 5677–5682.
- Olle, L., Bou, J., Shendrik, A., & Bacardit, A. (2014). Sustainable solvent-free finishing of patent leather using carbonyl-functional resins. *Journal of Cleaner Production*, *65*, 590–594. <https://doi.org/10.1016/j.jclepro.2013.07.058>
- Ozgunay, H., Colak, S., Mutlu, M. M., & Akyuz, F. (2007). Characterization of leather industry wastes. *Polish Journal of Environmental Studies*, *16*(6), 867–873.
- Pahlawan, I. F., Sutyasmi, S., & Griyanitasari, G. (2019). Hydrolysis of leather shavings waste for protein binder. *IOP Conference Series: Earth and Environmental Science*, *230*(1). <https://doi.org/10.1088/1755-1315/230/1/012083>
- Pathan, E., Ahmed, S., & Shakil, S. R. (2019). Utilization of Limed Flesh Through Fat Extraction and Soap Preparation. *European Journal of Engineering Research and Science*, *4*(10), 198–202. <https://doi.org/10.24018/ejers.2019.4.10.1575>

- Pereira, R. (2021, July 31). O sistema de Economia Circular e a Agenda 2030: análise da evolução em Portugal. *Revista de Economia, Empresas e Empreendedores Na CPLP*, 7(1), 097–124. <https://doi.org/10.29073/e3.v7i1.381>
- Polaina, Julio., & MacCabe, A. P. (2007). *Industrial Enzymes - Structure, Function and Applications*.
- Prabakar, S., Catherin, P., Henning, A. M., & Holmes, G. (2016). *The Effect of Cloisite® Na+ Nanoclay Filler on the Morphology and Mechanical Properties of Loose Leather*. <https://www.researchgate.net/publication/301348365>
- Purcell, B. Patrick., Williamson, D. Thomas., Marga, F. Suzanne., Shofer, S. J., & Cassingham, D. Miles. (2017). *METHOD FOR MAKING A BIOFABRICATED MATERIAL CONTAINING COLLAGEN FIBRILS*.
- Rabotyagova, O. S., Cebe, P., & Kaplan, D. L. (2008). Collagen structural hierarchy and susceptibility to degradation by ultraviolet radiation. *Materials Science and Engineering C*, 28(8), 1420–1429. <https://doi.org/10.1016/j.msec.2008.03.012>
- Riaz, T., Zeeshan, R., Zarif, F., Ilyas, K., Muhammad, N., Safi, S. Z., Rahim, A., Rizvi, S. A. A., & Rehman, I. U. (2018). FTIR analysis of natural and synthetic collagen. In *Applied Spectroscopy Reviews* (Vol. 53, Issue 9, pp. 703–746). Taylor and Francis Inc. <https://doi.org/10.1080/05704928.2018.1426595>
- Rosu, L., Varganici, C., Crudu, A., Rosu, D., & Bele, A. (2018). Ecofriendly wet–white leather vs. conventional tanned wet–blue leather. A photochemical approach. *Journal of Cleaner Production*, 177, 708–720. <https://doi.org/10.1016/j.jclepro.2017.12.237>
- Rýglová, Š., Braun, M., Hříbal, M., Suchý, T., & Vöröš, D. (2021). The proportion of the key components analysed in collagen-based isolates from fish and mammalian tissues processed by different protocols. *Journal of Food Composition and Analysis*, 103. <https://doi.org/10.1016/j.jfca.2021.104059>
- Sanchez-Olivares, G., Sanchez-Solis, A., Calderas, F., Medina-Torres, L., Manero, O., Di Blasio, A., & Alongi, J. (2014). Sodium montmorillonite effect on the morphology, thermal, flame retardant and mechanical properties of semi-finished leather. *Applied Clay Science*, 102, 254–260. <https://doi.org/10.1016/j.clay.2014.10.007>
- Sanden, K. W., Kohler, A., Afseth, N. K., Böcker, U., Rønning, S. B., Liland, K. H., & Pedersen, M. E. (2019). The use of Fourier-transform infrared spectroscopy to characterize connective tissue components in skeletal muscle of Atlantic cod (*Gadus morhua* L.). *Journal of Biophotonics*, 12(9). <https://doi.org/10.1002/jbio.201800436>
- Shi, J., Puig, R., Sang, J., & Lin, W. (2016). A comprehensive evaluation of physical and environmental performances for wet-white leather manufacture. *Journal of Cleaner Production*, 139, 1512–1519. <https://doi.org/10.1016/j.jclepro.2016.08.120>
- Shi, J., Zhang, R., Mi, Z., Lyu, S., & Ma, J. (2021). Engineering a sustainable chrome-free leather processing based on novel lightfast wet-white tanning system towards eco-leather manufacture. *Journal of Cleaner Production*, 282. <https://doi.org/10.1016/j.jclepro.2020.124504>

Shorter, R. (2014). *The mechanical behavior of elastomers when hollow microspheres are used as a particulate filler*.

Shoulders, M. D., & Raines, R. T. (2009). Collagen structure and stability. *Annual Review of Biochemistry*, 78, 929–958. <https://doi.org/10.1146/annurev.biochem.77.032207.120833>

Sivakumar, V., & Mohan, R. (2020). Sustainable solid waste management in leather and textile industry: Leather & textile waste fibre-polymer composite and nanocomposite - overview and review. In *Textile and Leather Review* (Vol. 3, Issue 2, pp. 54–63). Seniko studio Ltd. <https://doi.org/10.31881/TLR.2020.04>

Sivakumar, V., Mohan, R., & Muralidhara, C. (2019). Alternative methods for salt free/less salt short term preservation of hides and skins in leather making for sustainable development - a review. In *Textile and Leather Review* (Vol. 2, Issue 1, pp. 46–52). Seniko studio Ltd. <https://doi.org/10.31881/TLR.2019.19>

Sizeland, K. H., Basil-Jones, M. M., Edmonds, R. L., Cooper, S. M., Kirby, N., Hawley, A., & Haverkamp, R. G. (2013). Collagen orientation and leather strength for selected mammals. *Journal of Agricultural and Food Chemistry*, 61(4), 887–892. <https://doi.org/10.1021/jf3043067>

Sizeland, K. H., Edmonds, R. L., Basil-Jones, M. M., Kirby, N., Hawley, A., Mudie, S., & Haverkamp, R. G. (2015). Changes to collagen structure during leather processing. *Journal of Agricultural and Food Chemistry*, 63(9), 2499–2505. <https://doi.org/10.1021/jf506357j>

Solomon, B. B. (2021). *Leather cutting waste minimization Techniques in Ethiopian footwear industry: case study ELICO-Universal Leather Products Industry*. <https://doi.org/10.21203/rs.3.rs-274284/v1>

Stachel, I., Schwarzenbolz, U., Henle, T., & Meyer, M. (2010). Cross-linking of type I collagen with microbial transglutaminase: Identification of cross-linking sites. *Biomacromolecules*, 11(3), 698–705. <https://doi.org/10.1021/bm901284x>

Staroszczyk, H., Pielichowska, J., Sztuka, K., Stangret, J., & Kołodziejaska, I. (2012). Molecular and structural characteristics of cod gelatin films modified with EDC and TGase. *Food Chemistry*, 130(2), 335–343. <https://doi.org/10.1016/j.foodchem.2011.07.047>

Sundar, S., Vijayalakshmi, N., Gupta, S., Rajaram, R., & Radhakrishnan, G. (2006). Aqueous dispersions of polyurethane-polyvinyl pyridine cationomers and their application as binder in base coat for leather finishing. *Progress in Organic Coatings*, 56(2–3), 178–184. <https://doi.org/10.1016/j.porgcoat.2006.04.001>

Sundar, V. J., Gnanamani, A., Muralidharan, C., Chandrababu, N. K., & Mandal, A. B. (2011). Recovery and utilization of proteinous wastes of leather making: A review. In *Reviews in Environmental Science and Biotechnology* (Vol. 10, Issue 2, pp. 151–163). <https://doi.org/10.1007/s11157-010-9223-6>

Tannery Projects. (2022). *Valero Wooden Drum*. <https://www.tanneryprojects.com/used-machines/drums-paddles/>



- Taylor, M. M., Brown, E., Bumanlag, L., & Marmer, W. (2006). *Use of enzymatically modified gelatin and casein as fillers in leather processing*. <https://www.researchgate.net/publication/289148982>
- Taylor, M. M., Lee, J., Bumanlag, L. P., Cooke, P. H., & Brown, E. M. (2009). Treatment of low-quality hides with fillers produced from sustainable resources. Effect on properties of leather fillers from sustainable resources. *Journal of the American Leather Chemists Association*, *104*.
- Taylor, M. M., Lee, J., Bumanlag, L. P., Hernández Balada, E., & Brown, E. M. (2010). Treatments to enhance properties of chrome-free (wet white) leather. *Journal of the American Leather Chemists Association*, *105*, 35–43. <https://www.researchgate.net/publication/279714256>
- Taylor, M. M., Marner, W. N., & Brown, E. (2007). *Evaluation of polymers prepared from gelatin and casein or whey as potential fillers*. <https://www.researchgate.net/publication/285948284>
- Teferi, T. A. (2021). *Solid Leather Waste for Preparation of Value Added Composite Products: An Ethiopian Perspective*. [www.scireslit.com](http://www.scireslit.com)
- Tian, S. (2020). Recent advances in functional polyurethane and its application in leather manufacture: A review. *Polymers*, *12*(9), 1–16. <https://doi.org/10.3390/polym12091996>
- Tian, S., Zhang, P., Fan, H., Chen, Y., & Yan, J. (2018). Fabrication of retro-reflective polyurethane via covalently embedding with amino-functionalized glass microspheres. *Progress in Organic Coatings*, *115*, 115–121. <https://doi.org/10.1016/j.porgcoat.2017.10.026>
- Tracton, A. A. (2006). *Coatings technology handbook* (Arthur A. Tracton, Ed.; Third Edition). Taylor & Francis Group.
- Velmurugan, P., Singam, E. R. A., Jonnalagadda, R. R., & Subramanian, V. (2014). Investigation on interaction of tannic acid with type i collagen and its effect on thermal, enzymatic, and conformational stability for tissue engineering applications. *Biopolymers*, *101*(5), 471–483. <https://doi.org/10.1002/bip.22405>
- Vieira Kopp, V., Borges Agustini, C., Gutterres, M., & Henrique Zimnoch dos Santos, J. (2021). *Nanomaterials to help eco-friendly leather processing*. <https://doi.org/10.1007/s11356-021-16216-z>Published
- Watt, A. (1906). *Leather manufacture - A practical handbook of tanning, currying, and chrome leather dressing* (5th ed.).
- Wells, H. C., Edmonds, R. L., Kirby, N., Hawley, A., Mudie, S. T., & Haverkamp, R. G. (2013). Collagen fibril diameter and leather strength. *Journal of Agricultural and Food Chemistry*, *61*(47), 11524–11531. <https://doi.org/10.1021/jf4041854>
- Wells, H. C., Holmes, G., & Haverkamp, R. G. (2016). Looseness in bovine leather: Microstructural characterization. *Journal of the Science of Food and Agriculture*, *96*(8), 2731–2736. <https://doi.org/10.1002/jsfa.7392>

- Winey, K. I., & Vaia, R. A. (2007). *Polymer Nanocomposites*. [www.mrs.org/bulletin](http://www.mrs.org/bulletin)
- Wong, R. S. H., Ashton, M., & Dodou, K. (2015). Effect of crosslinking agent concentration on the properties of unmedicated hydrogels. *Pharmaceutics*, 7(3), 305–319. <https://doi.org/10.3390/pharmaceutics7030305>
- Wu, X., Qiang, X., Liu, D., Yu, L., & Wang, X. (2020). An eco-friendly tanning process to wet-white leather based on amino acids. *Journal of Cleaner Production*, 270. <https://doi.org/10.1016/j.jclepro.2020.122399>
- Xiao, Y., Zhou, J., Wang, C., Zhang, J., Radnaeva, V. D., & Lin, W. (2023). Sustainable metal-free leather manufacture via synergistic effects of triazine derivative and vegetable tannins. *Journal of Leather Science and Engineering*, 5(1). <https://doi.org/10.1186/s42825-022-00108-0>
- Yahia, M., Musa, A. E., Gasmelseed, G. A., Faki, E. F., Ibrahim, H. E., Haythem, O. A., Manal, M. A., & Haythem, S. B. (2019). Quebracho-Oxazolidine Combination Tanning for Leather Making. *International Journal of Advance Industrial Engineering*, 7(2), 104–110. <https://doi.org/10.14741/ijaie/v.7.2.2>
- Yang, L. (2008). *Mechanical properties of collagen fibrils and elastic fibers explored by AFM*. University of Twente.
- Zou, Y., & Ma, G. (2014). A new criterion to evaluate water vapor interference in protein secondary structural analysis by FTIR spectroscopy. *International Journal of Molecular Sciences*, 15(6), 10018–10033. <https://doi.org/10.3390/ijms150610018>